Non-Orthogonal Multiple Access (NOMA) for Cellular Wireless Communications

by

Md Shipon Ali

A Thesis submitted to The Faculty of Graduate Studies of

The University of Manitoba

in partial fulfillment of the requirements for the degree of

Master of Science

Department of Electrical and Computer Engineering

University of Manitoba

Winnipeg

April 2017

Abstract

This thesis begins with an overview of the basic concept of NOMA by identifying the key working principle of NOMA systems and their respective power allocation requirements in both of downlink and uplink transmissions. Then, for cell-throughput maximization in both of downlink and uplink NOMA transmissions, the joint problem of user clustering and transmit power allocation is formulated as a mixed integer non-linear program (MINLP). The formulated problem is solved in two steps: grouping users into disjoint cluster(s), and then optimizing power allocation at each cluster.

After investigating NOMA for conventional downlink and uplink systems, the application of NOMA is investigated in downlink multiuser multiple-input multiple-output (MIMO) systems, by proposing a novel MIMO-NOMA model with linear beamforming technique. In this MIMO-NOMA system, users' receive antennas are dynamically grouped into a number of disjoint clusters, and within each cluster a single beam is shared by all the receive antennas those adopt NOMA. The superiority of the proposed model is illustrated through extensive performance evaluations.

Finally, the application of coordinated multi-point (CoMP) transmission technique is investigated in downlink multi-cell NOMA systems, considering distributed power allocation at each cell. In the proposed CoMP-NOMA model, CoMP transmission is used for users experiencing strong receive-signals from multiple cells while each cell independently adopts NOMA for resource allocation. The applicability and necessary conditions to use different CoMP schemes are identified under various network scenarios, and the corresponding throughput formulas are derived. The spectral efficiency gains of the proposed CoMP-NOMA model are also quantified.

Acknowledgements

My deepest gratitude goes to Dr. Ekram Hossain for giving me the opportunity to work with him. I have been able to push myself beyond my expectations with his excellent supervision, motivation, encouragement and personal generosity. I would like to express my sincere appreciation to Dr. Pradeepa Yahampath and Dr. Yang Wang for their comprehensive advice and feedback. I also acknowledge University of Manitoba and the Government of Manitoba for providing me with financial support.

My utmost gratitude goes to my beloved wife Mojaiana Synthia for her undoubted faith in me and allowing me to be as ambitious as I wanted. I especially thank to my lovely wife and my son Nooraiz Nivaan for their unconditional loves, sacrifices, supports and cares to me and my career throughout.

My appreciation also extends to my lab mates, particularly Dr. Hina Tabassum for valuable suggestions and Md Monjurul Islam Khan for facilitating my initial accommodation. Finally I would like to pay gratitude to Allah almighty for directing in the course of my life.

This thesis is dedicated to the memory of my elder brother Md Sanowar Hossain, a great human being whom I miss every day.

Table of Contents

List of Figures

List of Tables

List of Abbreviations

NOMA	Non-Orthogonal Multiple Access
OMA	Orthogonal Multiple Access
SIC	Successive Interference Cancellation
CSI	Channel State Information
MIMO	Multiple-Input Multiple-Output
CoMP	Coordinated Multi-Point
OFDMA	Orthogonal frequency Division Multiple Access
TDMA	Time-Division Multiple Access
ZF-BF	Zero-Forcing Beam-Forming
MINLP	Mixed Integer Non-Linear Programing
LTE	Long Term Evolution
3GPP	Third Generation Partnership Project
QoE	Quality of user Experience
SINR	Signal-to-Interference-plus-Noise Ratio
5G	Fifth Generation
KKT	Karush-Kuhn-Tucker
BS	Base Station
UE	User Equipment

Publications

- Journal/Magazine:

1. **Md Shipon Ali**, Ekram Hossain, and Dong In Kim, "Coordinated multi-point (CoMP) transmission in downlink multicell NOMA systems: Models and spectral efficiency," submitted to *IEEE Wireless Communications*.
2. **Md Shipon Ali**, Ekram Hossain, and Dong In Kim, "Non-orthogonal multiple access (NOMA) for downlink multiuser MIMO systems: User clustering, beamforming, and power allocation," *IEEE Access*, vol. 5, Jan. 2017 pp. 565–577.
3. **Md Shipon Ali**, Ekram Hossain, and Dong In Kim, "LTE/LTE-A random access for massive machine-type communications in smart cities," *IEEE Communications Magazine*, vol. 4, no. 1, Jan. 2017, pp. 76–83.
4. **Md Shipon Ali**, Hina Tabassum, and Ekram Hossain, "Dynamic user clustering and power allocation for uplink and downlink non-orthogonal multiple access (NOMA) systems," *IEEE Access*, vol. 4, Aug. 2016, pp. 6325–6343.

- Conference:

1. Hina Tabassum, **Md Shipon Ali**, Ekram Hossain, Md Jahangir Hossain and Dong In Kim, "Uplink vs. downlink NOMA in cellular networks: Challenges and research directions," to be presented in *IEEE VTC*, Spring 2017.

Chapter 1

Introduction

To ensure the sustainability of mobile communication services in the coming decades, new technology solutions are being sought for the fifth generation (5G) and beyond 5G (B5G) cellular systems. In the view of the anticipated exponential growth of mobile traffic, these technologies are expected to provide significant gains in the spectral efficiency (and hence system capacity) and improved quality of user experience (QoE). In this context, non-orthogonal multiple access (NOMA) is considered as a promising multiple access technology for 5G systems. By scheduling multiple users over same spectrum resources but at different power levels, NOMA can yield a significant spectral efficiency gain and enhanced QoE when compared to traditional orthogonal multiple access (OMA) systems.

1.1 What is NOMA?

The basic principle of NOMA is to simultaneously serve multiple users over same spectrum resources (i.e. time, frequency, code and space) but with different power levels, at the expense of minimal inter-user interference [1] [2] [3] [4] [5]. In contrast

to conventional orthogonal multiple access (OMA), where every user is served on exclusively allocated spectrum resources, NOMA superposes the message signals of multiple users in power domain at transmitter end(s) by exploiting the users' respective channel gain. Successive interference cancellation (SIC) is then applied at the receiver(s) for multiuser detection and decoding. For an example, let us consider a downlink NOMA transmission where the base station (BS) schedules m users over the same spectrum resources B. Let also assume that the message signal for i-th user is s_i, where $E[|s_i|^2] = 1$, and transmit power is p_i. Then the superposed signal at transmitter end could be expressed as:

$$X = \sum_{i=1}^{m} \sqrt{p_i} s_i \tag{1.1}$$

where $\sum_{i=1}^{m} p_i \leq p_t$, for BS total transmit power budget of p_t. On the other hand, the received signal at i-th user end could be expressed as:

$$y_i = h_i X + w_i, \quad \forall i \tag{1.2}$$

where h_i is the complex channel gain between user i and the BS. The term w_i denotes the receiver Gaussian noise including the inter-cell interference at the i-th user's receiver.

1.1.1 NOMA in Downlink Transmission Scenarios

Let us consider a downlink NOMA transmission with a single antennas BS and single antenna m number of users with distinct channel gains. In such m-user downlink NOMA, the BS transmitter non-orthogonally transmits m different signals by superposing them over the same spectrum resources; whereas, all m UE receivers receive

their desired signals along with the interferences caused by the messages of other UEs. To obtain the desired signal, each SIC receiver first decodes the dominant[1] interferences and then subtracts them from the superposed signal. Since each UE receives all signals (desired and interfering signals) over the same channel, the superposing of different signals with different power levels is crucial to diversify each signal and to perform SIC at a given UE receiver.

Let us also consider that the messages of NOMA users are superposed with a power level which is inversely proportional to the their channel gains, that is, a particular user is allocated for low power than the users those have lower channel gain while that allocated power is higher than all the users those have higher channel gain than the particular user. As such, the lowest channel gain user (who receives low interferences due to relatively low powers of the messages of high channel gain users) cannot suppress any interferences. However, the highest channel gain user (who receives strong interferences due to relatively high powers of the messages of low channel gain users) can suppress all interfering signals.

Illustration: Fig. 1.1 illustrates a 3-user downlink NOMA system where h_1, h_2 and h_3 are the complex channel gains of UE_1, UE_2 and UE_3, respectively, and $h_1 > h_2 > h_3$. Let also consider that w_1, w_2 and w_3 are the inter-cell interference-plus-noise of UE_1, UE_2 and UE_3, respectively, where $w_1 \leq w_2 \leq w_3$. Also, it is assumed that x_1, x_2, and x_3 are the desired signal of UE_1, UE_2, and UE_3, respectively, where $x_i = \sqrt{p_i}s_i$ and $E[|s_i|^2] = 1$. Now, if the transmit power is allocated in inverse proportional to the normalized channel gains by inter-cell interference-plus-noise, then UE_1 can perform SIC to cancel interference from both UE_2 and UE_3; whereas, UE_2 can only cancel interference from UE_3. Also, UE_3 experiences interference from both

[1]Dominant interference refers to the interference which is sufficiently stronger than the receiver's desired signal.

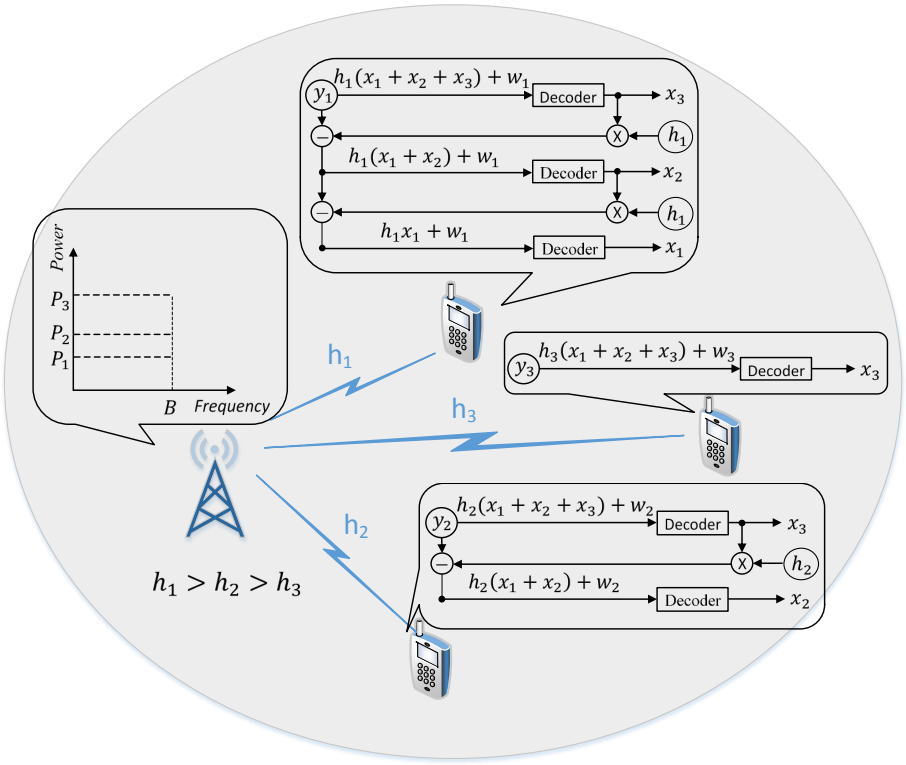

Figure 1.1: Illustration of a 3-user downlink NOMA transmission with SIC at user ends.

UE_1 and UE_2, but cannot cancel any of them. Therefore, the achievable throughput for UE_i in a 3-user downlink NOMA system can be expressed as:

$$\hat{R}_i = B \log_2 \left(1 + \frac{p_i \gamma_i}{\sum_{j=1}^{i-1} p_j \gamma_i + 1} \right), \quad \forall i = 1, 2, 3 \tag{1.3}$$

where B is the total transmission bandwidth for this NOMA system. The term $\gamma_i = \frac{h_i}{(I_i + N_i)B}$ denotes the normalized channel gain by inter-cell interference-plus-noise power for i-th user, where I_i and N_i are the inter-cell interference and receiver noise power density, respectively. To perform SIC, transmission power allocation to each

NOMA user needs to be designed properly. If p_1, p_2, and p_3 are the transmission powers for UE_1, UE_2, and UE_3, respectively, then the power allocation needs to adopt the following conditions for efficient SIC at UE_1 receiver:

$$p_3\gamma_1 - (p_1 + p_2)\gamma_1 \geq p_{tol}, \tag{1.4}$$

$$p_2\gamma_1 - p_1\gamma_1 \geq p_{tol}, \tag{1.5}$$

where $\sum_{i=1}^{3} p_i \leq p_t$, for downlink power budget of p_t for this 3-user NOMA system. The term p_{tol} denotes the minimum power difference needed to distinguish between the signal to be decoded and the remaining non-decoded message signals. (1.4) and (1.5) represent the power allocation conditions to cancel interference of UE_3 and UE_2, respectively, at UE_1 receiver. From (1.4) and (1.5), it is evident that the transmit power of any user must be the greater than sum transmit power of all users with relatively higher channel gains. That is, the transmit power of UE_3 needs to be greater than the sum transmit power of UE_1 and UE_2; while, the transmit power of UE_2 needs to be greater the transmit power of UE_1. Subsequently, the power allocation condition to cancel the interference of UE_3 at UE_2 receiver can be given as:

$$p_3\gamma_2 - (p_1 + p_2)\gamma_2 \geq p_{tol}. \tag{1.6}$$

Note that, since $\gamma_1 > \gamma_2$, (3.10) is automatically satisfied if (1.6) holds. Therefore, the necessary power constraints for efficient SIC in a 3-user downlink NOMA system can be given by (1.5) and (1.6).

Based on the above illustration, the necessary power constraints for efficient SIC

in an m-user downlink NOMA system can be expressed as follows:

$$p_i\gamma_{i-1} - \sum_{j=1}^{i-1} p_j\gamma_{i-1} \geq p_{tol}, \quad \forall i = 2, 3, \cdots, m. \tag{1.7}$$

1.1.2 NOMA in Uplink Transmission Scenarios

The working principle of uplink NOMA is quite different from the downlink NOMA. In uplink NOMA, multiple transmitters of different UEs non-orthogonally transmit to a single receiver at BS over same spectrum resources. Each UE independently transmits its own signal at either maximum transmit power or controlled transmit power depending on the channel gain differences among the NOMA users. All received signals at the BS are the desired signals, though they make interference to each other. Since the transmitters are different, each received signal at SIC receiver (BS) experiences distinct channel gain. Note that, to apply SIC and decode signals at BS, we need to maintain the distinctness among various message signals. As such, conventional transmit power control (typically intended to equalize the received signal powers of all users) is not feasible in NOMA-based systems.

Let us consider a general m-user uplink NOMA system in which m users transmit to a common BS over the same resources, at either maximum transmit power or controlled transmit power. The BS receives the superposed message signal of m different users and applies SIC to decode each signal. Since the received signal from the highest channel gain user is likely the strongest at the BS; therefore, this signal is decoded first. Consequently, the highest channel gain user experiences interference from all other users in the NOMA cluster. After that, the signal for second highest channel gain user is decoded and so on. As a result, in uplink NOMA, the achievable data rate of a user contains the interference from all users with relatively weaker

channels. That is, the highest channel gain user experiences interference from all users and the lowest channel gain user enjoys interference-free data rate.

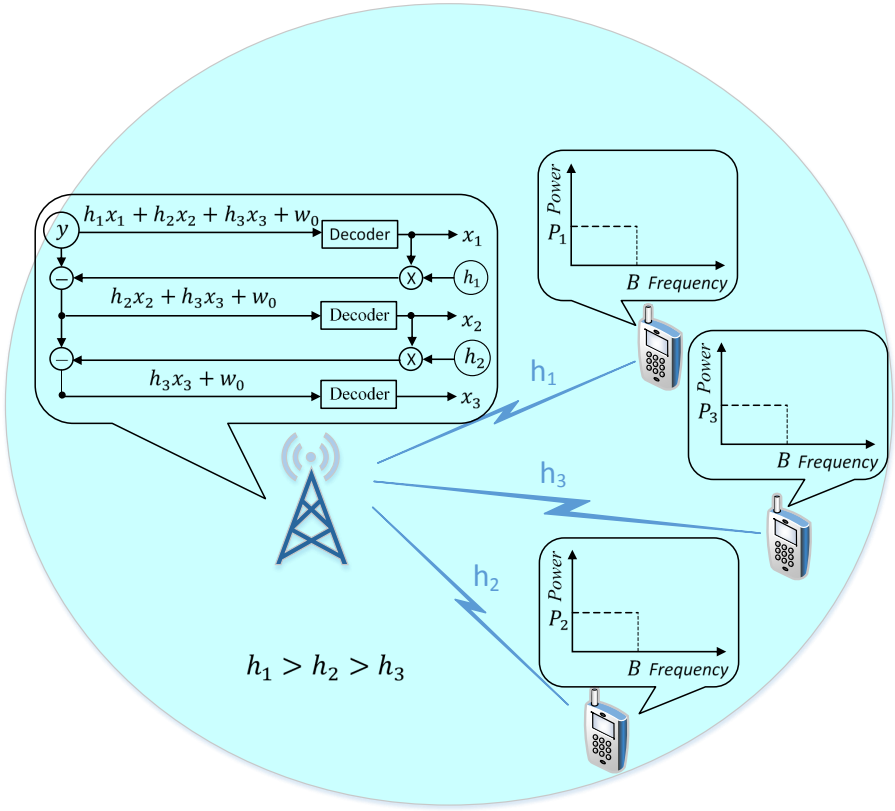

Figure 1.2: Illustration of a 3-user uplink NOMA system with SIC at BS end.

Illustration: Fig. 1.2 illustrates a 3-user uplink NOMA system in which UE_1, UE_2, and UE_3 experience complex channel gains h_1, h_2, and h_3, respectively, and $h_1 > h_2 > h_3$. As similar to downlink NOMA, it is assumed that x_1, x_2, and x_3 are the uplink signal for UE_1, UE_2, and UE_3, respectively, where $x_i = \sqrt{p_i}s_i$ and $E[|s_i|^2] = 1$. If each transmitter transmits their uplink message with the power level in such a way that the uplink signal of highest channel gain user is decoded first while other users' signals are sequentially decoded according to their channel gains at BS

receiver end, then the achievable throughput of UE_1 contains the interference from UE_2 and UE_3; whereas, UE_3 achieves interference free data rate. The throughput of UE_2 contains the interference from UE_3. Now, if p_i be the transmit power for i-th user, then the achievable throughput for UE_i in a 3-user uplink NOMA system can be expressed as:

$$\hat{R}_i = B \log_2 \left(1 + \frac{p_i \gamma_i}{\sum_{j=i+1}^{3} p_j \gamma_j + 1} \right), \quad \forall i = 1, 2, 3 \tag{1.8}$$

where B is the uplink bandwidth for this NOMA system. The term $\gamma_i = \frac{h_i}{(I_0+N_0)B}$ denotes the normalized channel gain by inter-cell interference-plus-noise power for i-th user measured at BS receiver end, where I_0 and N_0 are the inter-cell interference and receiver noise power density, respectively. However, to decode individual user's signal at BS receiver end with SIC processing, following conditions need to be satisfied, i.e.,

$$p_1 \gamma_1 - p_2 \gamma_2 - p_3 \gamma_3 \geq p_{tol} \tag{1.9}$$

$$p_2 \gamma_2 - p_3 \gamma_3 \geq p_{tol} \tag{1.10}$$

where $p_i \leq p'_t, \quad \forall i = 1, 2, 3$, for p'_t of the maximum transmit power budget of each UE end. (1.9) and (1.10) represent the necessary conditions for efficient decoding of UE_1 and UE_2 signals, respectively, prior to decoding the signal of UE_3.

Given the above illustration, the necessary power constraints for efficient SIC decoding in an m-user uplink NOMA cluster can be expressed as follows:

$$p_i \gamma_i - \sum_{j=i+1}^{m} p_j \gamma_j \geq p_{tol}, \quad \forall i = 1, 2, \cdots, (m-1) \tag{1.11}$$

1.2 Basic Principle of MIMO

Multiple-input multiple-output (MIMO) communications with multi-user beamforming is a potential technology for achieving significant gains in the overall system throughput. In downlink multiuser MIMO, each user is served by one or multiple beams depending on the number of BS transmit antennas and total number of receive antennas at the user ends in the cell. The inter-beam interference can be completely eliminated when the number of transmit antennas is more than or equal to the number of receive antennas, under the uncorrelated radio channels [6]. In such a conventional multiuser MIMO system, each user-end-receiver is supported by individual beamforming vector which is orthogonal to the other receivers' channel gains.

In a downlink multiuser MIMO-NOMA system, multiple receive antennas of different user equipments (UEs) with distinct channel gains are grouped into MIMO-NOMA clusters. All the users/receive-antennas in each cluster are scheduled on NOMA basis.

1.3 Basic Principle of CoMP

The fundamental principle of CoMP utilizes multiple transmit/receive antennas from multiple antenna site locations, which may or may not belong to the same physical cell, to enhance the received signal quality and effective coverage area by exploiting the co-channel interferences [7] [8]. CoMP mainly has been targeted to improve cell-edge users experience, but regardless the location it improves throughput performance to the users those experience strong signals of different BSs/cells. CoMP mainly categorized as inter-site CoMP and intra-site CoMP. In inter-site CoMP, the coordination is performed between BSs located at separated geographical areas. On

the other hand, intra-site CoMP enables the coordination between sectors of the same BS, where the coordination is performed through multiple antenna units that allow the coordination between the sectors.

In the CoMP-NOMA framework, CoMP transmission is used for users experiencing strong receive-signals from multiple cells while each cell adopts NOMA for resource allocation to its active users.

1.4 Motivation

As a potential multiple access technique for 5G mobile communication systems, NOMA is being received tremendous interests from communication research society. NOMA demonstrates a significant enhancement of spectral efficiency gain without requiring any additional infrastructure/resources. Although inter-user interference is the main obstacle for NOMA, efficient user clustering and power allocation can minimize inter-user interference and can provide high spectral efficiency performance. However, except this dissertation and subsequent publications, most of the research investigations on NOMA have been conducted by considering two users in the system with fixed power allocation strategies. Therefore, the necessity for the optimal user clustering and power allocation of NOMA systems toward the upcoming 5G standard is the key motivation of this thesis.

On the other hand, by using multiple antennas at the transmitter and receiver ends, MIMO technique can potentially multiply the spectral efficiency gain in proportion to the spatial multiplexing order. The inter-user interference in MIMO can be completely eliminated when the number of total receive antennas is equal to or less than the total transmit antennas in a cell. However, in MIMO-NOMA, the number of receive antennas is more than the number of transmit antennas, thus the resultant

interference for each user is very high. Therefore, another motivation is to develop a "robust" multiuser MIMO-NOMA system for downlink transmission which can minimize the net interference, and thus maximize the system capacity.

In addition, the coordinated multi-point (CoMP) technology for downlink transmission is a promising approach to enhance the quality of user experience (QoE) for interference-prone users, particularly for cell-edge users, by exploiting the co-channel inter-cell interferences. In downlink NOMA, a cell-edge user usually gets low signal-to-inter-user-interference-plus-noise ratio (SINR). Therefore, in co-channel multi-cell downlink NOMA, the use of CoMP is crucial to enhance QoE for cell-edge users, which is the main motivation to investigate the application of CoMP in downlink NOMA system in this thesis.

1.5 Related Work

Recently, numerous research activities have been initiated across the globe to identify the potential application of NOMA in upcoming 5G systems. Here I review the most recent and relevant research studies on NOMA in conventional downlink and uplink systems, downlink multiuser MIMO systems, and downlink multi-cell CoMP systems, in the following separate subsections.

1.5.1 NOMA in Conventional Downlink and Uplink Systems

The basic concept of NOMA was initially exploited in [1] [2] [3] [4] for downlink transmissions. The authors in [1] proposed power domain user multiplexing at the BSs and SIC-based signal reception at UE terminals. Various practical challenges of NOMA systems, such as multiuser power allocation and user scheduling schemes, error propagation in SIC, overall system overhead, user mobility, and the combination of

NOMA with Multiple-Input Multiple-Output (MIMO), was discussed in [2]. System-level and link-level simulations in [3] indicated clear benefits of NOMA over OMA in terms of overall system throughput as well as individual user's throughput. A test-bed for two-user NOMA system was presented in [4]. The experiments were performed by setting 5.4 MHz bandwidth for NOMA users. The results were compared to two OMA users each having the transmission bandwidth of 2.7 MHz [4].

Closed-form expressions for ergodic sum-rate and outage probability were presented for two users in [9] considering static power allocation. The impact of user pairing was studied in [10] for a two-user NOMA system. The authors proposed fixed and opportunistic user pairing schemes by statically allocating transmission powers among NOMA users. On the other hand, the impact of power allocation on the fairness of the downlink NOMA was investigated in [11], considering perfect channel state information (CSI) feedback as well as average CSI feedback. In [12], a cooperative NOMA system was studied, where the authors advocated the idea of pairing weak channel users with the strong channel users for cooperative data transmission.

On the other hand, for uplink transmissions, NOMA was first investigated in [13] where power control was applied at UE transmitter and minimum mean squared error (MMSE)-based SIC decoding was utilized at BS receiver. A joint subcarrier and power allocation problem was studied in [14]. Specifically, a sub-optimal solution was designed to maximize the sum-rate of a NOMA cluster. Closed-form expressions for sum-throughput and outage probability were derived for a two-user uplink NOMA system in [15] assuming static powers of different users. The authors in [15] also compared their results with TDMA-based OMA system and concluded that without proper selection of target data rate for each NOMA user, a user can always be in outage. This conclusion was also mentioned in [9] for downlink NOMA. Apart from

these, a robust user scheduling algorithm for uplink NOMA with SC-FDMA was designed in [16], where the distinct channel gains of different users were exploited to obtain efficient user grouping.

1.5.2 NOMA in Downlink MIMO Systems

Recently, application of NOMA in multiuser MIMO systems has drawn a significant attention of the researchers. The fundamentals of the combination of NOMA and MIMO in downlink transmission was studied in [2], where a random beamforming was considered for a 2-user MIMO-NOMA cluster of single antenna UEs, and 2 transmit antennas was assumed at the BS end. The authors in [2] utilized fixed power allocation strategies at the transmitter end, while a two-step interference cancellation method was considered at the UE receiver ends. In the first step, they used interference rejection combining (IRC) technique to suppress inter-beam/inter-cluster interference, while in the second step they used SIC for intra-beam/intra-cluster interference cancellation.

In [17], multiuser ZF-BF for downlink MIMO-NOMA was studied where each cluster contains only two single-antenna UEs (i.e., a 2-user MIMO-NOMA system). The authors in [17] utilized conventional MIMO-NOMA model in which ZF-BF was done by taking channel information of cluster-heads. The users are grouped into a cluster based on their channel gain correlations and differences with the channel gain of cluster-head. The authors also provided a user clustering algorithm which considers both of the channel correlation and gain differences among the users. The MIMO-NOMA system in [17] was only evaluated at highly correlated user cluster scenarios, but in practice, the radio channels for different UEs can be uncorrelated.

Another important study on downlink MIMO-NOMA can be found in [5], where

random beamforming was performed at the BS and each beam is utilized by all the users of a cluster. The authors in [5] utilized spatial filtering to suppress the inter-cluster/inter-beam interference. The system level simulations in [5] were performed by considering only 2 transmit antennas at the BS end, while up-to 4-user MIMO-NOMA cluster with fixed power allocation strategies were evaluated. In addition, similar power allocation was assumed for each beam in [5]. The authors in [18] utilized the same system and signal model of [5] and proposed coordinated frequency block-dependent inter-beam power allocation to have distinct power levels for different beams. Moreover, random beamforming-based downlink MIMO-NOMA was also studied in [19] where the UE receivers use the minimum mean squired error (MMSE) technique to eliminate inter-beam interference.

A study on downlink MIMO-NOMA was also presented in [20], where the outage probability of the users of a MIMO-NOMA cluster was evaluated. The number of receive antennas at each UE end was considered to be equal to or more than the number of transmit antennas at the BS end. The authors simulated their model by considering up to 3 antennas at the UE ends and the BS end, while up to 3 UEs with fixed power allocation strategies were considered in each MIMO-NOMA cluster. In [20], new precoding and decoding matrices were also proposed and it was claimed to obtain the ZF-BF characteristics. Another power allocation solution for a 2-user downlink MIMO-NOMA cluster was studied in [21] where equal number of antennas are assumed at BS and each UE. A non-convex power allocation problem for 2-user MIMO-NOMA was formulated in [21] and both optimal and sub-optimal solutions were proposed.

1.5.3 NOMA in Downlink CoMP Systems

Recently, some studies have investigated on combining CoMP with NOMA in downlink transmission scenarios. The author in [22] utilized Alamouti code for joint transmission to a cell-edge user in a two-cell CoMP set. In that work, 2-user NOMA was used in both the cells where the non-CoMP user is the cell-center user. Another work on downlink CoMP-NOMA was found in [23], where an opportunistic CoMP-NOMA system was used for a group of cell-edge users which receive strong signals from all the coordinating cells. In that work, a joint multi-cell power allocation strategy was used based on the CoMP users' channel gains. The joint multi-cell power allocation strategy was used in [23], depending on the the CoMP users equivalent channel gain determined by their channel vector at CoMP set.

Considering multiple antennas at transmitter and receiver ends, a downlink CoMP-NOMA system was studied considering a single CoMP-user[2] in [24]. Moreover, a downlink multi-cell NOMA application can be found in [25] where the authors considered only one user who receives CoMP transmission is grouped with one user who receives single non-CoMP transmission at each NOMA cluster among the coordinating cells.

1.6 Contributions and Novelty of the Thesis

1.6.1 Contributions

The specific contributions of this thesis can be classified into three main categories as follows: (i) NOMA in conventional downlink and uplink communications, (ii) NOMA in MIMO scenarios, and (iii) NOMA in CoMP scenarios.

[2]In this thesis, the users those get CoMP transmission are denoted as CoMP-user while the other users are denoted as non-CoMP-user under the CoMP-NOMA systems.

For NOMA in conventional downlink and uplink communications, the contribution are as follows:

- The working principle of downlink and uplink NOMA by identifying the key power allocation requirements are provided in this thesis. In particular, the differences in the working principle of uplink and downlink NOMA is clearly identified.

- For both downlink and uplink NOMA, the cell-throughput maximization problem is formulated such that the joint user clustering and power allocation in NOMA cluster(s) can be optimized under user clustering constraints, transmission power constraints, minimum rate requirements of the users constraints, and SIC processing constraints. The formulated optimization is a mixed-integer non-linear programing (MINLP) problem.

- For both of downlink and uplink NOMA, a low-complexity sub-optimal user clustering scheme is proposed by exploiting the channel gain differences among users in a NOMA cluster in the target of sum throughput maximization.

- For a given set of NOMA clusters, optimal power allocation solution is obtained that maximizes the sum throughput of all users in a cluster and in turn maximizes the overall system throughput. Using KKT optimality conditions, for both downlink and uplink NOMA, closed-form optimal power allocation solutions are obtained for any cluster size.

- A robust performances evaluation is carried out for both of downlink and uplink NOMA systems using the proposed user clustering and power allocation solutions. The guidelines are extracted related to the key design factors of NOMA systems.

For downlink multiuser MIMO-NOMA systems, the contributions can be summarized as follows:

- A novel system and signal model for downlink multiuser MIMO-NOMA is proposed which is applicable to any MIMO-NOMA scenario in downlink transmission.
- A new multi-cluster zero-forcing beamforming (ZF-BF) technique is proposed in which the precoding is performed by considering the equivalent channel gain of each MIMO-NOMA cluster, instead of that of any particular user.
- A low-complexity user clustering scheme is also proposed. The user clustering is performed with an objective to maximizing the sum-spectral efficiency in a cell by exploiting the NOMA and MIMO principles.
- A dynamic power allocation solution for downlink multiuser MIMO-NOMA is also proposed. The proposed power allocation is done in two steps: suboptimal inter-cluster power allocation and optimal intra-cluster power allocation.
- A comprehensive performance evaluation of the proposed MIMO-NOMA model is carried out, and the insights are discussed for a wide rage MIMO-NOMA applications.

Regarding the use of CoMP transmission in downlink multi-cell NOMA systems, the major contributions are summarized as follows:

- A novel model for the application of CoMP in downlink multi-cell NOMA is proposed, where multiple CoMP-users from a set of coordinating cells are utilized NOMA at each of the coordinating cells, by grouping NOMA cluster with non-CoMP-users.

- The proposed model analyzes the application of CoMP-NOMA under various CoMP schemes and various network deployment scenarios.
- At each CoMP schemes and network deployment scenarios, the necessary conditions those are needed to satisfy for CoMP-NOMA application are also derived.
- The numerical result of the proposed model is evaluated and compared with those for CoMP-OMA systems.

1.6.2 Novelty

The novelty of this thesis are as follows:

- A convex form of the throughput formula for downlink and uplink NOMA systems is formulated in this thesis. Subsequently, the closed-form solution of NOMA for downlink and uplink systems is derived. To date, this is the only solution of the optimal power allocation for NOMA systems in closed-form.
- A new multi-cluster zero-forcing beamforming (ZF-BF) technique is proposed in which the precoding is performed by considering the equivalent channel gain of each MIMO-NOMA cluster, instead of that of any particular user. Each user in a MIMO-NOMA cluster cancels the inter-cluster interference by estimating its own *cluster's equivalent channel gain*. To estimate the *cluster's equivalent channel gain*, a novel decoding scaling weight factor is introduced for each user.
- A concrete model is proposed for the application of CoMP in downlink multi-cell NOMA systems. To date, this is the only model which considers multiple CoMP-users those are utilized NOMA with the non-CoMP-users at each of the coordinating cells, simultaneously.

1.7 Organization of the Thesis

The rest of the thesis is organized into following four chapters:

- Chapter 2 presents the system model, assumptions and formulation of the joint optimization problem of user clustering and power allocation in conventional downlink and uplink NOMA systems. After that, a suboptimal user clustering algorithm and then the optimal power allocation closed-form solution for each cluster are derived. Numerical results of the proposed solution for user clustering and power allocation for conventional NOMA systems are also evaluated and discussed in chapter 2.

- In Chapter 3, the application of NOMA in MIMO system is analyzed for downlink transmission. The system model, signal model, user clustering algorithm, beamforming technique and power allocation solution of downlink MIMO-NOMA also presented in chapter 3. At the end of the chapter, a robust simulation results is presented for the proposed MIMO-NOMA model.

- Chapter 4 presents the system models, assumptions, signal models and numerical results for the application of CoMP in downlink multi-cell NOMA systems under various network deployment scenarios.

- Chapter 5 concludes the thesis by summarizing the work done and suggesting possible extensions of the work presented in this thesis.

Chapter 2

NOMA in Conventional Downlink and Uplink Cellular Systems

In this chapter, I provide the optimal power allocation solution for downlink and uplink NOMA which maximizes the cell sum-throughput performance. However, the requirement of power allocation among NOMA users at transmitter end(s) and the use of SIC application at receiver end(s) potentially bound the number of users scheduling in a NOMA system. Therefore, I propose cluster-based NOMA application in which users in a cell are grouped into a number of clusters and each cluster utilizes NOMA application. Toward that, this chapter is organized as follows: Section 2.1 presents the system model, assumptions, and the joint problem formulation for optimal user clustering and power allocation in both of downlink and uplink NOMA systems. Section 2.2 and Section 2.3, respectively, discuss the proposed sub-optimal user clustering solution and the optimal power allocation solutions for downlink and uplink NOMA systems. Section 2.4 evaluates the performance of the proposed solutions numerically. A summary of the chapter is provided in Section 2.5.

2.1 Joint User Clustering and Power Allocation

In general, NOMA enhances sum-spectral efficiency by offering all the users to share the same spectrum resources. Thus, it is appeared that the NOMA system with more users may provide higher spectral efficiency. However, the requirements of the received power differences among the NOMA users at each receiver end to perform SIC application may bound the maximum number of users that could be served in a NOMA system. In case of downlink throughput maximization, an important conclusion about the maximum transmit power of the highest channel gain user in a NOMA cluster can be obtained as follows:

Lemma 2.1.1 (Maximum Transmit Power for the Highest Channel Gain User in a Downlink NOMA Cluster)**.** *To maximize the sum-throughput, the maximum transmission power allocation to the highest channel gain user in the downlink NOMA cluster must be smaller than* $\frac{P_t}{2^{m-1}}$*, where* m *is the number of users in the cluster and* P_t *is the total transmission power budget for the given NOMA cluster.*

Proof. The proof follows by induction. Let us consider a 2-user downlink NOMA cluster where γ_1 and γ_2 are the normalized channel gains of the high and low channel gain users, respectively. As per the SIC constraints in (1.5), we have

$$P_2\gamma_1 - P_1\gamma_1 \geq P_{tol}, \quad \text{and} \quad P_1 + P_2 \leq P_t,$$

where P_1 and P_2 are the allocated powers for high and low channel users, respectively. The maximum allocated power to the highest channel gain user can thus be derived as

$$P_{1(max)} \leq \frac{P_t - \delta}{2},$$

where $\delta = \frac{P_{tol}}{\gamma_1}$ is the minimum power difference needed for SIC. δ can be sufficiently small as the value of γ_1 is high. Similarly, for 3-user downlink NOMA cluster, the maximum allocated transmit powers for second higher and highest channel gain user can be expressed, respectively, as:

$$P_{2(max)} \leq \frac{P_t - \delta}{2},$$
$$P_{1(max)} \leq \frac{P_t - \delta}{2^2} - \frac{\delta}{2}.$$

Consequently, for an m-user cluster, we have

$$P_{1(max)} \leq \frac{P_t - \delta}{2^{m-1}} - \frac{\delta}{2^{m-2}} - \cdots - -\frac{\delta}{2} \approx \frac{P_t}{2^{m-1}}.$$

This is the same result as given in **Lemma 2.1.1**. □

Lemma 2.1.1 indicates that for a large number of users the highest channel gain users may will not get sufficient transmit power to satisfy her required SINR, and thus the the clustering based NOMA application is adopted in this chapter.

2.1.1 System Model and Assumptions

Let us consider a macro base station (BS) serving N uniformly distributed user equipments (UEs) in downlink transmission and N uniformly distributed user equipments (UEs) in uplink transmission. The BS and UEs have single antenna configuration. The available system bandwidth B_T is divided into frequency resource blocks, each of bandwidth B. That is, the total number of frequency resource blocks are given as $\Omega = B_T/B$. Users those are non-orthogonally scheduled over the same resource blocks form a NOMA cluster. However, multiple NOMA clusters are operated on orthogonal

frequency resource blocks. The number of users per NOMA cluster is represented by m which ranges from $2 \leq m \leq N$. Also, the resource blocks allocated per cluster are represented by ω, where $1 \leq \omega \leq \Omega$. Provided the range of m, the number of clusters can vary between 1 and $N/2$. The maximum BS transmission power budget is p_T, the maximum transmission power budget per downlink NOMA cluster is p_t, and the maximum uplink transmit power at each UE end is P_t'. The normalized channel gain between i-th UE and the BS is represented by γ_i which accounts for both distance-based path-loss, fading and shadowing. The users are sorted according to the descending order of their channel gains as $\gamma_1 > \gamma_2 > \gamma_3 > \cdots > \gamma_N$.

Now, let us define a variable $\beta_{i,j}$ as:

$$\beta_{i,j} = \begin{cases} 1, & \text{if a user } i \text{ is grouped into cluster } j \\ 0, & \text{otherwise} \end{cases} \tag{2.1}$$

where $j = 1, 2, , \cdots, N/2$ and $i = 1, 2, \cdots, N$.

2.1.2 Joint Optimization Problem Formulation for Downlink NOMA

The joint user clustering (i.e., grouping of users into clusters) and power allocation problem for the throughput maximization in downlink NOMA can be formulated as:

$$\underset{\omega,\ \boldsymbol{\beta},\boldsymbol{P}}{\text{maximize}} \sum_{j=1}^{N/2}\sum_{i=1}^{N} \omega_j \beta_{i,j} \log_2\left(1+\frac{p_i\gamma_i}{\sum\limits_{k=1}^{i-1}\beta_{k,j}p_k\gamma_i+\omega_j}\right)$$

subject to:

$$\mathbf{C_1}: \sum_{j=1}^{N/2}\sum_{i=1}^{N}\beta_{i,j}p_i \le p_T$$

$$\mathbf{C_2}: \sum_{j=1}^{N/2}\omega_j\beta_{i,j}\log_2\left(1+\frac{p_i\gamma_i}{\sum\limits_{k=1}^{i-1}\beta_{k,j}p_k\gamma_i+\omega_j}\right) > R_i, \quad \forall i$$

$$\mathbf{C_3}: \left(\beta_{i,j}p_i - \sum_{k=1}^{i-1}\beta_{k,j}p_k\right)\gamma_{i-1} \ge p_{tol}, \quad \forall i$$

$$\mathbf{C_4}: \left(\sum_{j=1}^{N/2}\beta_{i,j}=1, \sum_{i=1}^{N}\beta_{i,j}\le N\right) \text{OR} \left(\sum_{i=1}^{N}\beta_{i,j}=0, \quad \forall j\right)\Bigg)$$

$$\mathbf{C_5}: \sum_{j=1}^{N/2}\beta_{i,j}\omega_j \le \Omega, \quad \forall i$$

$$\mathbf{C_6}: \omega_j \in \{1,2,\cdots,\Omega\}, \quad \forall j$$

$$\mathbf{C_7}: \beta_{i,j} \in \{0,1\}, \quad \forall i,j$$

where R_i is the minimum data rate requirement for i-th user, and p_{tol} is the minimum received power difference required to decode a signal from the non-decoded signals at SIC process. The **Constraint $\mathbf{C_1}$** denotes the total power constraint of the BS, **Constraint $\mathbf{C_2}$** ensures the minimum downlink data rate requirements of the users, **Constraint $\mathbf{C_3}$** are the SIC constraints as discussed in Chapter 1, **Constraint $\mathbf{C_4}$** ensures that one user can be assigned to at most one cluster, while at least two

users are grouped into each downlink NOMA cluster, **Constraint $\mathbf{C_5}$** provides the total downlink frequency resource constraint. In addition, **Constraint $\mathbf{C_6}$** and **$\mathbf{C_7}$** demonstrate that ω and β are integer variables.

2.1.3 Joint Optimization Problem Formulation for Uplink NOMA

Similarly, the joint user clustering and power allocation problem for the throughput maximization of uplink NOMA system can be formulated as follows:

$$\underset{\omega,\ \boldsymbol{\beta},\boldsymbol{P}}{\text{maximize}} \sum_{j=1}^{N/2}\sum_{i=1}^{N} \omega_j \beta_{i,j} \log_2\left(1+\frac{p_i\gamma_i}{\sum\limits_{k=i+1}^{N}\beta_{k,j}p_k\gamma_k+\omega_j}\right)$$

subject to:

$$\mathbf{C'_1}: \sum_{j=1}^{N/2}\beta_{i,j}p_i \le P'_t, \quad \forall i$$

$$\mathbf{C'_2}: \sum_{j=1}^{N/2}\omega_j\beta_{i,j}\log_2\left(1+\frac{p_i\gamma_i}{\sum\limits_{k=i+1}^{N}\beta_{k,j}p_k\gamma_k+\omega_j}\right) > R'_i, \quad \forall i$$

$$\mathbf{C'_3}: p_i\gamma_i\beta_{i,j} - \sum_{k=i+1}^{N}\beta_{k,j}p_k\gamma_k \ge p_{tol}, \quad \forall i$$

$$\mathbf{C'_4}: \left(\sum_{j=1}^{N/2}\beta_{i,j}=1, \quad \forall i\right)\text{AND}\left(\left(2\le\sum_{i=1}^{N}\beta_{i,j}\le N\right)\text{OR}\left(\sum_{i=1}^{N}\beta_{i,j}=0, \quad \forall j\right)\right)$$

$$\mathbf{C'_5}: \sum_{j=1}^{N/2}\beta_{i,j}\omega_j \le \Omega, \quad \forall i$$

$$\mathbf{C'_6}: \omega_j \in \{1,2,\cdots,\Omega\}, \quad \forall j$$

$$\mathbf{C'_7}: \beta_{i,j} \in \{0,1\}, \quad \forall i,j$$

where R'_i is the minimum uplink data rate requirement for i-th user, and p_{tol} is similarly defined as downlink case. **Constraint $\mathbf{C'_1}$** ensures the minimum rate re-

quirements of the users, **Constraint $\mathbf{C'_2}$** ensures the minimum uplink data rate requirements of the users, **Constraint $\mathbf{C'_3}$** ensures the SIC constraint as discussed in Chaper 1, and **Constraints $\mathbf{C'_4 - C'_7}$** are same as defined in Section 2.1.1.

2.1.4 Solution Methodology

As can be seen, the formulated problems are mixed integer non-linear programming (MINLP) problems whose solution is combinatorial by nature. Specifically, for throughput maximization, the optimal user clustering solution requires an exhaustive search to form a NOMA cluster [16]. That is, for every single user, we need to consider all possible combinations of user grouping. For example, let us consider an uplink/downlink NOMA system with N users. In such a system, the number of possible combinations for optimal user clustering, can be expressed as follows:

$$\Phi = \sum_{i=2}^{N} \binom{N}{i}.$$

Evidently, the computational complexity of optimal user clustering may not be suitable for practical systems with a large number of active users. As such, I resort to solve the problem in two steps, i.e., by developing a less complex solution for grouping users into different NOMA clusters and then optimizing their respective powers to maximize the sum throughput per cluster. Subsequently, Section 2.2 details the proposed low-complexity user clustering scheme. Given the user clustering, we derive optimal power allocation for users in Section 2.3.

2.2 User Clustering in NOMA

Low complex user clustering policy is one of the key design factor for efficient NOMA systems. In this section, I propose a less complex sub-optimal user clustering scheme for both downlink and uplink NOMA systems, in the target of sum-throughput maximization. The proposed scheme exploits the channel gain differences among users and aims to enhance the sum throughput of the considered cell. Prior to user grouping, this scheme relies on selecting a feasible number of clusters, i.e., decides the number of clusters and in turn the number of users per cluster. Once the number of users in a cluster is decided, user grouping is performed. In the following subsections, the key concepts of the proposed user paring policies and their algorithmic presentation are detailed.

2.2.1 Key Issues for User Clustering in Downlink NOMA

Let us consider an m-user downlink NOMA cluster to which B is the allocated spectrum resources. For such a system, the achievable per-user throughput in (1.3), where $i = 1, 2, 3, \cdots, m$, provides necessary insights to group users into a cluster. These insights are discussed below:

- In a NOMA cluster, only the cluster-head[1] can enjoy intra-cluster interference-free throughput while others get inter-user interference according to the ordering policy. After SIC, the throughput of the cluster-head is only depends on its own channel gain and the amount of allocated transmit power; it is noted that the inter-cell interference is not considered here. Although the allocated transmit power for the cluster-head is low (Lemma 2.1.1), the impact of this low power

[1]NOMA user who can cancel all the intra-cluster interference.

allocation on the sum-throughput is minimal. The reason is that the total transmission power is limited and generally measured in dBm, whereas the channel gain for cluster-head is usually high and measured in dB. Subsequently, if the channel gain of the cluster-head is sufficiently high, then the achievable data rate negligibly depends on the transmission power, unless the power becomes too low. Thus to maximize the sum-throughput in downlink NOMA transmission, the number of NOMA cluster should be determined upon the number of most higher channel gain users, and all the higher channel gain users need to be distributed into different NOMA clusters as cluster-head.

- The throughput of the remaining users in a NOMA cluster follows the same format. That is, the SINR contains same channel in both the denominator and numerator; whereas, the transmit power in numerator is greater than the sum power of denominator (this is given by the SIC constraint). As such, the throughput of the remaining users in a NOMA cluster depends mainly on the distribution of the transmit power levels.

- To increase the throughput of the lowest channel gain users in a downlink NOMA cluster, it is important to pair them with the high channel gain users. The reason is that the high channel gain users can achieve a high rate even with the low power levels while making the large fraction of power available for low channel gain users. As such, the key point of our proposed user clustering in downlink NOMA is to pair the highest channel gain user and the lowest channel gain user into same NOMA cluster, while second higher channel gain user and second lower channel gain user into another NOMA cluster, and so on.

2.2.2 Key Issues for User Clustering in Uplink NOMA

Let again consider an m-user uplink NOMA cluster to which B is the allocated spectrum resources. For such a system, the achievable per-user throughput in (1.8), where $i = 1, 2, 3, \cdots, m$, provides necessary insights to group users. These insights are discussed below:

- In an uplink NOMA cluster, all users' signals experience distinct channel gains. To perform SIC at BS, we need to maintain the distinctness of received signals. As such, the conventional transmit power control may not be feasible in a NOMA cluster. In addition, contrary to downlink NOMA, the power control at any user doesn't increase the power budget for any other user in a cluster. As such, the ultimate result of power control is sum-throughput degradation.

- In uplink NOMA, the distinctness among the channels of different users within a NOMA cluster is crucial to minimize inter-user interference and thus to maximize the cluster throughput. Therefore, the number of NOMA cluster should be determined upon the channel gain distinctness among the uplink users, while each uplink NOMA contains users with maximum channel gain distinctness by ensuring the least lower channel gain users as cluster-head.

- In uplink NOMA, the highest channel gain user does not interfere to weak channel users (actually his interference is canceled by SIC). Therefore, this user can transmit with maximum power to achieve a higher throughput. It is thus beneficial to include the high channel gain users transmitting with maximum powers in each NOMA cluster, as they can significantly contribute to the throughput of a cluster.

2.2.3 Algorithm for User Clustering

Based on the above discussions, let us classify the users into two classes: Class$-A$ and Class$-B$. The number of users in Class$-A$, denoted as α, have much higher channel gains compared to users in Class$-B$, i.e.,

$$\gamma_1, \gamma_2, \cdots, \gamma_\alpha \gg \gamma_{\alpha+1}, \gamma_{\alpha+2}, \cdots, \gamma_N$$

Then, the proposed sub-optimal user clustering algorithm can be given as in **Algorithm** 2.2.31.

Algorithm 2.2.3.1**: User Clustering in Downlink and Uplink NOMA**

---

1. **Sort users:** $\gamma_1 \geq \gamma_2 \geq \cdots \geq \gamma_\alpha \gg \gamma_{\alpha+1} \geq \gamma_{\alpha+2} \geq \cdots \geq \gamma_N$.

2. **Select cluster:** if $\alpha < \frac{N}{2}$, then number of cluster $\kappa = \alpha$
   else if $\alpha \geq \frac{N}{2}$ then number of cluster $\kappa = \frac{N}{2}$.

3. **(a) Group users in Downlink:** 1st cluster $= \{\gamma_1, \gamma_{\kappa+1}, \gamma_{2\kappa+1}, \cdots, \gamma_N\}$, 2nd cluster $= \{\gamma_2, \gamma_{\kappa+2}, \gamma_{2\kappa+2}, \cdots, \gamma_{N-1}\}, \cdots,$ κ-th cluster $= \{\gamma_\kappa, \gamma_{2\kappa}, \gamma_{3\kappa}, \cdots, \gamma_{N-\kappa-1}\}$.

   (b) Group users in Uplink: 1st cluster $= \{\gamma_1, \gamma_{\kappa+1}, \gamma_{2\kappa+1}, \cdots, \gamma_{N-\kappa-1}\}$, 2nd cluster $= \{\gamma_2, \gamma_{\kappa+2}, \gamma_{2\kappa+2}, \cdots, \gamma_{N-\kappa-2}\}, \cdots,$ κ-th cluster $= \{\gamma_\kappa, \gamma_{2\kappa}, \gamma_{3\kappa}, \cdots, \gamma_N\}$.

4. **Cluster size:** if N **mod** $\kappa = 0$, then uniform cluster size
   else if N **mod** $\kappa \neq 0$ then different cluster size.

For further illustrations, we demonstrate user grouping in Fig. 2.1 and Fig. 2.2, for 2-user, 3-user, and 4-user NOMA clusters in downlink and uplink, respectively, where the total number of users are taken as 12 (twelve).

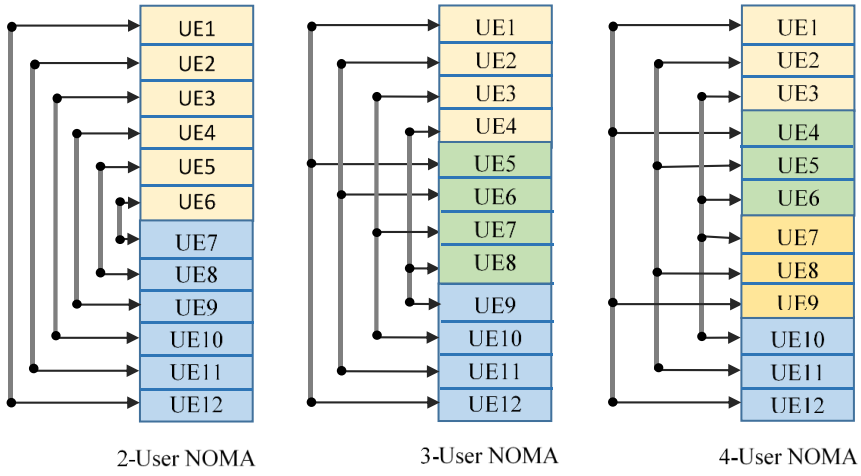

Figure 2.1: Illustration of 2-user, 3-user, and 4-user NOMA clustering for the downlink transmission of 12 active users in a cell.

2.3 Optimal power allocation in NOMA

Provided the NOMA clusters from Section 2.2, in this section, I derive optimal power allocation for a NOMA cluster with m users in the downlink and m users in uplink transmissions, where $2 \leq m \leq N$. Closed-form expressions for the optimal power allocation are derived using Karush-Kuhn-Tucker (KKT) optimality conditions.

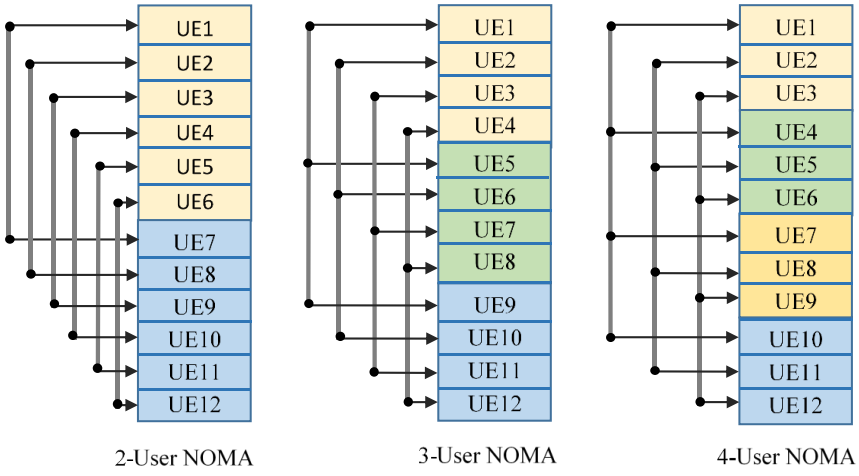

Figure 2.2: Illustration of 2-user, 3-user, and 4-user NOMA for uplink transmission of 12 active users in a cell.

2.3.1 Power Allocation Problem Formulation for Downlink NOMA

Let us consider an m-user downlink NOMA cluster, where the normalized channel gains of $UE_1, UE_2, \cdots, UE_m$ are assumed as $\gamma_1, \gamma_2, \cdots, \gamma_m$, respectively, and their respective minimum rate requirements are $R_1, R_2, \cdots, R_m$, where $R_i > 0$. It is assumed that ω units of resource blocks, each of bandwidth B, are allocated to the downlink NOMA cluster. If $p_1, p_2, \cdots, p_m$ are the transmission powers for $UE_1, UE_2, \cdots, UE_m$,

respectively, then the optimal power allocation problem can be given as:

$$\begin{aligned}
&\underset{P}{\text{maximize}} \quad \omega B \sum_{i=1}^{m} \log_2 \left(1 + \frac{p_i \gamma_i}{\sum\limits_{j=1}^{i-1} p_j \gamma_i + \omega}\right) \\
&\text{subject to:} \quad \mathbf{C_1}: \sum_{i=1}^{m} p_i \leq p_t, \\
&\qquad\qquad \mathbf{C_2}: \omega B \log_2 \left(1 + \frac{p_i \gamma_i}{\sum\limits_{j=1}^{i-1} p_j \gamma_i + \omega}\right) \geq R_i, \quad \forall i, \\
&\qquad\qquad \mathbf{C_3}: p_i \gamma_{i-1} - \sum_{j=1}^{i-1} p_j \gamma_{i-1} \geq p_{tol}, \quad \forall i = 2, 3, \cdots, m
\end{aligned}$$

where $\sum\limits_{j=1}^{i-1} p_j \gamma_i$ is the inter-user interference for i-th user in downlink NOMA cluster. **Constraint $\mathbf{C_1}$** is the total power constraint, **Constraint $\mathbf{C_2}$** is the minimum rate requirement per user, and **Constraint $\mathbf{C_3}$** denotes SIC constraints. Note that the aforementioned problem is convex under **Constraints $\mathbf{C_1} - \mathbf{C_3}$**.

2.3.2 *Closed-Form Optimal Power Solution for Downlink NOMA*

For the aforementioned problem, the Lagrangian can be expressed as:

$$\begin{aligned}
\mathcal{L}(P, \lambda, \mu, \psi) = \omega B \sum_{i=1}^{m} \log_2 \left(1 + \frac{p_i \gamma_i}{\sum\limits_{j=1}^{i-1} p_j \gamma_i + \omega}\right) + \lambda\Big(p_t - \sum_{i=1}^{m} p_i\Big) + \sum_{i=1}^{m} \mu_i \Big\{ p_i \gamma_i - \\
\Big(\sum_{k=1}^{i-1} p_k \gamma_i - \omega\Big) \times \Big(\varphi_i - 1\Big)\Big\} + \sum_{i=2}^{m} \psi_i \Big(p_i \gamma_{i-1} - \sum_{l=1}^{i} p_l \gamma_{i-1} - p_{tol}\Big) \quad (2.2)
\end{aligned}$$

where λ, μ_i, and ψ_j are the Lagrange multipliers, $\forall\, i = 1, 2, 3, \cdots, m$ and $\forall\, j = 2, 3, 4, \cdots, m$. Also, $\varphi_i = 2^{\frac{R_i}{\omega B}}$. Taking derivatives of (2.2) w.r.t. p_i, λ, μ_i, ψ_j, we can

write the KKT conditions as:

$$\frac{\partial \mathcal{L}}{\partial p_1^*} = \frac{\omega B \gamma_1}{p_1\gamma_1 + \omega} - \sum_{k=2}^{m} \frac{\omega B p_k \gamma_k^2}{\Big(\sum\limits_{l=1}^{k} p_l\gamma_k + \omega\Big)\Big(\sum\limits_{l'=1}^{k-1} p_{l'}\gamma_k + \omega\Big)} - \lambda + \mu_1\gamma_1 - \sum_{j=2}^{m}(\varphi_j - 1)\mu_j\gamma_j - \sum_{j=2}^{m}\psi_j\gamma_{j-1} \leq 0, \ \textbf{if } p_1^* \geq 0 \tag{2.3}$$

$$\frac{\partial \mathcal{L}}{\partial p_i^*} = \frac{\omega B \gamma_i}{\sum\limits_{j=1}^{i} p_j\gamma_i + \omega} - \sum_{k=i+1}^{m} \frac{\omega B p_k \gamma_k^2}{\Big(\sum\limits_{l=1}^{k} p_l\gamma_k + \omega\Big)\big(\sum\limits_{l'=1}^{k-1} p_{l'}\gamma_k + \omega\Big)} - \lambda + \mu_i\gamma_i - \sum_{k=i+1}^{m}(\varphi_k - 1)\mu_k\gamma_k + \psi_i\gamma_{i-1} - \sum_{j=i+1}^{m}\psi_j\gamma_{j-1} \leq 0, \ \textbf{if } p_i^* \geq 0, \quad \forall i = 2, 3, \cdots, m \tag{2.4}$$

$$\frac{\partial \mathcal{L}}{\partial \lambda^*} = p_t - \sum_{i=1}^{m} p_i \geq 0, \ \textbf{if } \lambda^* \geq 0 \tag{2.5}$$

$$\frac{\partial \mathcal{L}}{\partial \mu_i^*} = p_i\gamma_i - \Big(\sum_{j=1}^{i-1} p_j\gamma_i + \omega\Big)\Big(\varphi_i - 1\Big) \geq 0, \ \textbf{if } \mu_i^* \geq 0, \quad \forall i = 1, 2, 3, \cdots, m \tag{2.6}$$

$$\frac{\partial \mathcal{L}}{\partial \psi_i^*} = p_i\gamma_{i-1} - \sum_{j=1}^{i-1} p_j\gamma_{i-1} - p_{tol} \geq 0, \ \textbf{if } \psi_i^* \geq 0, \quad \forall i = 2, 3, 4, \cdots, m. \tag{2.7}$$

In addition, we have several KKT complementarity conditions whose treatment is detailed in the following.

In an m-user cluster, there are $2m$ Lagrange multipliers. Thus there are 2^{2m} com-

binations of Lagrange multipliers that need to be checked for satisfying the KKT conditions. However, checking 2^{2m} combinations is computationally complex. For example, if $m = 3, 4, \cdots, 10$, then the number of combinations are $64, 256, \cdots, 1048576$, respectively. In our problem $p_i > 0$, $\forall\, i = 1, 2, 3, \cdots, m$; therefore, to obtain finite solutions for m decision variables we need exactly m equations [26]. Thus, all 2^{2m} combinations need not to be checked, rather we need to check only $\binom{2m}{m}$ combinations. After solving for 2-, 3-, 4-, and 6-user NOMA clusters, we find that the Lagrange multiplier combinations satisfying KKT conditions are $2, 4, 8, 32$, respectively, thus in general 2^{m-1}.

The Lagrange multipliers for m-user downlink NOMA cluster belong to three sets of constraints. These sets are the total transmit power constraints, minimum data rate constraints, and SIC constraints, given mathematically as, $A = \{\lambda\}$, $\quad B = \{\mu_1, \mu_2, \mu_3, \mu_4, \cdots, \mu_m\}$, $\quad C = \{\psi_2, \psi_3, \psi_4, \cdots, \psi_m\}$, respectively. Therefore, the solution set is, $S = \{\lambda, \mu_2 \text{ or } \psi_2, \mu_3 \text{ or } \psi_3, \mu_4 \text{ or } \psi_4, \cdots, \mu_m \text{ or } \psi_m\}$. For example, for 2-user downlink NOMA, the satisfied KKT conditions are $S_1 = \{\lambda, \mu_2\}$ and $S_2 = \{\lambda, \psi_2\}$. For 3-user NOMA, the satisfied KKT conditions are $S_1 = \{\lambda, \mu_2, \mu_3\}$, $S_2 = \{\lambda, \mu_2, \psi_3\}$, $S_3 = \{\lambda, \psi_2, \mu_3\}$, and $S_4 = \{\lambda, \psi_2, \psi_3\}$. Now let us define two additional sets of Lagrange multipliers, $B' = S - B$ and $C' = S - C$. Then the closed-form solution of optimal power allocation to m-user downlink NOMA cluster can be given as in the following.

Lemma 2.3.1 (Optimal power allocation for m-User Downlink NOMA Cluster)**.** *The closed-form solution of the optimal power allocation for the highest channel gain user*

in downlink NOMA cluster can be given as follows:

$$p_1 = \frac{p_t}{\prod\limits_{\substack{j=2 \\ j\notin B'}}^{m} \varphi_j \prod\limits_{\substack{j=2 \\ j\in B'}}^{m} 2} - \sum_{\substack{j=2 \\ j\notin B'}}^{m} \frac{\omega(\varphi_j - 1)}{\gamma_j \prod\limits_{\substack{k=2 \\ k\notin B'}}^{j} \varphi_k \prod\limits_{\substack{k=2 \\ k\in B'}}^{j} 2} - \sum_{\substack{j=2 \\ j\notin C'}}^{m} \frac{p_{tol}}{2\gamma_{j-1} \prod\limits_{\substack{k=2 \\ k\notin B'}}^{j-1} \varphi_k \prod\limits_{\substack{k=2 \\ k\in B'}}^{j-1} 2}.$$

On the other hand, the optimal power allocation for remaining users (except the highest channel gain user) are given as:

(i) If $i \notin B'$,

$$p_i = \left[\frac{p_t}{\prod\limits_{\substack{j=i \\ j\notin B'}}^{m} \varphi_j \prod\limits_{\substack{j=i \\ j\in B'}}^{m} 2} - \sum_{\substack{j=i \\ j\notin B'}}^{m} \frac{\omega(\varphi_j - 1)}{\gamma_j \prod\limits_{\substack{k=i \\ k\notin B'}}^{j} \varphi_k \prod\limits_{\substack{k=i \\ k\in B'}}^{j} 2} - \sum_{\substack{j=i \\ j\notin C'}}^{m} \frac{p_{tol}}{2\gamma_{j-1} \prod\limits_{\substack{k=i \\ k\notin B'}}^{j-1} \varphi_k \prod\limits_{\substack{k=i \\ k\in B'}}^{j-1} 2} + \frac{\omega}{\gamma_i} \right] \times (\varphi_i - 1). \tag{2.8}$$

(ii) If $i \in B'$,

$$p_i = \frac{p_t}{\prod\limits_{\substack{j=i \\ j\notin B'}}^{m} \varphi_j \prod\limits_{\substack{j=i \\ j\in B'}}^{m} 2} - \sum_{\substack{j=i \\ j\notin B'}}^{m} \frac{\omega(\varphi_j - 1)}{\gamma_j \prod\limits_{\substack{k=i \\ k\notin B'}}^{j} \varphi_k \prod\limits_{\substack{k=i \\ k\in B'}}^{j} 2} - \sum_{\substack{j=i \\ j\notin C'}}^{m} \frac{p_{tol}}{2\gamma_{j-1} \prod\limits_{\substack{k=i \\ k\notin B'}}^{j-1} \varphi_k \prod\limits_{\substack{k=i \\ k\in B'}}^{j-1} 2} + \frac{p_{tol}}{\gamma_{i-1}}. \tag{2.9}$$

Proof. See Appendix A. □

2.3.3 Power Allocation Problem Formulation for Uplink NOMA

Let us consider an m-user uplink NOMA cluster, where the normalized channel gains of $UE_1, UE_2, \cdots, UE_m$ are assumed as $\gamma_1, \gamma_2, \cdots, \gamma_m$, respectively, and their respective minimum rate requirements are $R'_1, R'_2, \cdots, R'_m$, where $R'_i > 0$. Let also consider that the ω units of resource blocks are allocated to this m-user uplink NOMA cluster, where the bandwidth of each resource unit is B Hz. The problem for optimal power control can then be expressed as follows:

$$\begin{aligned}
&\underset{p}{\text{maximize}} \quad \omega B \sum_{i=1}^{m} \log_2 \left(1 + \frac{p_i \gamma_i}{\sum\limits_{j=i+1}^{m} p_j \gamma_j + \omega} \right) \\
&\text{subject to:} \quad \mathbf{C'_1}: p_i \leq p'_t, \, \forall \, i = 1, 2, \cdots, m \\
&\qquad \mathbf{C'_2}: \omega B \log_2 \left(1 + \frac{p_i \gamma_i}{\sum\limits_{j=i+1}^{m} p_j \gamma_j + \omega} \right) \geq R'_i, \, \forall i = 1, 2, \cdots, m \\
&\qquad \mathbf{C'_3}: p_i \gamma_i - \sum_{j=i+1}^{m-1} p_j \gamma_j \geq p_{tol}, \, \forall \, i = 1, 2, \cdots, (m-1)
\end{aligned}$$

where $\sum_{j=i+1}^{m} p_j \gamma_j$ is the inter-user interference for i-th user in uplink NOMA cluster, and p'_t is the uplink maximum transmission power budget for each user. It is noted that the aforementioned optimization problem is also convex under the **Constraints** $\mathbf{C'_1} - \mathbf{C'_3}$.

2.3.4 Closed-Form Optimal Solution Formulation for Uplink NOMA

The Lagrange function for the above problem can then be expressed as:

$$\mathcal{L}(p,\lambda,\mu,\psi) = \omega B \sum_{i=1}^{m} \log_2 \left(1 + \frac{p_i\gamma_i}{\sum\limits_{j=i+1}^{m} p_j\gamma_j + \omega}\right) + \sum_{i=1}^{m} \lambda_i \Big(p_t' - p_i\Big) + \sum_{i=1}^{m} \mu_i \Big(p_i\gamma_i - \sum_{j=i+1}^{m} \phi_i p_j \gamma_j - \phi_i\omega\Big) + \sum_{i=1}^{m-1} \psi_i \Big(p_i\gamma_i - \sum_{j=i+1}^{m} p_j\gamma_j - p_{tol}\Big) \tag{2.10}$$

where λ_i, μ_i and ψ_i are the Lagrange multipliers, and $\phi_i = \Big(2^{\frac{R_i'}{\omega B}} - 1\Big)$. Taking derivatives of equation (2.10) w.r.t. p_i, λ_i, μ_i, and ψ_i, we obtain:

$$\frac{\partial \mathcal{L}}{\partial p_i} = \frac{\omega B\gamma_i}{\sum\limits_{j=1}^{m} p_j\gamma_j + \omega} - \lambda_i + \mu_i\gamma_i - \sum_{k=1}^{i-1} \phi_k\mu_k\gamma_i + \gamma_i\psi_i - \sum_{l=1}^{i-1} \psi_l\gamma_l \le 0,$$

$$\textbf{if } p_i^* \ge 0 \quad \forall i = 1, 2, \cdots, m-1 \tag{2.11}$$

$$\frac{\partial \mathcal{L}}{\partial p_m} = \frac{\omega B\gamma_m}{\sum\limits_{j=1}^{m} p_j\gamma_j + \omega} - \lambda_m + \mu_m\gamma_m - \sum_{k=1}^{m-1} \phi_k\mu_k\gamma_m - \sum_{l=1}^{m} \psi_l\gamma_l \le 0,$$

$$\textbf{if} \quad p_m^* \ge 0 \tag{2.12}$$

$$\frac{\partial \mathcal{L}}{\partial \lambda_i^*} = p_t' - p_i \ge 0, \ \textbf{if } \lambda_i^* \ge 0 \qquad \forall i = 1, 2, \cdots, m \tag{2.13}$$

$$\frac{\partial \mathcal{L}}{\partial \mu_i^*} = p_i\gamma_i - \sum_{j=i+1}^{m} \phi_i p_j\gamma_j - \phi_i\omega \ge 0, \ \textbf{if } \mu_i^* \ge 0 \quad \forall i = 1, 2, \cdots, m \tag{2.14}$$

$$\frac{\partial \mathcal{L}}{\partial \psi_i^*} = p_i\gamma_i - \sum_{j=i+1}^{m} p_j\gamma_j - p_{tol} \ge 0, \ \textbf{if } \psi_i^* \ge 0 \quad \forall i = 1, 2, \cdots, m-1 \tag{2.15}$$

In an m-user cluster, there are $(3m-1)$ Lagrange multipliers, thus there are 2^{3m-1} combinations of Lagrange multipliers. Each combination needs to be checked whether it satisfies the KKT conditions or not. However, checking 2^{3m-1} combina-

tions is computationally complex. For example, if $m = 3, 4, \cdots, 10$, then the number of combinations are $256, 2048, \cdots, 536870912$, respectively. However, in our problem $p_i > 0, \forall\, i = 1, 2, 3, ..., m$; therefore, we need not to check all Lagrange multiplier combinations. To obtain finite solutions for m decision variables we need exactly m equations [26]. Thus, only $\binom{3m-1}{m}$ combinations need to be checked. After solving for 2-, 3-, 4-, and 6-user NOMA clusters, we find that the Lagrange multiplier combinations satisfying KKT conditions are 3 for all cases.

Note that $(3m - 1)$ Lagrange multipliers belong to three sets of constraints. These sets are total transmit power constraints, minimum data rate constraints, and SIC constraints, given mathematically as, $A = \{\lambda_1, \lambda_2, \lambda_3, \cdots, \lambda_m\}$, $B = \{\mu_1, \mu_2, \mu_3, , ..., \mu_m\}$, and $C = \{\psi_1, \psi_2, \psi_3, ..., \psi_{m-1}\}$, respectively. Therefore, the solution set is, $S = \{\lambda_1, \lambda_2\, \lambda_3, ..., \lambda_{m-1}, \lambda_m \,\text{or}\, \mu_{m-1} \,\text{or}\, \psi_{m-1}\}$. For example, for 3-user uplink NOMA cluster, the satisfied KKT conditions are $S_1 = \{\lambda_1, \lambda_2, \lambda_3\}$, $S_2 = \{\lambda, \lambda_2, \mu_2\}$, and $S_3 = \{\lambda, \lambda_2, \psi_2\}$. Now let us define three additional sets of Lagrange multipliers as, $A' = S - A$, $B' = S - B$, and $C' = S - C$. Then the closed-form solution of optimal power allocation to m-user uplink NOMA cluster can be given as in the following lemma.

Lemma 2.3.2 (Optimal power allocation for m-User Uplink NOMA Cluster)**.** *The closed-form solutions of the optimal power allocation in an m-user uplink NOMA cluster can be given as follows:*

(i) If $A' = \{\varnothing\}$, $B' = B$ and $C' = C$, then the optimal power allocation solution

$$p_i = p'_t \quad \forall i = 1, 2, 3, \cdots, m$$

(ii) If $A' \neq \{\varnothing\}$, $B' \neq B$ and $C' = C$, then the optimal power allocation solution

$$p_i = p'_t \quad \forall i = 1, 2, \cdots, m-1, \text{ and } p_m = \frac{p'_t \gamma_{m-1}}{\phi_{m-1}\gamma_m} - \frac{\omega}{\gamma_m}$$

(iii) If $A' \neq \{\varnothing\}$, $B' = B$ and $C' \neq C$, then the optimal power allocation solution

$$p_i = p'_t \quad \forall i = 1, 2, 3, \cdots, m-1, \text{ and } p_m = \frac{p'_t \gamma_{m-1}}{\gamma_m} - \frac{p_{tol}}{\gamma_m}$$

Proof. See Appendix B. □

Remark: In an uplink NOMA cluster, power control needs to be applied only at the weakest channel gain user. For example, for 4-user uplink NOMA cluster UE_1, UE_2, and UE_3 transmits with full power, while power control may be needed at UE_4 under the following conditions:

- to maintain minimum data rate for second weakest channel user (UE_3 in 4-user NOMA cluster), and
- to maintain minimum receive power difference between least two channel gain users (UE_3 and UE_4 in a 4-user NOMA cluster) at BS receiver.

2.4 Numerical Results and Discussions

2.4.1 Simulation Assumptions

In this section, I investigate the throughput performances of the downlink and uplink NOMA systems in LTE/LTE-advanced systems, using my proposed suboptimal user grouping and optimal power allocation solutions. In these simulations, 2, 3, 4, and 6 units of resource blocks are allocated for 2-, 3-, 4-, and 6-user NOMA clus-

ters, respectively. Both uplink and downlink NOMA systems are also compared with OFDMA based LTE/LTE-Advanced systems. In addition, the total downlink transmission power is uniformly allocated among the available resource blocks. The major simulation parameters are presented in **Table 2.1**.

Table 2.1: Simulation parameters for conventional NOMA in downlink and uplink transmissions

Parameters	**value**
Unit resource bandwidth, B	180 kHz
Downlink Transmit power budget, p_T	46 dBm
Uplink Transmit power budget, p'_t	24 dBm
SIC receiver's detection threshold, p_{tol}	20 dBm
Number of transmit antenna at both of BS and UE end	1
Number of receive antenna at both of BS and UE end	1

2.4.2 Throughput Comparison between NOMA and OMA Systems in Downlink Transmission

In this subsection, I compare the performance of NOMA with OFDMA in terms of sum-throughput and individual user's throughput.

Fig. 2.3 and Fig. 2.4 show the sum-throughput and individual throughput of 2-user downlink NOMA cluster as well as its corresponding OMA system for minimum data rate requirements of 100 Kbps and 1 Mbps, respectively. The channel gain of the higher channel gain user is fixed at 40 dB whereas the channel gain of weak user varies. Further, Fig. 2.5 represents the sum-throughput of 4-user downlink NOMA cluster and its corresponding OMA system as a function of each user channel variations. In

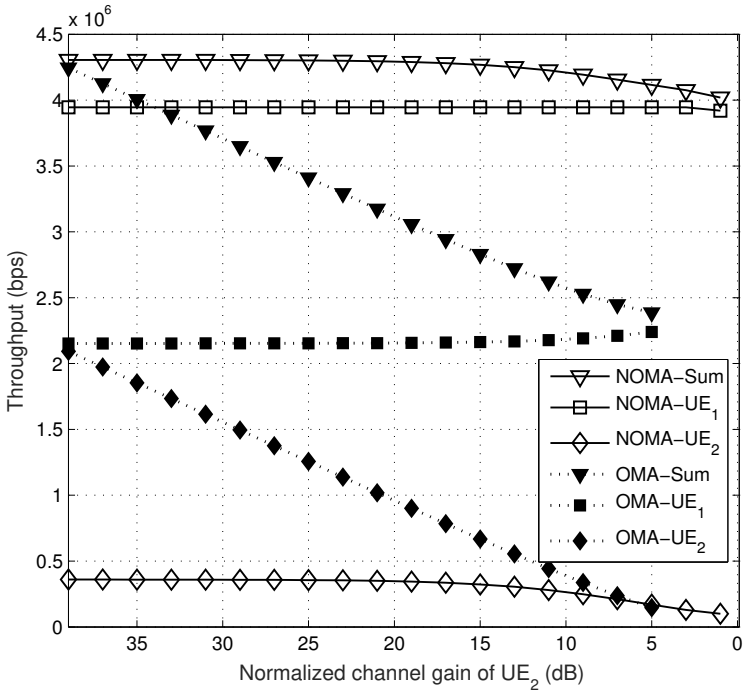

Figure 2.3: Throughput performance of 2-user downlink NOMA and OMA systems assuming 100 Kbps minimum data rate. Normalized channel gain of UE_1 is 40 dB.

Fig. 2.5, the initial channel gains of UE_1, UE_2, UE_3, and UE_4 are set as $\gamma_1 = 40$ dB, $\gamma_2 = 32$ dB, $\gamma_3 = 24$ dB, and $\gamma_4 = 16$ dB, respectively, and in each sub-figure only one user's channel is varied by ensuring $\gamma_1 > \gamma_2 > \gamma_3 > \gamma_4$.

From the above simulation results, the following observations can be made:

- ✓ Sum-throughput of downlink NOMA is observed to be always better than OMA at any channel conditions. However, a significant throughput gain can be achieved for more distinct channel conditions of users in a cluster.

- ✓ Individual throughput of the highest channel gain user in a NOMA cluster is significantly higher than in OMA. However, the lowest channel gain user's throughput is limited by its minimum rate requirements. To overcome this issue

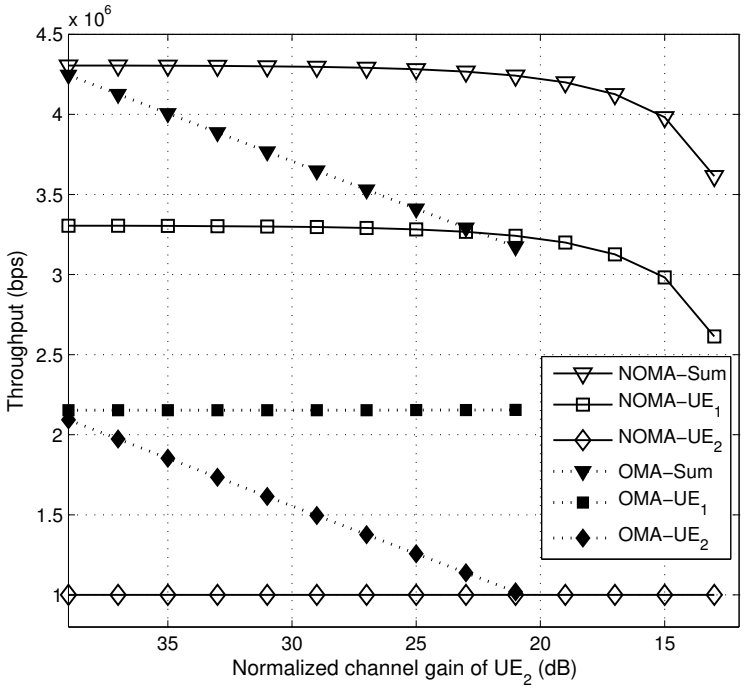

Figure 2.4: Throughput performance of 2-user downlink NOMA and OMA systems assuming 1 Mbps minimum data rate. Normalized channel gain of UE_1 is 40 dB.

in NOMA, minimum rate requirements of different users can be dynamically adjusted (by the system) to enhance the fairness among users.

✓ Sum-throughput of downlink NOMA strongly depends on the highest channel gain user within a cluster. The reason behind is that the strongest channel gain user can cancel all interfering signals before decoding its own signal, thus its achievable data rate does not contain any inter-user interference.

✓ The impact of the lowest channel gain user is minimal on the cluster sum throughput, unless there is a such poor channel gain where a huge power is required by the lowest channel gain user. At this point, a sharp decay of sum-throughput is observed. It is noted that the traditional OMA is unable to

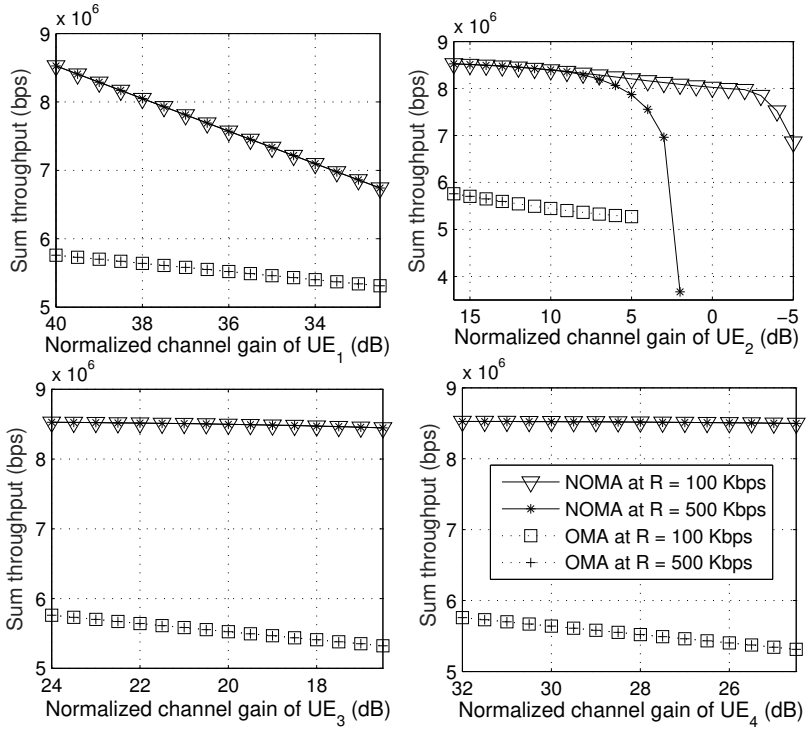

Figure 2.5: Impact of channel variation on the sum-throughput of 4-user downlink NOMA and OMA systems. Initial normalized channel gains of UE_1, UE_2, UE_3, and UE_4 are 40 dB, 32 dB, 24 dB and 16 dB, respectively. We assume R =100 Kbps and R =500 Kbps, where $R = R_1 = R_2 = R_3 = R_4$.

operate at such poor channel gains.

✓ The channel variations of all users, except the highest and lowest channel gain users, in a downlink NOMA cluster do not considerably affect the sum-throughput of a NOMA cluster (see Fig. 2.5(b) and Fig. 2.5(c)).

2.4.3 Throughput Comparison Among Various Downlink NOMA Systems

In this subsection, I compare the overall throughput performance of 2-user, 3-user, and 4-user downlink NOMA systems by considering 12 (twelve) active downlink users.

As given in **Lemma 2.1.1**, the higher number of users in a downlink NOMA cluster significantly reduces the portion of power for the strongest channel user, who generally contributes maximum throughput in a cluster. Therefore, it is crucial to investigate the correct cluster size. However, the throughput performance of a NOMA cluster depends significantly on three parameters, i.e., cluster size, transmit power, and channel gains of users. For a particular set of transmit powers and channel gains of users, we can find a cluster size that generally maximizes the sum throughput. **Table 2.2** represents the sum-throughput of different NOMA and OMA systems with 12 downlink users for various channel conditions while the transmit power is fixed in all cases.

Table 2.2: Throughput performance of NOMA and OMA systems in downlink transmission with twelve active users.

Case	Normalized channel gain (dB)												Sum-throughput (Mbps)			
													NOMA			OMA
	γ_1	γ_2	γ_3	γ_4	γ_5	γ_6	γ_7	γ_8	γ_9	γ_{10}	γ_{11}	γ_{12}	4-UE	3-UE	2-UE	
1	40	15	14.5	14	13.5	13	12.5	12	11.5	11	10.5	10	**12.78**	11.72	10.3	8.15
2	40	39.5	15	14.5	14	13.5	13	12.5	12	11.5	11	10.5	**18.36**	16.13	13.39	9.85
3	40	39.5	39	15	14.5	14	13.5	13	12.5	12	11.5	11	**23.74**	20.37	16.38	11.51
4	40	39.5	39	38.5	15	14.5	14	13.5	13	12.5	12	11.5	24.08	**24.45**	19.25	13.1
5	40	39.5	39	38.5	38	15	14.5	14	13.5	13	12.5	12	24.4	**24.62**	22	14.64
6	40	39.5	39	38.5	38	37.5	15	14.5	14	13.5	13	12.5	24.7	**24.77**	24.65	16.13
7	40	39.5	39	38.5	38	37.5	37	15	14.5	14	13.5	13	24.89	**24.91**	24.71	17.56
8	40	39.5	39	38.5	38	37.5	37	36.5	15	14.5	14	13.5	**25.07**	25.04	24.76	18.93
9	40	39.5	39	38.5	38	37.5	37	36.5	36	15	14.5	14	**25.23**	25.11	24.81	20.25
10	40	39.5	39	38.5	38	37.5	37	36.5	36	35.5	15	14.5	**25.32**	25.18	24.86	21.51
11	40	39.5	39	38.5	38	37.5	37	36.5	36	35.5	35	15	**25.4**	25.24	24.9	22.72
12	40	39.5	39	38.5	38	37.5	37	36.5	36	35.5	35	34.5	**25.47**	25.29	24.93	23.86
13	40	37	34	31	28	25	22	19	16	13	10	7	**22.84**	22.03	20.11	14.24
14	11	10.5	10	9.5	9	8.5	8	7.5	7	6.5	6	5.5	4.25	4.46	**4.54**	4.11

In **Table 2.2**, I order users according to their channel gains in descending order. There are 6, 4, and 3 number of clusters for 2-user, 3-user, and 4-user cluster sizes, respectively. The throughput performance of the aforementioned downlink NOMA clusters and their respective OMA counterparts is demonstrated in **Table 2.2**. The main observations are listed as follows:

- ✓ ***Less distinct channel gains of users (cases 12 and 14)***: In this case, the

throughput of different downlink NOMA systems is nearly the same. However, the 4-user NOMA achieves higher throughput at better channel gains *(case 12)*, while 2-user NOMA obtains higher throughput at lower channel gains *(case 14)*. As such, we can conclude that higher cluster size is preferred for higher channel gains of the users and lower cluster size should be preferred for lower channel gains of the users. The overall throughput gains of downlink NOMA over OMA are very limited.

- ✓ ***More distinct channel gains of users (case 13):*** In this case, NOMA systems outperform their OMA counterparts. It can be seen that the 4-user NOMA achieves better throughput than 2-user and 3-user NOMA systems. Therefore, higher cluster size can be selected in such cases until the power allocation to the highest channel gain user reduces significantly **(Lemma 1)**.

- ✓ ***Number of higher channel gain users equals to the number of clusters (cases 3, 4, 6):*** In such a case, each downlink NOMA system achieves maximum relative throughput gain compared to OMA. In **Table 2.2**, the 4-user downlink NOMA system (i.e., 3 clusters) achieves maximum 106.3% throughput gain over OMA system when the number of good channels are equal to 3 (*case 3*). However, for three good channel users, the 3-user (i.e., 4 clusters) and 2-user (i.e., 6 clusters) systems achieve maximum throughput gains of 86.6% and 52.8%, respectively, over OMA systems (*case 4* and *case 6*). Thus, a NOMA system with the number of higher channel gain users equal to the number of clusters either achieves maximum or close to maximum throughput among all NOMA systems.

- ✓ In general, the throughput of all NOMA systems are quite similar when 50%

or more users experience good channels (*case 6 to 12*). However, if the higher channel gain users become limited, then the higher cluster sizes should be selected to enhance throughput (*case 1 to 3*).

2.4.4 Fairness in Downlink NOMA systems

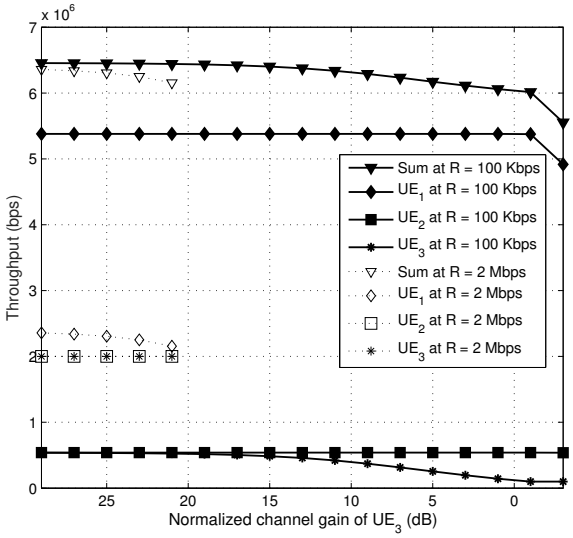

Figure 2.6: Throughput performances of 3-user downlink NOMA system, for $R = R_1 = R_2 = R_3 = 100$ Kbps and 2 Mbps. Normalized channel gain of UE_1 is 40 dB, and UE_2 is 30 dB.

Fig. 2.6 shows the individual users' throughput for 3-user downlink NOMA cluster considering two different minimum rate requirements of users, i.e., 100 Kbps and 2 Mbps. In general, the proposed optimal power allocation maximize the transmit power of the highest channel gain user while maintaining the minimum rate requirements of all users in a NOMA cluster. However, in such a case, the lower channel gain users may experience significant throughput difference when compared to the highest channel gain user, as discussed in Section 2.2.1. As such, to improve the throughput fairness among users, the minimum data rate requirements of the users

can be adjusted further to balance the trade-off between fairness and the overall system throughput.

2.4.5 Throughput Comparisons Between NOMA and OMA in Uplink Transmission

The sum-throughput and individual throughput of 2-user uplink NOMA cluster is shown in Fig. 2.7, where the minimum user rate requirement is 100 Kbps. It can be seen that the sum throughput of NOMA outperforms OMA with more distinct channel gains of users in a cluster. Also, the NOMA sum-throughput remains higher than OMA, regardless of the weakest channel. On the other hand, when UE_1 and UE_2 have nearly the same channel gains, UE_2 achieves better data rate. However, due to high interference of UE_2, UE_1 obtains very low data rate. As the channel gain of UE_2 reduces, its throughput gradually reduces. However, the interference on UE_1 also reduces which improves the achievable throughput of UE_1. As such, the sum throughput of uplink NOMA cluster remains almost unchanged.

When the minimum rate requirement of both users is set as high as 1 Mbps, Fig. 2.8 depicts the sum-throughput and individual throughput of 2-user NOMA cluster as well as the sum throughput of 2-user OMA system. It is observed that the sum-throughput of NOMA becomes less than the corresponding OMA system in the region when the channel gains are less distinct and power control is applied. The reason is that, without power control, the sum data rate of 2-user uplink NOMA system and corresponding OMA system is nearly similar. Therefore, after applying power control in NOMA, sum data rate is further reduced and goes below OMA. We further noted, since the power control is only applicable at the weakest channel gain user, its impact keeps diminishing gradually for 3-user and beyond uplink NOMA clusters (see in

Fig. 2.9). Fig. 2.9 shows the sum throughput and individual throughput of 3-user uplink NOMA cluster and corresponding sum throughput of OMA system, where the minimum individual rate requirement is 1 Mbps. It is evident that the sum throughput of 3-user and beyond uplink NOMA clusters remain always better than the OMA systems.

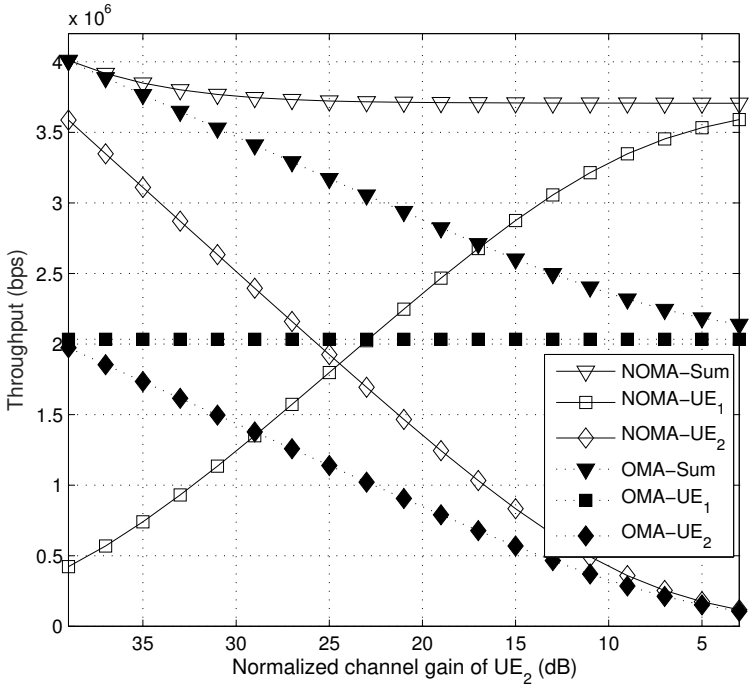

Figure 2.7: Throughput performance of 2-user uplink NOMA and OMA systems assuming 100 Kbps minimum data rate. Normalized channel gain of UE_1 is 40 dB.

Fig. 2.10 demonstrates the sum throughput of 4-user uplink NOMA cluster as a function of individual user's channel gain variation. The channel gains of UE_1, UE_2, UE_3, and UE_4 are set at 40 dB, 32 dB, 24 dB and 16 dB, respectively. In each sub-figure, one user's channel gain is varied while others remain fixed. For example, in case (a) UE_1 is varied from 40 dB to 32.5 dB while others are fixed. It is observed that the sum-throughput of uplink NOMA mainly depends on the channel conditions

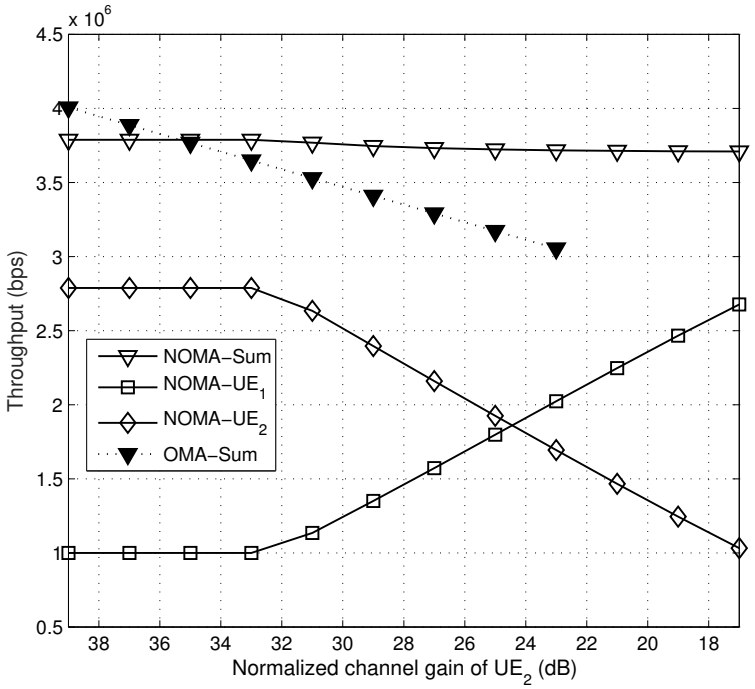

Figure 2.8: Throughput performance of 2-user uplink NOMA and OMA systems assuming 1 Mbps minimum data rate. Normalized channel gain of UE_1 is 40 dB.

of the highest channel gain user.

2.4.6 Throughput Comparisons Among Various Uplink NOMA Systems

Similar to downlink, in this subsection, I compare the overall and individual user's throughput of 2-user, 3-user, 4-user, and 6-user uplink NOMA systems for 12 uplink users. The important feature of uplink NOMA system is that all lower channel gain users in a NOMA cluster interfere significantly to the higher channel gain users. Note that, due to SIC, low channel gain users do not experience any interference from high channel gain users. In contrast to downlink NOMA, the impact of transmission

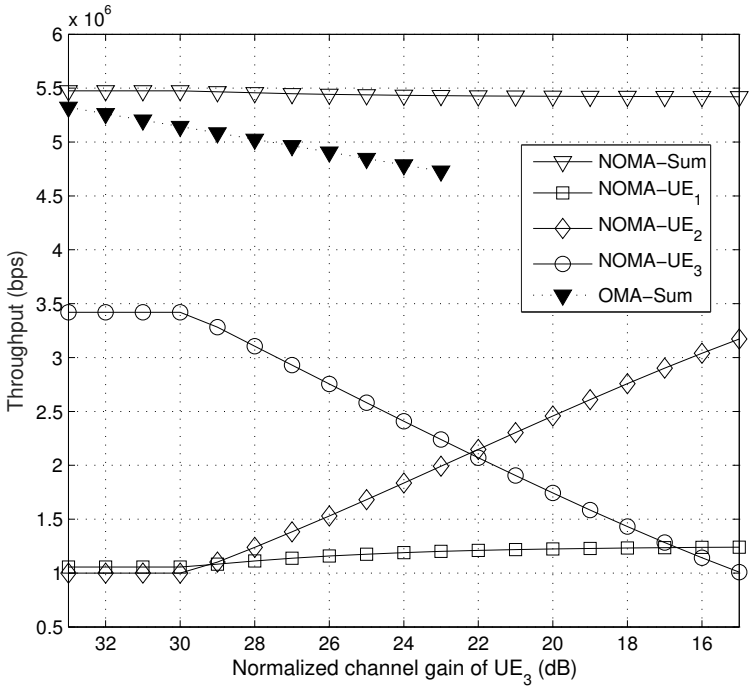

Figure 2.9: Throughput performance of 3-user uplink NOMA and OMA systems assuming 1 Mbps minimum data rate. Normalized channel gains of UE_1 and UE_2 are 40 dB and 34 dB, respectively.

power control in not significant in uplink NOMA. If more users are grouped into a cluster in uplink NOMA, more distinct channels are required. With different channel conditions of 12 (twelve) uplink active users, I measure the throughput performances of 2-user, 4-user, and 6-user uplink NOMA systems as well as OMA system, shown in **Table 2.3**. The users are clustered according to the method discussed in Section 2.2. The channel gains in Table **2.3** are chosen in order to ensure the minimum channel distinctness required for 6-user uplink NOMA system.

In Table **2.3**, we sort 12 (twelve) users according to the descending order of their channel gains. There are 6, 4 and 2 clusters available for 2-user, 3-user, and 6-user uplink NOMA systems, respectively. From Table **2.3** we find the following key

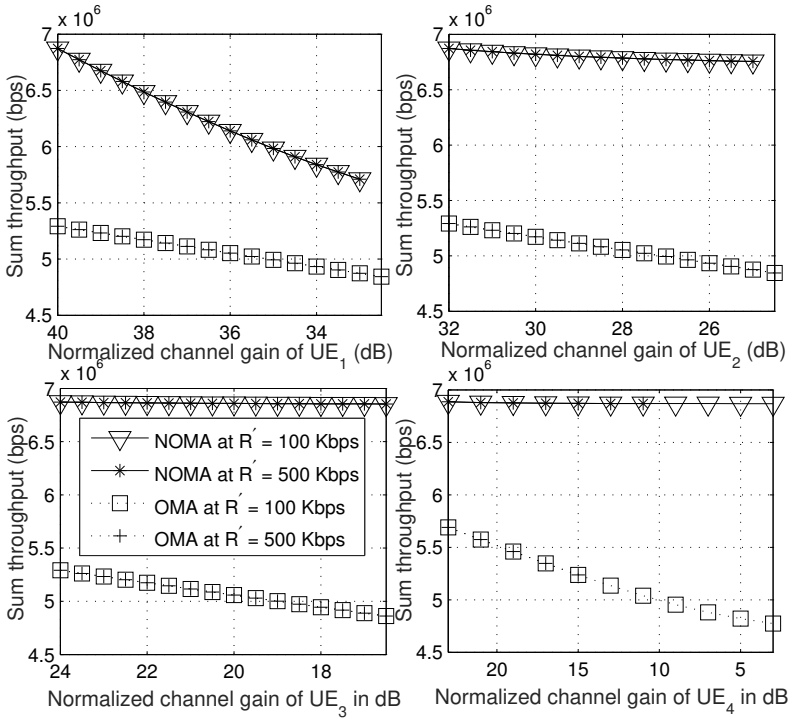

Figure 2.10: Impact of channel variation on the sum-throughput of 4-user uplink NOMA and OMA systems. Initial normalized channel gains of UE_1, UE_2, UE_3, and UE_4 are 40 dB, 32 dB, 24 dB, and 16 dB, respectively. We assume R' =100 Kbps and R' =500 Kbps, where $R' = R'_1 = R'_2 = R'_3 = R'_4$.

Table 2.3: Throughput performance of NOMA and OMA systems in uplink transmission with twelve active users.

Case	Normalized channel gain (dB)												Sum-throughput (Mbps)			
													NOMA			OMA
	γ_1	γ_2	γ_3	γ_4	γ_5	γ_6	γ_7	γ_8	γ_9	γ_{10}	γ_{11}	γ_{12}	6-UE	4-UE	2-UE	
1	40	20	18.5	17	15.5	14	12.5	11	9.5	8	6.5	5	**12.90**	11.28	9.17	7.14
2	40	38.5	20	18.5	17	15.5	14	12.5	11	9.5	8	6.5	**18.34**	15.50	11.91	8.93
3	40	38.5	37	20	18.5	17	15.5	14	12.5	11	9.5	8	18.97	**19.05**	14.33	10.59
4	40	38.5	37	35.5	20	18.5	17	15.5	14	12.5	11	9.5	**19.59**	19.37	16.42	12.11
5	40	38.5	37	35.5	34	20	18.5	17	15.5	14	12.5	11	**19.83**	19.68	18.17	13.48
6	40	38.5	37	35.5	34	32.5	20	18.5	17	15.5	14	12.5	**20.06**	19.98	19.58	14.69
7	40	38.5	37	35.5	34	32.5	31	20	18.5	17	15.5	14	**20.17**	20.08	19.65	15.75
8	40	38.5	37	35.5	34	32.5	31	29.5	20	18.5	17	15.5	**20.27**	20.17	19.72	16.64
9	40	38.5	37	35.5	34	32.5	31	29.5	28	20	18.5	17	**20.32**	20.25	19.78	17.36
10	40	38.5	37	35.5	34	32.5	31	29.5	28	26.5	20	18.5	**20.36**	20.28	19.84	17.91
11	40	38.5	37	35.5	34	32.5	31	29.5	28	26.5	25	20	**20.38**	20.30	19.89	18.29
12	40	38.5	37	35.5	34	32.5	31	29.5	28	26.5	25	23.5	**20.40**	20.32	19.92	18.49
13	40	37	34	31	28	25	22	19	16	13	10	7	**18.65**	18.35	16.93	12.89
14	20	18.5	17	15.5	14	12.5	11	9.5	8	6.5	5	3.5	**6.47**	6.41	6.11	5.23

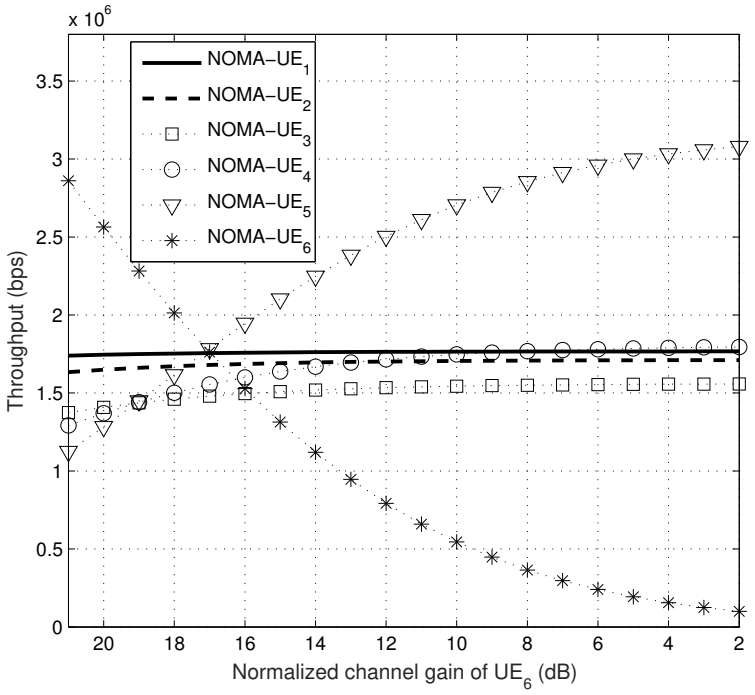

Figure 2.11: Throughput performance of 6-user uplink NOMA cluster for 100 Kbps minimum data rate. Normalized channel gain of UE_1 to UE_5 are 40, 35, 30, 26, and 22 dB, respectively, while UE_6 varies.

observations:

- ✓ ***More distinct channel gains of users (case 13):*** In this case, the performance of any uplink NOMA is much better than the OMA system (*case 13*), whereas the higher order NOMA achieves higher throughput.
- ✓ ***Less distinct channel gains of users (cases 12 and 14)***: In this case, higher order uplink NOMA still performs better, though the throughput performance of various NOMA systems are quite similar. However, in this case, the throughput gains of NOMA over OMA are marginal.
- ✓ ***Number of good channel users equals the number of clusters (cases***

2, 3, 4, 6): In such a case, each uplink NOMA system achieves maximum relative throughput gain compared to OMA. In **Table 2.3**, *case 2* shows 105.4% throughput gain of 6-user uplink NOMA system in comparison to OMA system, while *case 3, 4* and *case 6* show the maximum throughput gain of 4-user and 2-user uplink NOMA systems, respectively, where the gains are 79.9% and 33.3%, respectively. Thus, a NOMA system with the number of higher channel gain users equal to the number of clusters either achieves maximum or close to maximum throughput among all NOMA systems.

✓ When one or couple of users experience higher channel gains, higher order uplink NOMA systems perform much better than OMA systems *(case 1, 2 and 3)*. As the number of users experiencing higher channel gains increases, different uplink NOMA systems perform nearly similar *(case 4 to 12)*.

2.4.7 Fairness in Uplink NOMA Systems

Fig. 2.11 shows the individual throughput of 6-user uplink NOMA cluster, where UE_1 to UE_5 experience 40, 35, 30, 26, and 22 dB channel gains, respectively. Fig. 2.11 shows good throughput fairness among UE_1 to UE_4, whilst, by selecting proper channel gains for UE_5 and UE_6, all six users can get good throughput fairness. Therefore, the exploitation of channel gain differences among the NOMA users is the key design issue of uplink NOMA.

2.5 Summary

Efficient user clustering and power allocation among NOMA users are the key driving factors for successful NOMA operations. In this chapter, for both downlink and up-

link NOMA, I have formulated a joint user clustering and power allocation optimization problem for sum throughput maximization, under the user clustering constraint, transmission power budget constraint, individual user's minimum rate requirement constraint, and NOMA power allocation constraint for SIC application at receiver end(s). Due to the MINLP nature of the formulated joint optimization problem, I opt to develop a low-complexity sub-optimal user clustering scheme by exploiting users channel gain differences. Provided the user clustering, I have derived closed-form optimal power allocation for sum-throughput maximization of a general m-user downlink and uplink NOMA systems. Numerical results demonstrate a significant spectral efficiency gain of NOMA systems in comparison to those for OFDMA systems. Along the superior spectral efficiency performance, NOMA also can able to provide better fairness among the users in both of downlink and uplink transmissions.

Chapter 3

NOMA in Downlink Multi-user MIMO Systems

In this chapter, I investigate the application of NOMA with SIC processing in downlink MIMO systems, where the total number of receive antennas at UE ends is more than the number of transmit antennas at the BS in a single cell network.

3.1 Preliminaries

MIMO communication with multiuser beamforming has been studied widely as a potential technology for achieving significant gains in the overall system throughput [6]. In downlink multiuser MIMO, each UE is served by one or multiple beams depending on the number of BS transmit antennas and total number of receive antennas at the UEs in the cell. The inter-beam interference can be completely eliminated when the number of transmit antennas is more than or equal to the number of receive antennas. In such a conventional multiuser MIMO system, each UE receiver is supported by individual beamforming vector which is orthogonal to the other receivers' channel

gains.

In a downlink multiuser MIMO-NOMA system, multiple receive antennas of different UEs with distinct channel gains are grouped into MIMO-NOMA clusters. All the users/receive-antennas in each cluster are scheduled on NOMA basis. The number of clusters is generally equal to the number of BS transmit antennas, i.e., the number of transmit beams. A single beam is utilized by all the receivers of a cluster which adopt NOMA. In case of more clusters than the BS transmit antennas, multiple clusters may share the same beam but utilize orthogonal spectrum resources, while each cluster individually is scheduled on a NOMA basis. However, since the number of UE receive antennas in downlink MIMO-NOMA system is much higher than the number of BS transmit antennas, it results in strong inter-cluster interference. Therefore, multi-cluster beamforming is a key to reducing inter-cluster interference in MIMO-NOMA systems. In this paper, we propose a new multi-cluster zero-forcing beamforming (ZF-BF) technique for downlink multiuser MIMO-NOMA systems.

In this chapter, the MIMO-NOMA system in which beamforming is performed by using the channel information of the highest channel gain users of each cluster is denoted as *conventional MIMO-NOMA*, while orthogonal spectrum resource allocation among the users of each MIMO-NOMA cluster is denoted as *conventional MIMO-OMA or MIMO-OMA*. Also, a NOMA system with single antennas BS is referred as *conventional NOMA*. In addition, I define the highest channel gain user of each MIMO-NOMA cluster as the *cluster-head*, and each receive antenna in a cluster is defined as a *user*.

3.2 System and Signal Models

3.2.1 System Model

For a downlink multiuser MIMO-NOMA system, it is assumed that a single cell BS is equipped with N_t transmit antennas for beamforming. The total number of UEs in the cell is X, where each UE can be equipped with one or more receive antenna(s). The total number of UE receive antennas in the cell is L, where $L > N_t$. The receive antennas are grouped into N clusters, where $N \geq N_t$. In a cluster, no more than one user/receive-antenna belongs to one UE, while one user/receive-antenna only belongs to one cluster. However, if $N > N_t$, then multiple clusters may utilize the same BF vector but use orthogonal spectrum resources to each other, while users in each cluster are scheduled on a NOMA basis. For $N = N_t$, all the clusters use the same spectrum resources (full bandwidth) and each BF vector serves individual cluster. Each MIMO-NOMA cluster (*each cluster is defined as a MIMO-NOMA cluster*) consists of K users/receive-antennas such that $\sum_{n=1}^{N} |K| = L$.

For the sake of simplicity, the number of clusters are assumed to be equal to the number of transmit antennas, i.e., $N = N_t$.

3.2.2 Signal Model

Let us consider $\mathbf{x} = [x_1 \ x_2 \ x_3 \ \cdots \ x_N]^T \in \mathbb{C}^{N\times 1}$ to be the transmitted data vector, where $x_n = \sum_{k=1}^{K} p_{n,k} s_{n,k}$ is the data stream for n-cluster in which $p_{n,k}$ and $s_{n,k}$ are the transmit power and message signal, respectively, for the k-th user in the n-th cluster. Let us also assume that the data vector is modulated by a beamforming precoding matrix $\mathbf{M} \in \mathbb{C}^{N\times N}$, and then transmitted over the radio channel $\mathbf{H} = [\mathbf{H}_1^T \ \mathbf{H}_2^T \ \mathbf{H}_3^T \ \cdots \ \mathbf{H}_N^T]^T \in \mathbb{C}^{L\times N}$, where $\mathbf{H}_n \in \mathbb{C}^{K\times N}$ corresponds to the radio channel

of all K users of n-th cluster. Therefore, the transmitted superposed signal $\tilde{\mathbf{x}} \in \mathbb{C}^{N\times 1}$ can be expressed as

$$\tilde{\mathbf{x}} = \mathbf{M}\mathbf{x}. \tag{3.1}$$

Now, we define $d_{n,k} \in \mathbb{C}$ to be the decoding scaling weight factor in which the received signal is multiplied prior to decode at k-th user of n-th cluster end. Thus, the received signal for k-th user of n-th cluster can be expressed as

$$y_{n,k} = d_{n,k}[\mathbf{h}_{n,k}\mathbf{M}\mathbf{x} + z_{n,k}] \tag{3.2}$$

where $\mathbf{h}_{n,k} \in \mathbb{C}^{1\times N}$ is the radio channel gain column vector for k-th user of n-th cluster, and $z_{n,k} \in \mathbb{C}$ represents circularly symmetric complex Gaussian noise with variance σ^2. However, if $\mathbf{m}_n$ denotes the n-th column of the BF precoding matrix $\mathbf{M}$, then (3.2) can be expressed as follows:

$$\begin{aligned} y_{n,k} = \; & d_{n,k}\mathbf{h}_{n,k}\mathbf{m}_n x_n + d_{n,k}\mathbf{h}_{n,k}\sum_{i=1,i\neq n}^{N}\mathbf{m}_i x_i + d_{n,k}z_{n,k} \\ = \; & d_{n,k}\mathbf{h}_{n,k}\mathbf{m}_n p_{n,k}s_{n,k} + d_{n,k}\mathbf{h}_{n,k}\mathbf{m}_n\sum_{j=1,j\neq k}^{K} p_{n,j}s_{n,j} \\ & + d_{n,k}\mathbf{h}_{n,k}\sum_{i=1,i\neq n}^{N}\mathbf{m}_i x_i + d_{n,k}z_{n,k}. \end{aligned} \tag{3.3}$$

In this downlink MIMO-NOMA system, the dynamic power allocation within each MIMO-NOMA cluster is performed in such a way that the higher channel gain user can perfectly decode and then suppress the intra-cluster interference from lower chan-

nel gain users. Thus, (3.3) can be rewritten as follows:

$$\begin{aligned} y_{n,k} = \; & d_{n,k}\mathbf{h}_{n,k}\mathbf{m}_n p_{n,k} s_{n,k} + d_{n,k}\mathbf{h}_{n,k}\mathbf{m}_n \sum_{j=1}^{k-1} p_{n,j} s_{n,j} \\ & + d_{n,k}\mathbf{h}_{n,k} \sum_{i=1, i\neq n}^{N} \mathbf{m}_i x_i + d_{n,k} z_{n,k}. \end{aligned} \tag{3.4}$$

Therefore, the received signal-to-intra-cell interference-plus-noise ratio (SINR) for k-th user of n-th cluster can be expressed as follows:

$$\mathrm{SINR}_{n,k} = \frac{|(d_{n,k}\mathbf{h}_{n,k})\mathbf{m}_n|^2 p_{n,k}}{\underbrace{|(d_{n,k}\mathbf{h}_{n,k})\mathbf{m}_n|^2 \sum_{j=1}^{k-1} p_{n,j}}_{\text{Intra-beam interference}} + \underbrace{\sum_{i=1, i\neq n}^{N} |(d_{n,k}\mathbf{h}_{n,k})\mathbf{m}_i|^2 p_i}_{\text{Inter-beam interference}} + \underbrace{d_{n,k} z_{n,k}}_{\text{Noise}}} \tag{3.5}$$

where p_i is the total transmit power for i-th cluster, and we assume that $\mathrm{E}[|s_{i,j}|^2] = 1 \; \forall i, j$. The achievable throughput for k-th user of n-th cluster can be expressed as

$$\bar{R}_{n,k} = B \log_2 \left(1 + \frac{g_{n,k} p_{n,k}}{g_{n,k} \sum_{j=1}^{k-1} p_{n,j} + 1} \right) \tag{3.6}$$

where B is the total system bandwidth utilised by each transmit beam, and the resultant normalized channel gain $g_{n,k}$ could be defined as follows:

$$g_{n,k} = \frac{|(d_{n,k}\mathbf{h}_{n,k})\mathbf{m}_n|^2}{\sum_{i=1, i\neq n}^{N} |(d_{n,k}\mathbf{h}_{n,k})\mathbf{m}_i|^2 p_i + d_{n,k} z_{n,k} B}. \tag{3.7}$$

For this proposed downlink MIMO-NOMA system, the overall achievable cell system throughput can be expressed as

$$\bar{R}_{cell} = R \sum_{n=1}^{N} \sum_{k=1}^{K} B \log_2 \left(1 + \frac{g_{n,k} p_{n,k}}{g_{n,k} \sum_{j=1}^{k-1} p_{n,j} + 1} \right) \tag{3.8}$$

where $\mathcal{U}_{n,k} \cap \mathcal{U}_{n',k} = \emptyset$, $\forall n \neq n'$ and $\forall k$, $\mathcal{U}_{n,k}$ represents the k-th user in n-th cluster. The maximization of (3.8) depends on three key factors: beamforming technique, user clustering approach, and inter-cluster and intra-cluster power allocation, which are discussed in subsequent sections.

3.3 Beamforming in Downlink MIMO-NOMA

In ZF-BF method, the inter-cluster interference could be completely removed when the number of total receive antennas is less than or equal to the number of total transmit antennas in a cell, thus each cluster contains maximum one receive antenna. In case of equal transmit and receive antennas, the ZF-BF can simply be achieved by taking the inversion of the receivers' channel gains. On the other hand, singular value decomposition (SVD) of the receivers' channel gains is used to achieve the ZF-BF in case of equal or less receive antennas than the transmit antennas in a cell. However, in a MIMO-NOMA system, the number of receive antennas is much higher than the number of transmit antennas, thus the multiuser ZF-BF may not be achieved. In this proposed downlink MIMO-NOMA system, we utilize a precoding technique that was suggested in [6], where the actual channel matrix $\mathbf{H} \in \mathbb{C}^{K \times N}$ for all n-th MIMO-NOMA clusters consisting of K users are manipulated to form an equivalent channel matrix $\bar{\mathbf{H}} \in \mathbb{C}^{1 \times N}$ which provides compatible dimension for ZF-BF. Unfortunately, the performance of this precoding technique not much better than the conventional

MIMO-NOMA precoding. To improve the MIMO-NOMA performance with this precoding technique, I introduce a decoding scaling weight factor which potentially reduces the inter-cluster interference while increasing the desired signal strength. The details of the precoding and decoding techniques will be discussed in the following subsections.

3.3.1 Precoding Matrix

Let us consider the n-th MIMO-NOMA cluster which consists of K users, then the radio channel matrix $\mathbf{H}_n \in \mathbb{C}^{K\times N}$ can be expressed as follows:

$$\mathbf{H}_n = [\mathbf{h}_{n,1}^T \;\; \mathbf{h}_{n,2}^T \;\; \mathbf{h}_{n,3}^T \;\; \cdots \;\; \mathbf{h}_{n,K}^T]^T \tag{3.9}$$

where $\mathbf{h}_{n,k} \in \mathbb{C}^{1\times N}$ is the radio channel vector for the k-th user of n-th cluster. Now taking the SVD of the channel matrix $\mathbf{H}_n$ we obtain

$$\mathbf{H}_n = \mathbf{U}_n \mathbf{\Sigma}_n \mathbf{V}_n^H. \tag{3.10}$$

In our proposed MIMO-NOMA system, each beamforming vector is utilized by one MIMO-NOMA cluster. Thus, the equivalent radio channel matrix $\bar{\mathbf{H}}_n \in \mathbb{C}^{1\times N}$ for the n-th cluster is obtained as follows:

$$\bar{\mathbf{H}}_n = \mathbf{U}_n^{(1)H} \mathbf{H}_n \tag{3.11}$$

where $\mathbf{U}_n^{(1)H} \in \mathbb{C}^{1\times K}$ is the Hermitian transpose of the first column of $\mathbf{U}_n$ of (3.10). Thus, the equivalent radio channel matrix $\bar{\mathbf{H}} \in \mathbb{C}^{N\times N}$ consisting of all MIMO-NOMA

clusters can be expressed as follows:

$$\bar{\mathbf{H}} = [\bar{\mathbf{H}}_1^T \ \bar{\mathbf{H}}_2^T \ \bar{\mathbf{H}}_3^T \ \cdots \ \bar{\mathbf{H}}_N^T]^T. \tag{3.12}$$

Finally, the BF precoding matrix $\mathbf{M} \in \mathbb{C}^{N \times N}$ can be obtained by taking the right pseudo-inverse of the equivalent matrix $\bar{\mathbf{H}}$ as follows:

$$\mathbf{M} = \frac{\bar{\mathbf{H}}^\dagger}{||\bar{\mathbf{H}}^\dagger||_F} = \left[\frac{\bar{\mathbf{m}}_1}{||\bar{\mathbf{m}}_1||_F} \frac{\bar{\mathbf{m}}_2}{||\bar{\mathbf{m}}_2||_F} \cdots \frac{\bar{\mathbf{m}}_N}{||\bar{\mathbf{m}}_N||_F} \right] \tag{3.13}$$

where $||\bullet||_F$ represents the Frobenius norm, and $\bar{\mathbf{m}}_n$ indicates the n-the column of the pseudo-inverse of $\bar{\mathbf{H}}$.

3.3.2 Scaling Weight Factor

In this proposed downlink MIMO-NOMA system, the users/receive-antennas are clustered in such a way that each cluster contains maximum distinctive channel gain users (the details of user clustering will be presented in Section IV). Also, within each cluster, the users are sorted according to the ascending order of their channel gains, thus the strongest user is the 1st user (*which is also defined as cluster-head*) and the weakest user is the K-th user of a MIMO-NOMA cluster consisting of K users. On the other hand, according to the properties of the SVD of a matrix $\mathbf{A}$, the elements of first column of the left singular matrix ($\mathbf{U}^{(1)}$) is nearly-proportional to the normalized value of the corresponding rows of the matrix $\mathbf{A}$. If the channel gain differences between the cluster-head and other users of a MIMO-NOMA cluster are sufficiently large, the equivalent channel gain is then nearly similar to the cluster-head's channel gain. Therefore, in such a channel condition, the cluster-head of each MIMO-NOMA cluster can almost completely cancel inter-cluster interference. All the

cluster members except the cluster-head can achieve a better inter-cluster interference cancellation if they estimate their equivalent cluster channel or cluster-head's channel at their ends. To obtain the best estimation of cluster-head's channel for k-th user of n-th MIMO-NOMA cluster, his own channel need to be scaled up by the following weight factor prior to the decoding:

$$d_{n,k} = \frac{\mathbf{U}_{n,1}^{(1)}}{\mathbf{U}_{n,k}^{(1)}}, \quad \forall n \text{ and } \forall k \tag{3.14}$$

where $\mathbf{U}_{n,k}^{(1)}$ is the k-th row of first column of the left singular matrix $\mathbf{U}_n$ of n-th MIMO-NOMA cluster's channel matrix $\mathbf{H}_n$. In this proposed downlink MIMO-NOMA system, the BS sends the decoding scaling weight factor to the specific users before it starts sending the data streams. This is easy for MIMO-NOMA system to send such information before sending data streams, since the NOMA with dynamic power allocation requires to share the allocated transmit power information to the participating NOMA users in order to perform SIC at the receiver ends.

3.4 Dynamic User Clustering in Downlink MIMO-NOMA

As mentioned in Chapter 2, the optimal user clustering for conventional NOMA system requires an exhaustive search among all the users in a cell. That is, for every single user, it is required to consider all possible combinations of user grouping. In downlink transmission, the working principle of MIMO-NOMA and conventional NOMA are nearly similar. Each cluster of a conventional NOMA is served by orthogonal spectrum resources, while MIMO-NOMA clusters equal to the number of BS antennas use same spectrum resources by utilizing MIMO principle. Therefore, the computational complexity of optimal user clustering for downlink MIMO-NOMA is also extremely

high, and thus may not be affordable for practical systems with a moderate to large number of transmit and receive antennas.

In this section, we propose a low-complexity sub-optimal user clustering scheme for downlink MIMO-NOMA system. The proposed scheme exploits the channel gain differences and correlations among the NOMA users, and targets to enhance the overall sum-spectral efficiency in the cell. Note that, in this paper, the channel gain correlation between two users refers to their Rayleigh fading gain correlation. By utilizing the channel gain differences, a low-complexity user clustering scheme was also proposed in Chapter 2 for a conventional NOMA system. However, the user clustering of MIMO-NOMA is little bit different from that of conventional NOMA. Along with the channel gain differences and correlations among the NOMA users, the precoding and decoding techniques of MIMO system play a vital role in MIMO-NOMA user clustering.

3.4.1 Key Issues in User Clustering for Downlink MIMO-NOMA

With an objective of sum-throughput maximization in a cell, the key factors that need to be considered for user clustering in downlink MIMO-NOMA system are as follows.

- A mentioned in Chapter 2, the cluster-head (the highest channel gain user) of a downlink NOMA cluster can completely cancel intra-cluster interference, and thus achieves maximum throughput gain. Therefore, a key point to maximizing the overall system capacity (or spectral efficiency) is to ensure that the high channel gain users in a cell are selected as the cluster-heads of different MIMO-NOMA clusters.

- As discussed in Section 3.3.2, the equivalent channel gain of this proposed

MIMO-NOMA cluster is almost similar to the channel gain of the cluster-head when the differences in channel gains of the cluster-head and the other users are sufficiently high. In addition, the proposed decoding scaling weight factor can sufficiently improve the desired signal and eliminate the inter-cluster interference for the remaining users of a MIMO-NOMA cluster when their channel gains are significantly much lower than that of the cluster-head. Therefore, the second key point of downlink MIMO-NOMA user clustering is to make the cluster-head much distinctive from the remaining users of the cluster. This point also indicates that all the users under a MIMO cell may not be able to use NOMA.

- In both the proposed and conventional MIMO-NOMA clusters, the cluster members with more correlated channel gains with the cluster-head can effectively eliminate the inter-cluster interference, and thus improve the resultant capacity gain. In general, the channel gains between two users would be correlated when they are closely located, i.e., difference in their channel gains is small. However, the beamforming technique proposed for the MIMO-NOMA system requires high channel gain differences between the cluster-head and the other users of a MIMO-NOMA cluster. Therefore, both the channel gain differences and correlations need to be considered while forming downlink MIMO-NOMA clusters.

3.4.2 User Clustering Algorithm

Let us consider a downlink MIMO-NOMA system where the number of transmit antennas at the BS is N_t. The total number of receive antennas at all UEs in the cell is L. Here, we first provide a low-complexity MIMO-NOMA user clustering algorithm

in which the number of clusters $N = N_t$ and each cluster contains K (equal) number of receive antennas of different UEs. Afterwards, a more sophisticated version of MIMO-NOMA user clustering algorithm will be presented. In addition, we define ρ as the minimum correlation coefficient for which two users' Rayleigh fading channel gains are considered to be correlated. Moreover, we use $(\mathcal{U}_i \neq \mathcal{U}_j)$ to indicate that both of the i-th and j-th receive antennas in the cell do not belong to the same UE. The low-complexity MIMO-NOMA user clustering algorithm is given in **Algorithm** 3.4.1.

Algorithm 3.4.1**: User Clustering for Downlink MIMO-NOMA**

---

1. **Sort users according to the ascending channel gain:**

   $h_1 \geq h_2 \geq \cdots \geq h_L$, $h_i = i$-th user's channel gain.

2. **Select number of clusters and cluster-heads:**

   Number of MIMO-NOMA clusters is N, and the n-th higher channel gain user in a cell is the cluster-head of n-th MIMO-NOMA cluster.

3. **Include second users into each cluster:**

   Initiate user sets: $\mathcal{A} = \{1, 2, \cdots, N\}$, $\mathcal{B} = \{N+1, N+2, \cdots, 2N\}, \mathcal{R}_{i,j} =$ correlation coefficient between h_i and h_j.

($\boldsymbol{a}$) ***Clustering of users with correlated channel gains:***

for $i = 1 : N$

for $j = N + 1 : 2N$

if $\left(\mathcal{R}_{i,j} > \mathcal{R}_{i,k} \geq \rho, \forall k \neq j \in \mathcal{B}\right)$ AND $\left(\mathcal{U}_i \neq \mathcal{U}_j\right)$

include j-th user into i-th cluster,

update $\mathcal{A} \leftarrow \mathcal{A} - \{i\}$, $\mathcal{B} \leftarrow \mathcal{B} - \{j\}$.

end

end

end

(***b***) ***Clustering of users with uncorrelated channel gains:***

for $i = 1 : N$

for $j = N + 1 : 2N$

if $\left(i \in \mathcal{A}\right)$ AND $\left(j \in \mathcal{B}\right)$ AND $\left(\mathcal{U}_i \neq \mathcal{U}_j\right)$

include j-th user into i-th cluster,

update $\mathcal{A} \leftarrow \mathcal{A} - \{i\}$, $\mathcal{B} \leftarrow \mathcal{B} - \{j\}$.

end

end

end

4. Include k-th users into each cluster:

Repeat Step 3,

while $3 \leq k \leq K$

set $i = 1 : N$, $j = kN - N + 1 : kN$, $\mathcal{A} = \{1, 2, \cdots,$

$N\}$, $\mathcal{B} = \{kN - N + 1, kN - N + 2, \cdots, kN\}$.

end

In **Algorithm** 3.4.1, it is assumed that all the users in a downlink MIMO cellular system can utilize NOMA-based resource allocation. However, the lower channel gain users of a NOMA cluster usually experience high intra-cluster interference. The lower channel gain users in a MIMO-NOMA cluster also experience strong inter-cluster interference which results in a low SINR. Although our proposed MIMO-NOMA system can significantly cancel inter-cluster interference for lower channel

gain users, the performances of these users deteriorate as their channel gains become closer to that of the cluster-head. Therefore, only a portion of the users may use NOMA in a MIMO system. In addition, a higher order MIMO-NOMA system (i.e., a system with more users in a cluster) requires more transmit power for the lowest channel gain user of that cluster, while the transmit power budget per antenna in MIMO system is generally limited. Therefore, a higher order clustering may not to be possible in downlink MIMO-NOMA system. On the other hand, to maximize the cell sum-spectral efficiency, the users utilizing MIMO-NOMA should be clustered in such a way that each cluster contains users with the maximum channel gain differences, in case of uncorrelated channel gains.

Based on the aforementioned practical considerations, a sophisticated user clustering algorithm for 2-user clusters for the proposed MIMO-NOMA system is given in **Algorithm** 3.4.2. Note that the clustering process for 3-user and higher order MIMO-NOMA systems would be similar to that given by **Algorithm** 3.4.2.

Algorithm 3.4.2**: User Clustering for** 2**-User Downlink MIMO-NOMA**

---

1. **Input, Initialization and Assumption:**

   Input: Tx antennas N_t, Rx antennas L, channel gain h_i.

   Initialize: $\mathcal{C}_{i,j} = 1$, if i-th and j-th users can cluster, $\mathcal{C}'(t) = [i, j]$, if i-th and j-th users form t-th cluster.

   Assumption: In uncorrelated channel gain, if j-th user can cluster with i-th user, it also can cluster with all i' users such that $h_{i'} > h_i$.

2. **Sort users according to the ascending channel gain:**

   $h_1 \geq h_2 \geq \cdots \geq h_L$, $h_i = i$-th user's channel gain.

3. **Initial selection of the number of clusters:**

   If $N_t < L \leq 2N_t$, then initial clusters are $N = N_t$, elseif $L > 2N_t$, then initial clusters are $N = \lceil L/2 \rceil$.

4. **User selection for clustering:**

   Initialise user set: $\mathcal{A} = \{1, 2, \cdots, N\}$, $\mathcal{B} = \{N{+}1, N{+}2, \cdots, L\}$. Also, initialize two arrays $\mathcal{A}'$ and $\mathcal{B}'$ which contain the users, who are able to use NOMA, from set $\mathcal{A}$ and $\mathcal{B}$, respectively. Define $\mathcal{R}_{i,j}$ = correlation coefficient between h_i and h_j. Initialise $t = 1$, $t' = 1$.

($\boldsymbol{a}$) ***Clustering of users with correlated channel gains:***

for $i = 1 : N$

 for $j = N + 1 : L$

  if $\big(\mathcal{R}_{i,j} > \mathcal{R}_{i,k} \geq \rho, \forall k \neq j \in \mathcal{B}\big)$ AND $\big(\mathcal{C}_{i,j} = 1\big)$ AND $\big(\mathcal{U}_i \neq \mathcal{U}_j\big)$

   $\mathcal{C}'(t) = [i, j]$, $t \leftarrow t + 1$,

   update $\mathcal{A} \leftarrow \mathcal{A} - \{i\}$, $\mathcal{B} \leftarrow \mathcal{B} - \{j\}$.

  end

 end

end

($\boldsymbol{b}$) ***Clustering of users with uncorrelated channel gains:***

set $i = N$, $j = L$

while $j \geq N + 1$

 while $i \geq 1$

  if $\big(i \in \mathcal{A}\big)$ AND $\big(j \in \mathcal{B}\big)$ AND $\big(\mathcal{C}_{i,j} = 1\big)$ AND $\big(\mathcal{U}_i \neq \mathcal{U}_j\big)$

   $\mathcal{A}'(t') = i$, $\mathcal{B}'(t') = j$,

   update: $\mathcal{A} \leftarrow \mathcal{A} - \{i\}$, $\mathcal{B} \leftarrow \mathcal{B} - \{j\}$,

$t' \leftarrow t'+1$, $j \leftarrow j-1$, $i \leftarrow i-1$.

elseif $\big(i \in \mathcal{A}\big)$ AND $\big(j \in \mathcal{B}\big)$ AND $\big(\mathcal{C}_{i,j} \neq 1\big)$ AND $\big(\mathcal{U}_i \neq \mathcal{U}_j\big)$

update: $\mathcal{A} \leftarrow \mathcal{A} - \{i\}$, $i \leftarrow i-1$.

elseif $\big(j \notin \mathcal{B}\big)$ AND $\big(\mathcal{B} \neq \emptyset\big)$ AND $\big(\mathcal{A} \neq \emptyset\big)$ AND $\big(\mathcal{U}_i \neq \mathcal{U}_j\big)$

update: $\mathcal{A} \leftarrow \mathcal{A} - \{i\}$, $\mathcal{B} \leftarrow \mathcal{B} - \{j\}$,

$i \leftarrow i-1$, $j \leftarrow j-1$.

elseif $\big(i \notin \mathcal{A}\big)$ AND $\big(j \in \mathcal{B}\big)$ AND $\big(\mathcal{A} \neq \emptyset\big)$ AND $\big(\mathcal{U}_i \neq \mathcal{U}_j\big)$

update: $\mathcal{A} \leftarrow \mathcal{A} - \{i\}$, $i \leftarrow i-1$.

elseif $\big(i \in \mathcal{A}\big)$ AND $\big(j \notin \mathcal{B}\big)$ AND $\big(\mathcal{B} = \emptyset\big)$ AND $\big(\mathcal{U}_i \neq \mathcal{U}_j\big)$

for $k = 1 : t'-2$

$\mathcal{A}'(k) = \mathcal{A}'(k+1)$, $\mathcal{B}'(k) = \mathcal{B}'(k+1)$

end

$\mathcal{A}'(k+1) = i$, $\mathcal{B}'(k+1) = j$,

update: $\mathcal{A} \leftarrow \mathcal{A} - \{i\}$, $i \leftarrow i-1$, $k \leftarrow k+1$.

end

end

end

5. Final MIMO-NOMA clusters:

while $k \geq 1$

$\mathcal{C}'(t) = [\mathcal{A}'(k), \mathcal{B}'(k)]$,

update: $t \leftarrow t+1$, $k \leftarrow k-1$.

end

The Step 4(a) in **Algorithm** 3.4.2 indicates that, for clustering, the users, which have higher channel gain correlations with the cluster-head, can have a more re-

laxed requirement of the maximum gain differences. However, in case of uncorrelated channel gain, for every cluster of a downlink multiuser MIMO-NOMA system, the Step 4(b) in **Algorithm** 3.4.2 ensures maximum channel gain differences among the cluster-head and the other users of a cluster. It is important to note that the BS first utilizes **Algorithm** 3.4.2 for higher order user clustering, and then successively utilizes that to make the lower order user clustering for the users who are unable to form higher order MIMO-NOMA clusters.

3.5 Dynamic Power Allocation in Downlink MIMO-NOMA

For the proposed MIMO-NOMA system, we utilize a two-step power allocation method. Since each beam is utilized by all the users of a cluster, the total BS transmit power is divided into the number of transmit beams such that the transmit power for a beam is proportional to the number of users served by that beam. If all the transmit beams serve equal number of users (same cluster size), then the beam transmit powers are equally allocated. This approach can be said as nearly optimal since each MIMO-NOMA cluster contains users with similar channel gain distinctness. However, the users in each cluster are scheduled according to the NOMA principle, and thus the intra-cluster/intra-beam dynamic power allocation is crucial. For intra-cluster power allocation, I provide a dynamic power allocation solution under the constraints of the beam transmit power budget which is determined at inter-beam/inter-cluster power allocation step, minimum rate requirements of the users of the subjected MIMO-NOMA cluster, and the requirement of the minimum power differences among the NOMA received signals to perform SIC at the receiver ends.

Let us consider one MIMO-NOMA cluster, say the n-th cluster, in which the resultant normalized channel gains defined by (3.7) of all the K users are

$g_{n,1}, g_{n,2}, \cdots, g_{n,K}$, respectively, where $g_{n,1} > g_{n,2} > \cdots > g_{n,K}$. The respective guaranteed throughput requirements of all K users are assumed as $R_{n,1}, R_{n,2}, \cdots, R_{n,K}$, where $R_{n,k} > 0$, $\forall n$ and $\forall k$. If the number of MIMO-NOMA clusters is equal to the number of BS transmit antennas, then each beam utilizes the total system bandwidth B to serve the users of a cluster. If $p_{n,1}, p_{n,2}, \cdots, p_{n,K}$ are the transmit powers for 1st, 2nd, and K-th users of the n-th MIMO-NOMA cluster, respectively, then the optimal intra-cluster power allocation problem for n-th MIMO-NOMA cluster can be formulated as follows:

$$\begin{aligned}
&\underset{p}{\text{maximize}} \sum_{k=1}^{K} B \log_2 \left(1 + \frac{g_{n,k} p_{n,k}}{g_{n,k} \sum_{j=1}^{k-1} p_{n,j} + 1}\right) \qquad (3.15)\\
&\text{s.t.: } \mathbf{C_1}\text{:} \ \sum_{k=1}^{K} p_{n,k} \leq p_n \\
&\qquad \mathbf{C_2}\text{:} \ B \log_2 \left(1 + \frac{g_{n,k} p_{n,k}}{g_{n,k} \sum_{j=1}^{k-1} p_{n,j} + 1}\right) \geq R_{n,k}, \ \forall k \\
&\qquad \mathbf{C_3}\text{:} \ \Big(p_{n,k} - \sum_{j=1}^{k-1} p_{n,j}\Big) g_{n,k-1} \geq p_{tol}, \ \forall k \neq 1
\end{aligned}$$

where p_{tol} indicates the minimum received power differences among different users' signals of a MIMO-NOMA cluster to perform SIC. The optimization problem in (3.15) is similar to the dynamic power allocation in downlink NOMA for single antenna BS presented in Chapter 2. By using the closed-form solution of Chapter 2, we can find the dynamic intra-cluster power allocation solution for our proposed downlink multiuser MIMO-NOMA system. Therefore, the optimal power allocation for 1st user

of n-th MIMO-NOMA cluster is obtained as follows:

$$p_{n,1} = \frac{p_n}{\prod\limits_{\substack{j=2 \\ j\notin\mathcal{B}'}}^{K} \varphi_{n,j} \prod\limits_{\substack{j=2 \\ j\in\mathcal{B}'}}^{K} 2} - \sum_{\substack{j=2 \\ j\notin\mathcal{B}'}}^{K} \frac{(\varphi_{n,j}-1)}{g_{n,j} \prod\limits_{\substack{j'=2 \\ j'\notin\mathcal{B}'}}^{j} \varphi_{n,j'} \prod\limits_{\substack{j'=2 \\ j'\in\mathcal{B}'}}^{j} 2} - \sum_{\substack{j=2 \\ j\notin\mathcal{C}'}}^{K} \frac{p_{tol}}{2g_{n,j-1} \prod\limits_{\substack{j'=2 \\ j'\notin\mathcal{B}'}}^{j-1} \varphi_{n,j'} \prod\limits_{\substack{j'=2 \\ j'\in\mathcal{B}'}}^{j-1} 2}$$

On the other hand, the optimal power allocation solution for k-th user ($\forall k \neq 1$) of the n-th MIMO-NOMA cluster could be expressed as follows:

(i) If $k \notin \mathcal{B}'$, then

$$p_{n,k} = \frac{p_n(\varphi_{n,k}-1)}{\prod\limits_{\substack{j=k \\ j\notin\mathcal{B}'}}^{K} \varphi_{n,j} \prod\limits_{\substack{j=k \\ j\in\mathcal{B}'}}^{K} 2} - \sum_{\substack{j=k \\ j\notin\mathcal{B}'}}^{K} \frac{(\varphi_{n,j}-1)(\varphi_{n,k}-1)}{g_{n,j} \prod\limits_{\substack{j'=k \\ j'\notin\mathcal{B}'}}^{j} \varphi_{n,j'} \prod\limits_{\substack{j'=k \\ j'\in B'}}^{j} 2} - \sum_{\substack{j=k \\ j\notin\mathcal{C}'}}^{K} \frac{p_{tol}(\varphi_{n,k}-1)}{2g_{n,j-1} \prod\limits_{\substack{j'=k \\ j'\notin\mathcal{B}'}}^{j-1} \varphi_{n,j'} \prod\limits_{\substack{j'=k \\ j'\in\mathcal{B}'}}^{j-1} 2} + \frac{\varphi_{n,k}-1}{g_{n,k}}$$

(ii) If $k \in \mathcal{B}'$, then

$$p_{n,k} = \frac{p_n}{\prod\limits_{\substack{j=k \\ j\notin\mathcal{B}'}}^{K} \varphi_{n,j} \prod\limits_{\substack{j=k \\ j\in\mathcal{B}'}}^{K} 2} - \sum_{\substack{j=k \\ j\notin\mathcal{B}'}}^{K} \frac{(\varphi_{n,j}-1)}{g_{n,j} \prod\limits_{\substack{j'=k \\ j'\notin\mathcal{B}'}}^{j} \varphi_{n,j'} \prod\limits_{\substack{j'=k \\ j'\in\mathcal{B}'}}^{j} 2} - \sum_{\substack{j=k \\ j\notin\mathcal{C}'}}^{K} \frac{p_{tol}}{2g_{n,j-1} \prod\limits_{\substack{j'=k \\ j'\notin\mathcal{B}'}}^{j-1} \varphi_{n,j'} \prod\limits_{\substack{j'=k \\ j'\in\mathcal{B}'}}^{j-1} 2} + \frac{p_{tol}}{g_{n,k-1}}$$

where $\mathcal{B}'$ and $\mathcal{C}'$ are the complementary set of the minimum rate requirements of the users of n-th MIMO-NOMA cluster and the SIC constraints, respectively, which were defined in Chapter 2. In addition, $\varphi_{n,k} = 2^{\frac{R_{n,k}}{B}}$ was also defined in Chapter 2.

3.6 Numerical Results and Discussion

3.6.1 Simulation Assumptions

In this section, I provide simulation results to demonstrate the throughput/spectral-efficiency gain of the proposed MIMO-NOMA system and also compare the results

with those of conventional MIMO-OMA and conventional MIMO-NOMA (i.e., particular user specific beamforming MIMO-NOMA) systems. The major simulation parameters are listed in Table 3.1.

Table 3.1: Simulation parameters for MIMO-NOMA model

Parameter	Value
Cell radius	0.6 Km
System effective bandwidth, B	8.64 MHz
Bandwidth of one resource block	180 kHz
Number of available resource units	48
Number of antennas at BS end, N_t	$3, 5, 10$
Number of antennas at each UE end	1
Number of users/Rx-antennas in each cluster	$2, 3, 4$
BS per antenna transmit power budget, p_n	43 dBm
Antenna gain at BS/UE end	0 dBi
SIC receiver's detection threshold, p_{tol}	20 dBm
Path-loss exponent, α	4
Receiver noise density, N_0	-139 dBm/Hz

The radio channel is assumed to be the product of free-space path loss and Rayleigh fading with zero mean and unit variance. In these single-cell simulations, a single sector BS consisting of the whole hexagon is considered, where the BS is located at a corner of the cell areas. The cluster-heads are assumed to be randomly distributed around the BS. On the other hand, the random distributions of the other users of each MIMO-NOMA cluster are measured in terms of the *cell-edge coverage distance*. As an example, for an inter-site distance of 600 meter, 150m cell-edge cov-

erage distance means that the users in a cell (except the cluster-head) are distributed within 450m to 600m from the BS. Perfect CSI is assumed to be available at BS end. All the simulations are done for a single transmission time interval (TTI), that is, I only consider the instantaneous channel gains for a particular TTI. However, these instantaneous channel gains are averaged over twenty thousands of channel realizations. In addition, the number of MIMO-NOMA clusters is assumed to be equal to the number of BS transmit antennas, thus all the clusters use full spectrum resources by utilizing the MIMO principle. Fig. 3.1 demonstrates the simulation model for a 3-user MIMO-NOMA setup.

For MIMO-OMA, the spectral efficiency is calculated by considering orthogonal spectrum resource allocation among the users of each cluster and the transmit power allocation for each user of a cluster is proportional to the spectrum resource allocated to it. Also, before transmitting the data streams, the BS provides the decoding scaling weight factor and the transmit power information to the participating users in a cluster. Moreover, the users are clustered according to the sophisticated user clustering procedure presented in **Algorithm** 3.4.2. For a particular simulation, I consider same size of all MIMO-NOMA clusters, and the guaranteed throughput requirement of a particular user is same for all clusters in that simulation setup. As an example, $R_{1,2} = R_{2,2} = R_{3,2}$ is the throughput requirement for the second higher channel gain user of clusters 1, 2, and 3. For brevity, I use R_2, instead of $R_{1,2} = R_{2,2} = R_{3,2}$. Similarly, R_3 indicates the guaranteed throughput requirement for the third higher channel gain user of all cluster in a particular simulation. The throughput/spectral-efficiency calculation is performed by using Shanon's capacity formula.

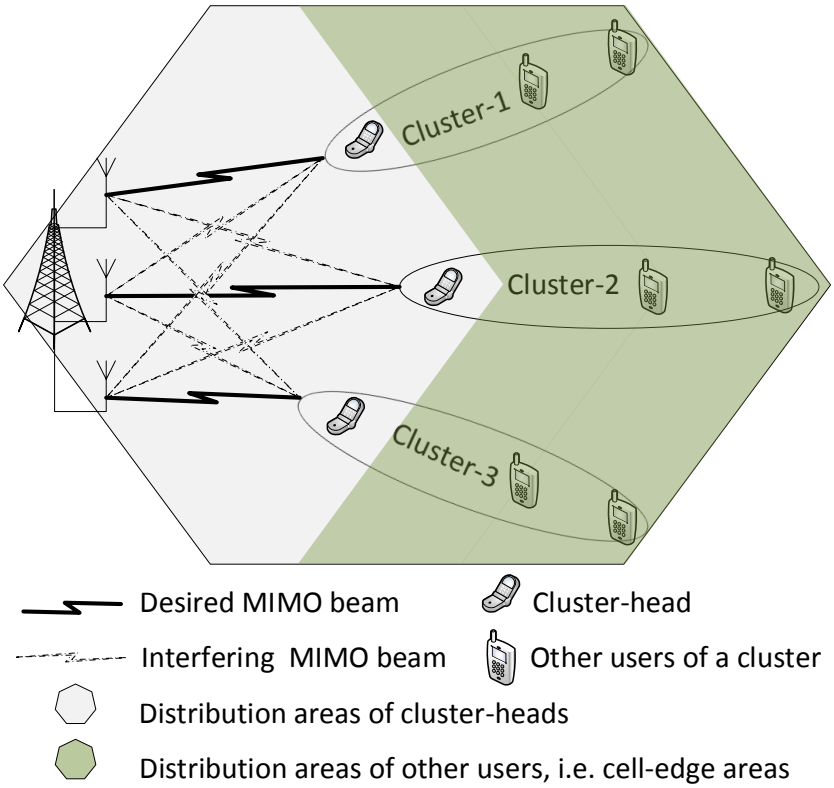

Figure 3.1: Illustrations of the simulation model for a 3-user MIMO-NOMA system, where the number of the transmit antennas, receive antennas and UEs is $3, 9$, and 9, respectively (i.e., $N_t = 3, L = 9, X = 9$).

3.6.2 Simulation Results

The performance evaluation of the proposed MIMO-NOMA system is performed at two different cases: uncorrelated Rayleigh fading channel gain users in each MIMO-NOMA cluster and correlated Rayleigh fading channel gain users in each MIMO-NOMA cluster.

Users With Uncorrelated Channel Gains

In a MIMO-NOMA system, all the users of a cluster might belong to different UEs. In addition, the throughput gain of the NOMA system increases if the channel gain differences among the participating users of a cluster increase. Therefore, it can be generally assumed that the channel gains of the users in a MIMO-NOMA cluster are uncorrelated and identically and independently distributed (iid).

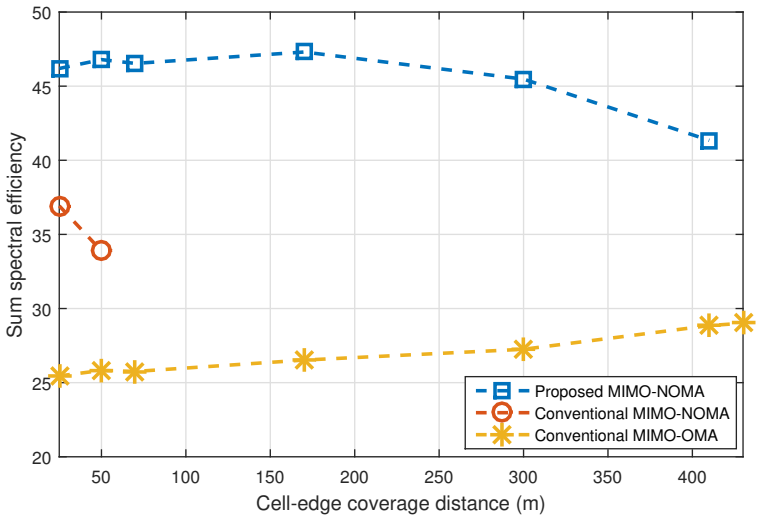

Figure 3.2: Spectral efficiency of a 2-user MIMO-NOMA system for $N_t = 3$ and $R_2 =$ OMA throughput with 50% bandwidth. The cluster-heads are distributed within 150m of the BS.

Figs. 3.2-3.3 show the sum spectral efficiencies for the proposed MIMO-NOMA, conventional MIMO-NOMA, and MIMO-OMA systems, where the guaranteed throughput requirement for the lower channel gain user of each 2-user cluster is equal to its achievable OMA throughput by considering 50% and 25% of their cluster-bandwidth, respectively. The spectral efficiency performances in Figs. 3.2-3.3 are obtained by considering 3 transmit antennas at BS end, while each MIMO-NOMA cluster contains 2 users (i.e., 2 single antenna UEs). The cluster-heads are randomly

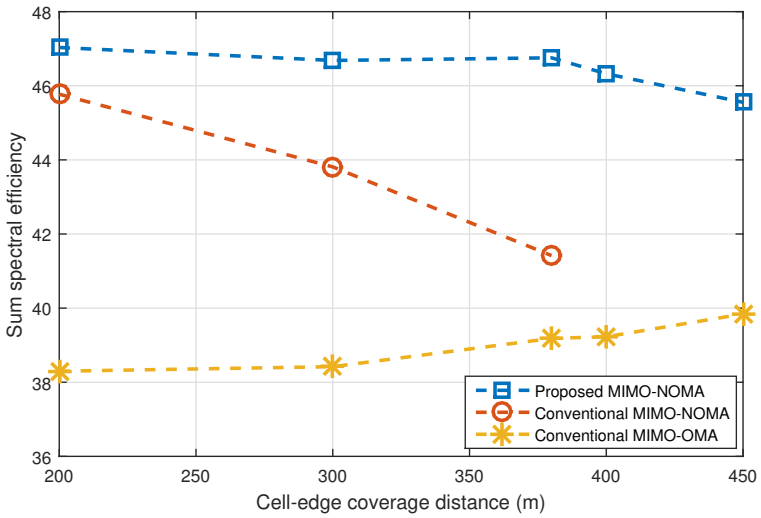

Figure 3.3: Spectral efficiency of a 2-user MIMO-NOMA system for $N_t = 3$ and $R_2 =$ OMA throughput with 25% bandwidth. The cluster-heads are distributed within 150m of the BS.

distributed within 150m closer to the BS, while the lower channel gain users are distributed in the cell edge areas. The key observation from Figs. 3.2-3.3 is that the spectral efficiency (or throughput) gain of a MIMO-NOMA system is very high in comparison to that of a MIMO-OMA system, and the comparative gain of MIMO-NOMA over MIMO-OMA is much higher at higher guaranteed throughput requirements for lower channel gain users. These results are expected because high throughput for the lower channel gain users require allocation of more spectrum resources to them in an OMA system, while NOMA can simply meet such requirements by providing higher power to the lower channel gain users. However, at high throughput requirements, the lower channel gain users are more confined within limited cell-edge areas to form NOMA clusters (Fig. 3.2). In our proposed MIMO-NOMA model, as the lower channel gain users come closer to the cluster-heads, the inter-cluster interference increases. In such a case, the amount of transmit power required to meet their

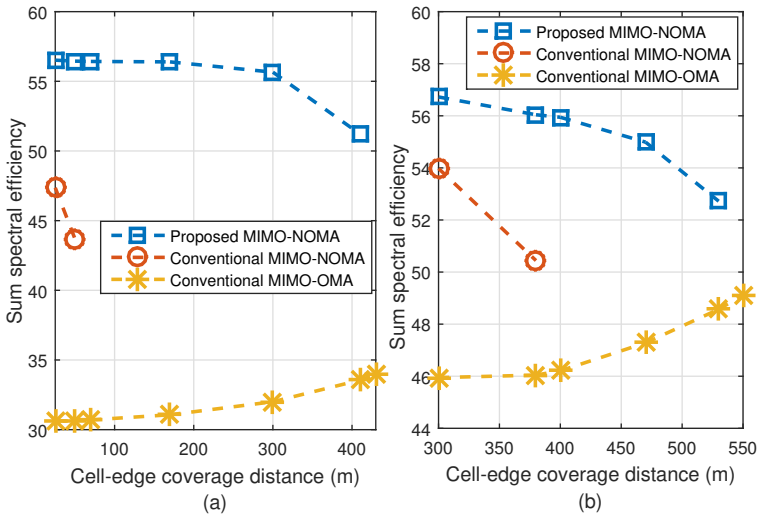

Figure 3.4: Spectral efficiency of a 2-user MIMO-NOMA system for $N_t = 3$. (a) R_2 = OMA throughput with 50% bandwidth, (b) R_2 = OMA throughput with 25% bandwidth. The cluster-heads are distributed within 50m of the BS.

higher throughput requirements may not be available at the BS end.

Figs. 3.4(a)-3.4(b) show spectral efficiency performances similar to those in Figs. 3.2-3.3, respectively, for a scenario where the cluster-heads are randomly distributed within 50m closer to the BS. As can be observed from Fig. 3.4, the spectral efficiency of MIMO-NOMA is higher at higher throughput requirements of lower channel gain users, but for such high data requirements, user clustering is limited by a certain coverage areas. In spite of similar performance trends, the spectral efficiency gains shown in Fig. 3.4 are much higher in comparison to those in Figs. 3.2-3.3. This performance enhancement is due to the improvement of the cluster-heads' channel gains since they are distributed closer to the BS. The results also show that the spectral efficiency of the proposed MIMO-NOMA system is much higher than that of a conventional MIMO-NOMA system thanks to the proposed precoding and decoding mechanisms which effectively reduces the inter-cluster interference.

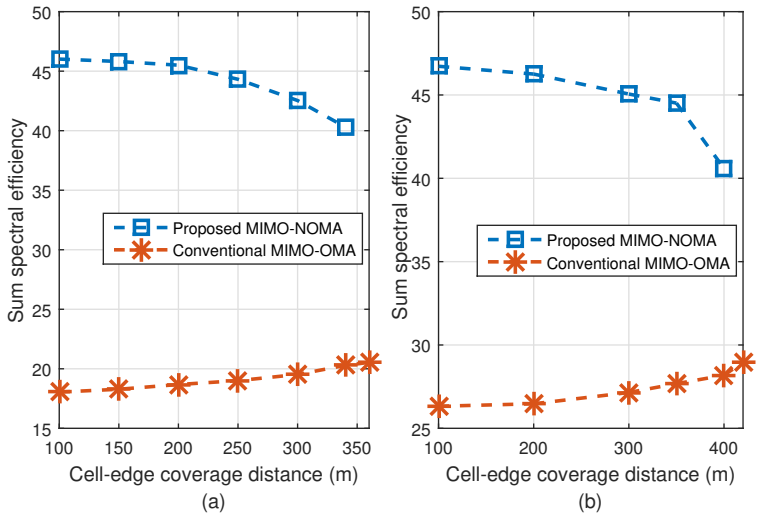

Figure 3.5: Spectral efficiency of a 3-user MIMO-NOMA system for $N_t = 3$. (a) R_i = OMA throughput with 33.33% bandwidth, (b) R_i = OMA throughput with 25% bandwidth. The cluster-heads are distributed within 150m of the BS ($i = 2, 3$).

For 3-user and 4-user clusters with 3 transmit antennas at BS, the spectral efficiency performances of the proposed MIMO-NOMA and MIMO-OMA systems are presented in Fig. 3.5 and Fig. 3.6, respectively. In Figs. 3.5-3.6, the cluster-heads are assumed to be randomly distributed within 150m closer to the BS and the other users are randomly distributed at the cell edge areas. It is to be noted that, for these system parameters, the conventional MIMO-NOMA is unable to support more than 2-user cluster. Fig. 3.5(a) and Fig. 3.5(b) are obtained, respectively, by considering the guaranteed throughput requirements for the lower channel gain users (i.e., users except the cluster-head) of each cluster to be equal to their achievable OMA throughput utilizing 33.33% and 25% of their cluster-bandwidth, respectively. Similar requirements for Fig. 3.6(a) and Fig. 3.6(b) are 25% and 16.67% of their cluster-bandwidth, respectively. By comparing all of the aforementioned results, it becomes evident that the comparative gain of the spectral efficiency of proposed MIMO-NOMA over the

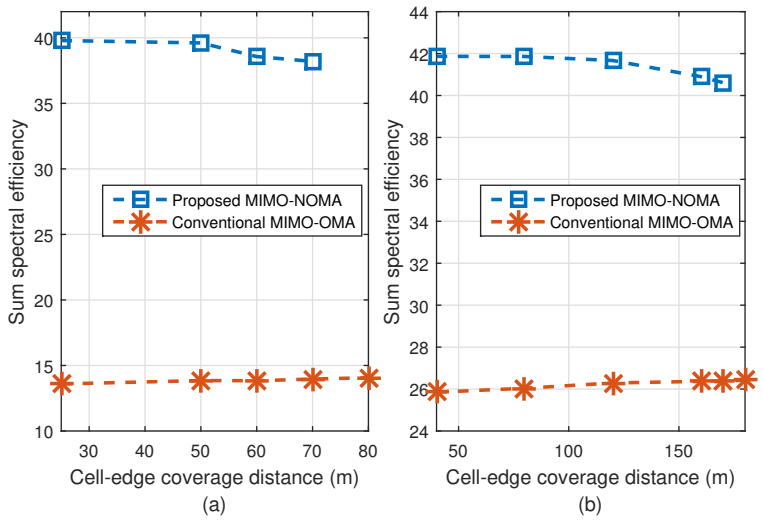

Figure 3.6: Spectral efficiency of a 4-user MIMO-NOMA system for $N_t = 3$. (a) $R_i =$ OMA throughput with 25% bandwidth, (b) $R_i =$ OMA throughput with 16.67% bandwidth. The cluster-heads are distributed within 150m of the BS ($i = 2, 3, 4$).

MIMO-OMA is much higher for higher order of user clusters, but the higher order user clusters would be confined within much smaller coverage areas. In addition, more users are required at the cell-edge areas to form higher order MIMO-NOMA systems, and the performance gain is improved if the data requirements for the cell-edge users are high. However, due to the strong inter-cluster interference and transmit power limitation, the proposed MIMO-NOMA cluster for more than 4-user is not possible for the system parameters assumed for Fig. 3.6.

With 5 transmit antennas at the BS, Figs. 3.7(a)-3.7(b) show the spectral efficiencies of the 2-user proposed MIMO-NOMA and the MIMO-OMA systems, where the throughput requirements and user distributions are similar to those used for Figs. 3.2-3.3, respectively. Fig. 3.7 shows the higher spectral efficiency for both of the MIMO-NOMA and MIMO-OMA systems in comparison of 2-user cluster systems with 3 transmit antennas at the BS (Figs. 3.2-3.4). These gains are obtained due to

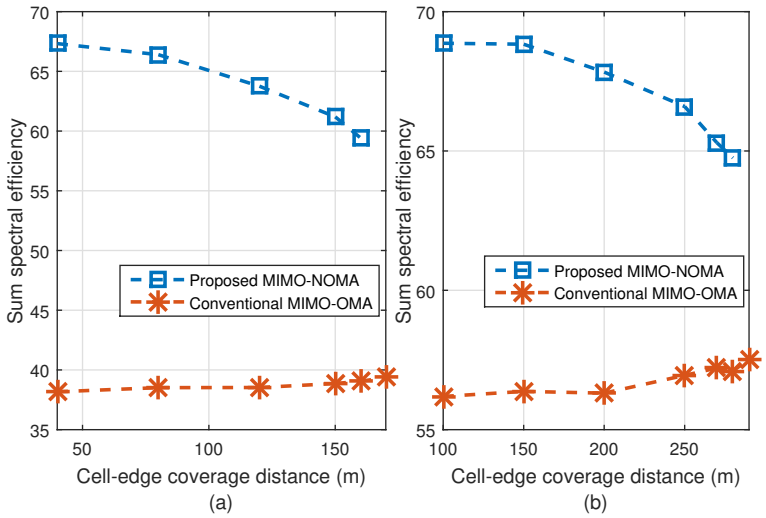

Figure 3.7: Spectral efficiency of a 2-user MIMO-NOMA system for $N_t = 5$. (a) R_2 = OMA throughput with 50% bandwidth, (b) R_2 = OMA throughput with 25% bandwidth. The cluster-heads are distributed within 150m of the BS.

the use of higher order MIMO. However, it is important to note that the inter-cluster interference of MIMO-NOMA increases in proportion to the number of transmit antennas at the BS end, i.e., for higher order MIMO. Therefore, the coverage areas for the lower channel gain users are reduced for higher order MIMO scenarios, which can be clearly observed from Fig. 3.7.

In high inter-cluster interference scenarios, higher order user clustering may not be possible to meet higher throughput requirements for lower channel gain users. Fig. 3.8 shows the spectral efficiency of a 3-user proposed MIMO-NOMA system and a MIMO-OMA system with 5 transmit antennas at the BS. The throughput requirements for the lower channel gain users are equal to their achievable OMA throughput by considering 16.67% of their cluster-bandwidth. This 3-user MIMO-NOMA is unable to meet the high throughput requirements by considering equal resource allocation among all the users in a cluster. With even more transmit antennas at the BS (10

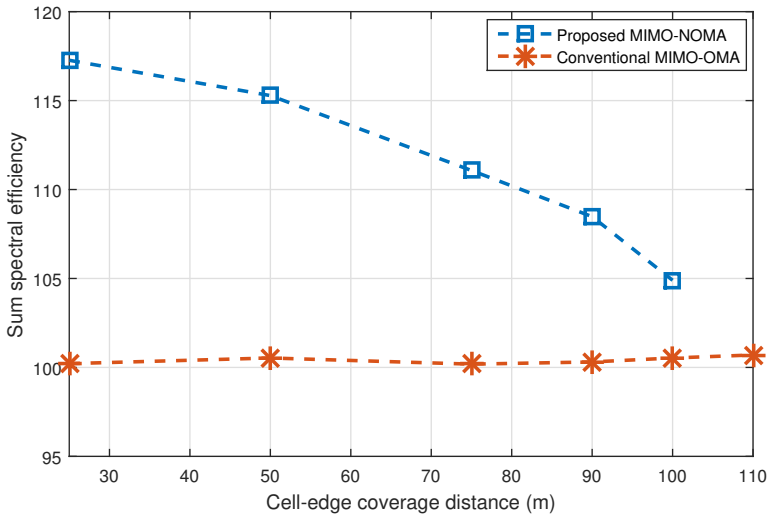

Figure 3.8: Spectral efficiency of a 3-user MIMO-NOMA system for $N_t = 5$. $R_i =$ OMA throughput with 16.67% bandwidth. The cluster-heads are distributed within 50m of the BS ($i = 2, 3$).

transmit antennas), Fig. 3.9 shows the spectral efficiency of the proposed MIMO-NOMA system and that of a MIMO-OMA system.

The performance of NOMA with higher order MIMO is vulnerable to high inter-cluster interference. One straightforward way to reduce inter-cluster interference is to control the transmit powers of different non-orthogonal clusters. In higher order MIMO systems, only a portion of the randomly distributed users can use NOMA, while the others can be scheduled on an OMA basis. In such a scenario, some of the clusters would have only one user and transmit powers can be controlled for these single-user clusters. However, the clusters utilizing NOMA should not be subjected to power control. With power control, Fig. 3.10 shows the spectral efficiency of the proposed MIMO-NOMA and the MIMO-OMA systems with 10 transmit antennas at BS. In fig. 3.10, five 2-user clusters utilize 43 dBm transmit power, while another five single-user clusters utilize 40 dBm transmit power. Fig. 3.10(a) indicates the perfor-

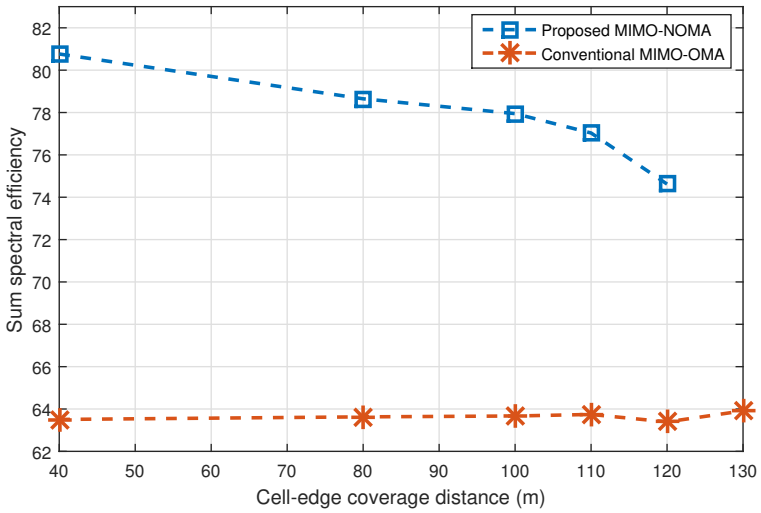

Figure 3.9: Spectral efficiency of a 2-user MIMO-NOMA system for $N_t = 10$ and R_2 = OMA throughput with 25% bandwidth. The cluster-heads are distributed within 150m of the BS.

mance when the guaranteed throughput requirements of the NOMA users are equal to the their achievable OMA throughput for equally allocated cluster-bandwidth. Note that Fig. 3.10(b) is obtained by considering 25% of the cluster-bandwidth for lower channel gain users' guaranteed throughput requirement.

Users with Correlated Channel Gains

The correlated multi-path fading between the cluster-head and other users of a cluster is beneficial for MIMO-NOMA. In conventional MIMO-NOMA, the transmit beamforming is performed based on the channel information of cluster-head, and thus the other users of a MIMO-NOMA cluster can completely remove inter-cluster interference if their channel gains are fully correlated with that of the cluster-head. Our proposed MIMO-NOMA model also provides superior throughput performance under correlated channel gain scenarios. All the simulations under correlated channel

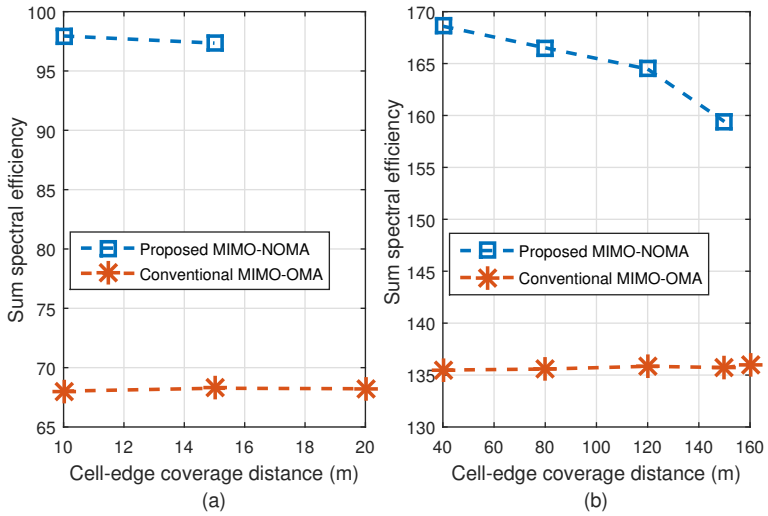

Figure 3.10: Spectral efficiency of a 2-user MIMO-NOMA system for $N_t = 10$ with power control and $L = 15$. The number of NOMA clusters is 5, another 5 users utilize OMA. (a) R_2 = OMA throughput with 50% bandwidth, (b) R_2 = OMA throughput with 25% bandwidth. The cluster-heads are distributed within 150m of the BS. For OMA spectral efficiency, all 15 users utilize OMA.

gains are performed for 2-user MIMO-NOMA clusters and the BS is assumed to be equipped with 5 transmit antennas.

For a correlation coefficient of $\rho = 0.5$ between the Rayleigh fading channel gains of the cluster-head and that of each of the other users of a MIMO-NOMA cluster, Fig. 3.11(a) and Fig. 3.11(b) show the spectral efficiency of the MIMO-NOMA and MIMO-OMA for the guaranteed throughput requirements similar to Fig. 3.2 and Fig. 3.3, respectively. Fig. 3.11 clearly demonstrates the improvement of spectral efficiency of MIMO-NOMA (both for the proposed and conventional models) in comparison of their MIMO-OMA counterpart, while the proposed MIMO-NOMA model provides much higher spectral efficiency than the conventional MIMO-NOMA. Fig. 3.11 is obtained by considering the cluster-heads' random distribution within 150m closer to the BS, while other users are considered to randomly be distributed in the cell edge

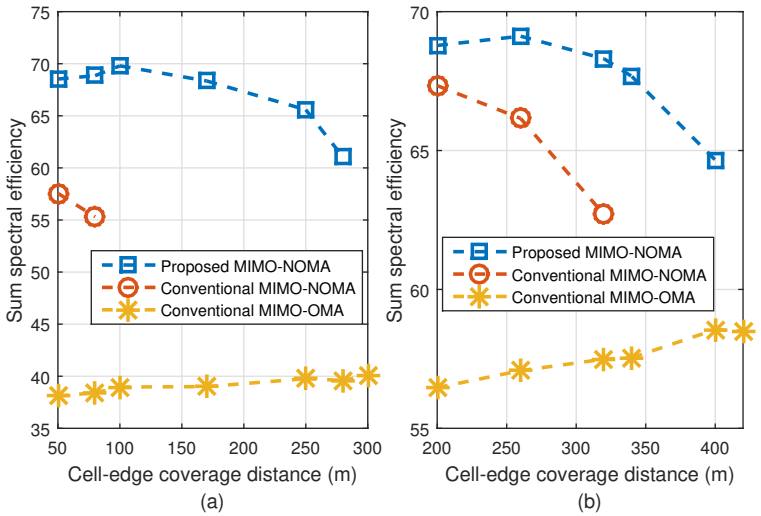

Figure 3.11: Spectral efficiency of a 2-user MIMO-NOMA system for $\rho = 0.5$ and $N_t = 5$. (a) $R_2 =$ OMA throughput with 50% bandwidth, (b) $R_2 =$ OMA throughput with 25% bandwidth. The cluster-heads are distributed within 150m of the BS.

areas.

The spectral efficiencies for the MIMO-NOMA and MIMO-OMA systems for different correlation coefficient ($\rho = 0$ to 1) are demonstrated in Fig. 3.12. The cluster-heads in Fig. 3.12 are assumed to be randomly be distributed within 150m closer to the BS, while the other users are considered to randomly be distributed within 200m of cell edge distance. In addition, the guaranteed throughput requirements of the users considered in Fig. 3.12(a) and Fig. 3.12(b) are similar to those of the users considered in Fig. 3.2 and Fig. 3.3, respectively. Fig. 3.12 shows a huge improvement of the spectral efficiency of MIMO-NOMA system when highly correlated users are clustered. MIMO-NOMA clusters with very high correlated channel gains could completely cancel inter-cluster interference, thus the throughput performance is not affected by the number of transmit antennas. In such a channel condition, higher order MIMO-NOMA cluster (i.e., more users in a cluster) can provide higher

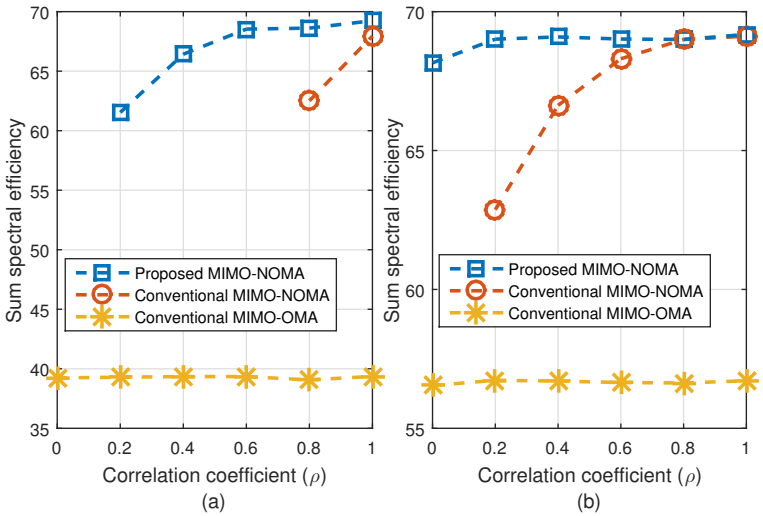

Figure 3.12: Spectral efficiency of a 2-user MIMO-NOMA system for different values of ρ for $N_t = 5$. (a) R_2 = OMA throughput with 50% bandwidth, (b) R_2 = OMA throughput with 25% bandwidth. The cluster-heads are distributed within 150m of the BS and other users are distributed within 200m of cell edge.

throughput gains.

3.7 Summary

For a downlink transmission with more receive antennas than the transmit antennas, the application of MIMO-NOMA has been investigated in this chapter. After providing system and signal models, robust user clustering algorithm has been proposed to group the UE receive antennas into a number of clusters equal to or more than the number of BS transmit antennas. A single beamforming vector is then shared by all the receive antennas in a cluster. After that, a linear beamforming technique also has been proposed which significantly cancel the inter-cluster interference for all the users of each cluster. On the other hand, the receive antennas in each cluster are scheduled on power domain NOMA basis with SIC at the receiver ends. For

inter-cluster and intra-cluster power allocation, dynamic power allocation solution has been provided with an objective to maximizing the overall cell capacity. An extensive performance evaluation has been carried out for the proposed MIMO-NOMA system and the results are compared with those for conventional OMA-based MIMO systems and other existing MIMO-NOMA solutions. The numerical results quantify the capacity gain of the proposed MIMO-NOMA model over MIMO-OMA and other existing MIMO-NOMA solutions.

Chapter 4

CoMP in Downlink Multi-cell NOMA Systems

To maximize the overall spectral efficiency and/or minimize the total power consumption in downlink NOMA, the BS allocates transmit power in such a way that the SIC decoding is performed according to an ascending order of the channel gains of the NOMA users. This power allocation strategy results in a low received signal-to-intra-cell-interference ratio for lower channel gain users (e.g., cell-edge users) those are also vulnerable to inter-cell interference. Therefore, inter-cell interference management will be crucial in multi-cell downlink NOMA systems. To mitigate inter-cell interference for traditional downlink OMA-based 4G cellular systems, third generation partnership project (3GPP) adopted CoMP transmission technique in which multiple cells, called *CoMP set*, coordinately schedule/transmit to the interference-prone users [8] [7] [27]. This Chapter focuses on the application of CoMP in NOMA-based multi-cell downlink transmission scenarios in order to improve the spectral efficiency performance of the system.

4.1 System Model of Downlink CoMP-NOMA

In this purposed CoMP-NOMA model for downlink transmission, CoMP transmission is used for users experiencing strong receive-signals from multiple cells under a downlink co-channel homogeneous network. Various CoMP schemes are applied to the CoMP-users experiencing inter-cell interference under two-cell coMP set, while distributed power allocation for NOMA users is utilized in each coordinating cell. This model first determines the users requiring CoMP transmissions from multiple cells and those requiring single transmissions from their serving cells. After that, different NOMA clusters are formed in individual cells in which the CoMP-users are clustered with the non-CoMP-users in a NOMA cluster. After clustering the users, each cell independently allocates transmit power to its NOMA users by utilizing the optimal power allocation solution proposed in Chapter 2. However, in a CoMP-NOMA system, the decoding order for the users in a NOMA cluster will be different from that in a conventional single-cell NOMA system as in Chapter 2, and thus the power allocation solution will also be different although it can be solved in a way similar to that in Chapter 2. In addition, This proposed CoMP-NOMA model considers single antenna at transmitter and receiver ends.

4.2 CoMP Schemes for Downlink CoMP-NOMA

In the proposed CoMP-NOMA model, I utilize the NOMA throughput formula in a different order than previous chapters but the working principle is exactly same. Here, in each NOMA cluster, the CoMP-users are defined prior than the non-CoMP-users regardless their respective channel gains, in order to ensure the clustering of a CoMP-user at multiple cells in a the CoMP set. First I define the achievable throughput for a NOMA user according to their decoding order under the proposed COMP-NOMA

model. After that, different CoMP schemes are discussed considering single antenna BS and user equipment (UE), and identify their applicability for a NOMA-based transmission model.

4.2.1 Achievable Downlink Throughput for a NOMA User

Let us assume a downlink NOMA cluster with n users and the following decoding order: UE_1 is decoded first, UE_2 is decoded second, and so on. Therefore, UE_1's signal will be decoded at all the users' ends, while UE_n's signal will be decoded only at her own end. Since UE_1 can only decode her own signal, it experiences all the other users' signals as interference, while UE_n can decode all users' signals and removes inter-user interference by applying SIC. Therefore, the achievable throughput for the i-th user can be written as follows:

$$R_i = B \log_2 \left(1 + \frac{p_i \gamma_i}{\sum\limits_{j=i+1}^{n} p_j \gamma_i + 1} \right), \quad \forall i = 1, 2, \cdots, n \tag{4.1}$$

where γ is the normalized channel gain with respect to noise power density over NOMA bandwidth B, and p_i is the allocated transmit power for UE_i. The necessary condition for power allocation to perform SIC is:

$$\Big(p_i - \sum_{j=i+1}^{n} p_j \Big) \gamma_j \geq p_{tol}, \quad \forall i = 1, 2, \cdots, n-1 \tag{4.2}$$

where p_{tol} is the minimum difference in received power (normalized with respect to noise power) between the decoded signal and the non-decoded inter-user interference signals. To maximize the overall cell throughput and/or minimize the power consumption, the decoding should be performed in an ascending order of the chan-

nel power gains of the NOMA users. That is, the aforementioned decoding order will provide maximum sum-throughput if the channel gain for NOMA users are such that: $\gamma_n > \gamma_{n-1} > \cdots > \gamma_1$. In such a optimal scenario, the power allocation condition could be simplified as follows:

$$\Big(p_i - \sum_{j=i+1}^{n} p_j\Big)\gamma_i \geq p_{tol}, \quad \forall i = 1, 2, \cdots, n-1 \tag{4.3}$$

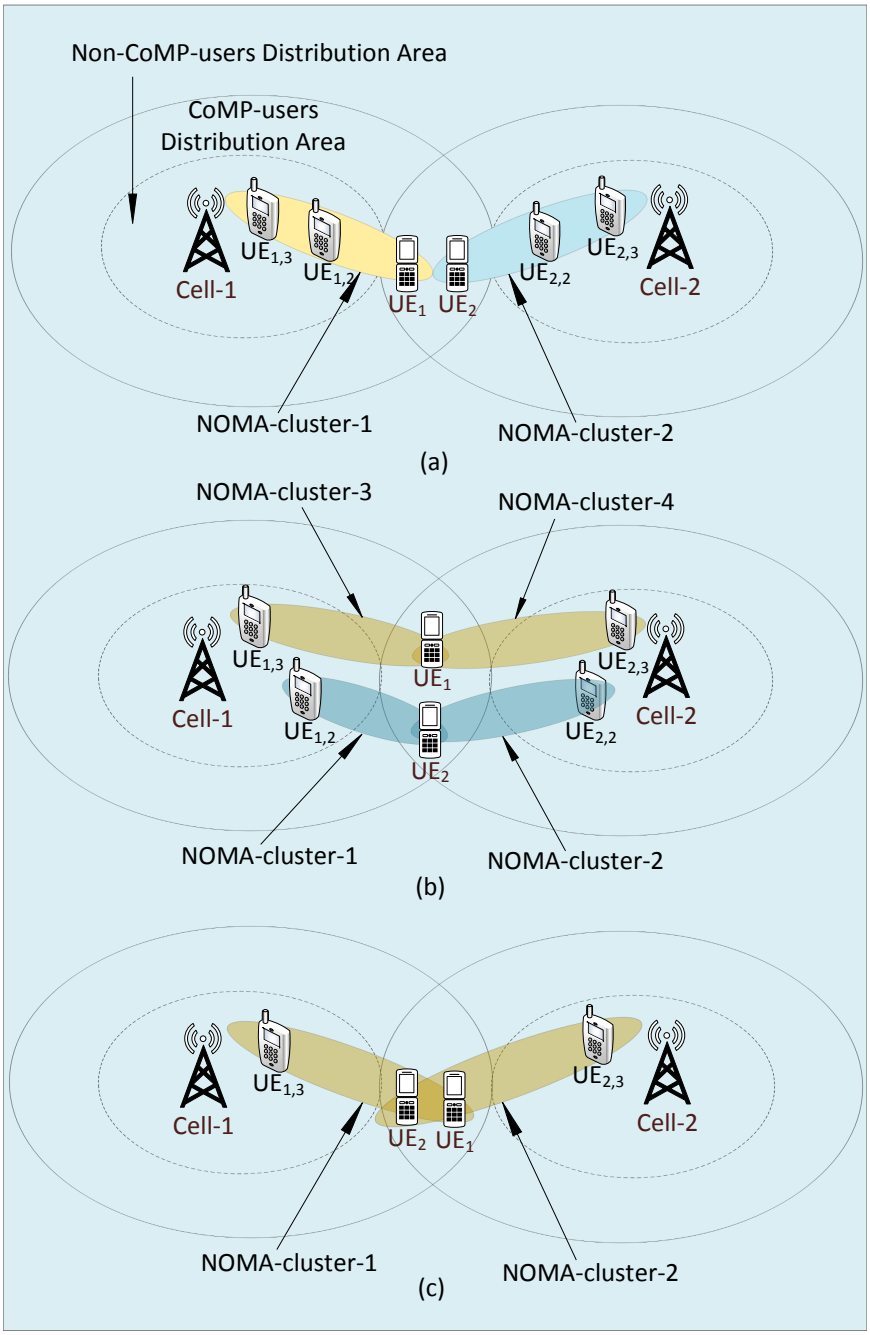

Figure 4.1: Illustrations of the various CoMP schemes for a downlink NOMA system: (a) CS-CoMP-NOMA, (b) JT-CoMP-NOMA for multiple CoMP-users and multiple non-CoMP-users, and (c) JT-CoMP-NOMA for multiple CoMP-users and a single non-CoMP-user.

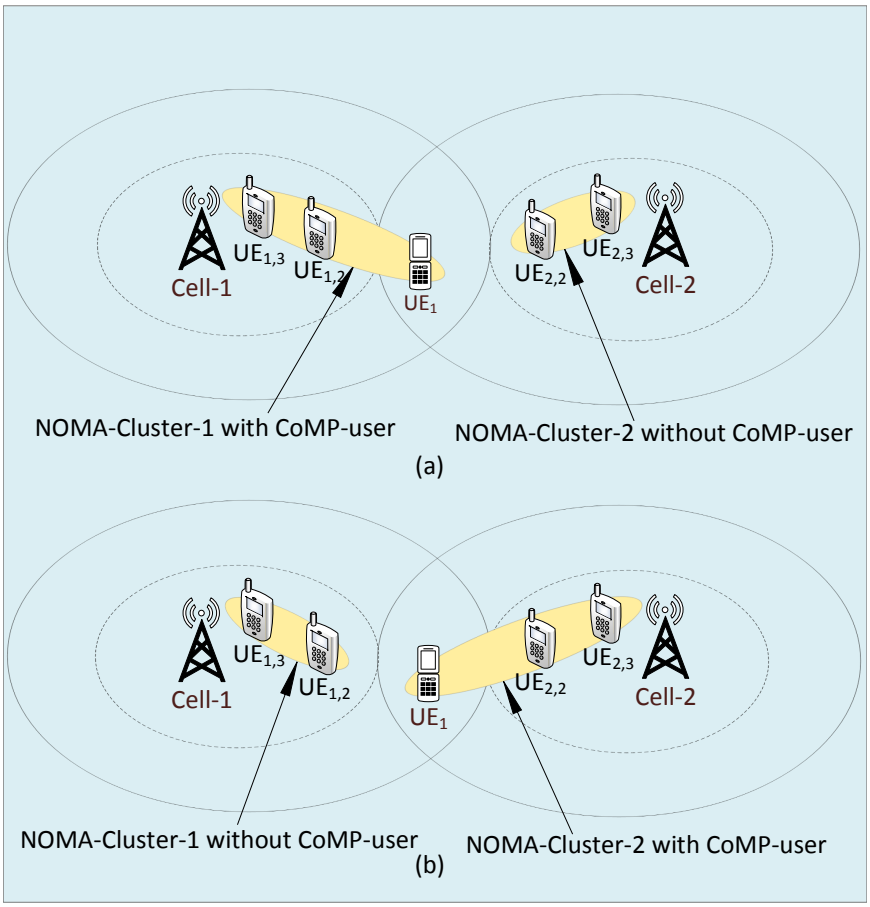

Figure 4.2: Illustrations of the DPS-CoMP schemes at downlink NOMA system for a single CoMP-user: (a) CoMP-user is clustered in cell−1, (b) CoMP-user is clustered in cell−2.

4.2.2 Coordinated Scheduling (CS)-CoMP in Downlink NOMA

In CS-CoMP, CoMP-users are scheduled on orthogonal spectrum resources and receive desired signals only from their serving cells, respectively, while an orthogonal spectrum allocation is done based on coordination among the CoMP-cells. In CS-CoMP-NOMA, each CoMP-user is grouped into one NOMA cluster and does not experience inter-cell interference due to the orthogonal spectrum allocation among

the CoMP-cells. Therefore, the working principle of CS-CoMP-NOMA is similar to that of traditional single-cell NOMA.

Fig. 4.1(a) illustrates CS-CoMP-NOMA for a homogeneous two-cell CoMP scenario, where two CoMP-users, UE_1 and UE_2, are allocated orthogonal spectrum resources from cell-1 and cell-2, respectively. In cell-1, UE_1 is grouped into a NOMA cluster with the non-CoMP-users $UE_{1,2}$ and $UE_{1,3}$ of cell-1. Similarly, UE_2 forms a NOMA cluster with the non-CoMP-users $UE_{2,2}$ and $UE_{2,3}$ at cell-2. After spectrum resources are allocated to each NOMA cluster, the CS-CoMP-NOMA is similar to the traditional single-cell NOMA which offers spectral efficiency gains over its OMA counterparts Chapter 2.

4.2.3 Joint Transmission (JT)-CoMP in Downlink NOMA

In JT-CoMP schemes under single antenna BS and UE, multiple cells (i.e., CoMP-cells) simultaneously transmit the same data to a CoMP-user by using the same spectrum resources.Since the same data is sent by all CoMP-cells, the reception performance for CoMP-users is improved. In a JT-CoMP-OMA system with multiple CoMP-users served by the same CoMP set, the users are scheduled on orthogonal spectrum resources. However, in JT-CoMP-NOMA, one or multiple non-CoMP-users from each cell form NOMA cluster with one or multiple CoMP-users.

In Fig. 4.1(b), a JT-CoMP-NOMA scheme is illustrated where two CoMP-users are grouped into two different NOMA clusters with different non-CoMP users. Thus, UE_1 receives the same message from cell-1 and cell-2 simultaneously over the same spectrum resource which is orthogonal to that for the other CoMP-user (i.e., UE_2). On the other hand, in Fig. 4.1(c), two CoMP-users are in the same NOMA cluster and both of them receive transmissions from the two CoMP cells simultaneously

over the same spectrum resource. The CoMP-users in a NOMA cluster receive their desired signals by utilizing SIC according to their decoding order. However, in a JT-CoMP-NOMA system, for successful decoding in presence of multiple CoMP-users in a NOMA cluster, the two following necessary conditions need to be satisfied:

- **The signals for users receiving CoMP transmissions will be decoded prior to those for the users receiving single transmissions from their serving cells**. To illustrate this condition, let us consider Fig. 4.1(c), where two CoMP-users, UE_1 and UE_2, receive CoMP transmission from both cells, while two non-CoMP-users, $UE_{1,3}$ and $UE_{2,3}$, receive their desired signals only from cell-1 and cell-2, respectively. Now, with the JT-CoMP scheme, the message signals for UE_1 and UE_2 will need to be decoded prior to decoding the signals for $UE_{1,3}$ and $UE_{2,3}$. In other words, $UE_{1,3}$ and $UE_{2,3}$ will decode and cancel the message signals for UE_1 and UE_2 prior to decoding their own signals. To verify the condition, let us consider the opposite scenario, that is, UE_1 and UE_2 need to decode the message signals for $UE_{1,3}$ and $UE_{2,3}$ before decoding their desired signals. To decode $UE_{1,3}$'s signal at UE_1 or UE_2 end, the received power for $UE_{1,3}$ need to be higher than the summation of the received powers for UE_1 and UE_2. Note that, UE_1, UE_2, and $UE_{1,3}$ are in the same NOMA cluster. Although cell-1 can allocate more power for $UE_{1,3}$ than the sum power for UE_1 and UE_2, the received power for $UE_{1,3}$ cannot be guaranteed to be higher than the sum of the received powers for UE_1 and UE_2. The reason is that both UE_1 and UE_2 will receive the same signal from both of the CoMP-cells, and thus their received powers will be improved. In addition, for the opposite decoding scenario, the CoMP-users need to decode all the non-CoMP users from all CoMP-cells those are clustered together, and

thus more SIC application need to perform at CoMP-users' ends in comparison of aforementioned necessary condition for decoding order.

- **The decoding order for a CoMP-user will be same in all NOMA clusters formed at different CoMP-cells in which the CoMP-user is clustered**. To illustrate this condition, let us again consider Fig. 4.1(c). If the decoding order for UE_1 is prior than UE_2 in cell-1, then it would be similar for cell-2 regardless the channel gains of UE_1 and UE_2 in cell-2. SIC is only possible at CoMP-user ends if this condition is satisfied. This condition also implies that the traditional power allocation for cell-throughput maximization will not hold in a JT-CoMP-NOMA system.

4.2.4 Dynamic Point Selection (DPS)-CoMP in Downlink NOMA

In a DPS-CoMP system, the data streams for each CoMP-user become available in all of the CoMP-cells but only one cell sends data at a time. In each subframe, all the CoMP-cells check the channel quality for each CoMP-user, and based on the maximum channel gain only one cell is dynamically selected for data transmission. Therefore, DPS-CoMP can be applied in a NOMA system where the user clustering and power allocation need to be performed at each subframe. After determining the serving cell in DPS-CoMP, a CoMP-user is grouped into a NOMA cluster with the non-CoMP-users served by that cell.

Fig. 4.2(a) and fig. 4.2(b) illustrate the working principle of DPS-CoMP-NOMA at two different subframes, by assuming that the CoMP-user has better channel gain with cell-1 in subframe-1 and with cell-2 in subframe-2. Since each CoMP-user is grouped into one cluster at a time and does not experience any inter-cell interference, the decoding order and power allocation for DPS-CoMP-NOMA is exactly similar to

that for the convention NOMA for a single cell system with dynamic power allocation Chapter 2.

4.2.5 Coordinated Beamforming (CB)-CoMP in Downlink NOMA

The fundamental principle of coordinated beamforming (CB)-CoMP is similar to that of the distributed MIMO system, where the coordinating cells act as a distributed antenna array under a virtual BS. One CoMP-user is associated with one CoMP-cell, while all the CoMP-cells use same spectrum resources to serve their associated CoMP-users by utilizing the distributed MIMO principle. To apply CB-CoMP scheme in downlink NOMA system, one or multiple non-CoMP-users need to be clustered with a CoMP-user at each CoMP-cell. However, to cancel the inter-cell interference for CoMP-users using the same spectrum resources, the zero-forcing MIMO beamforming need to be performed by using the CoMP-users' channel vector corresponding to the CoMP-cells. Since the same beam will be used for all non-CoMP-users and a CoMP-user in a CB-CoMP-NOMA cluster, the non-CoMP-user may will not be able to decode the message signals due to the mismatch in dimension between their channel vector (which has single dimension since only one channel exists with the serving cell) and precoding vector (which has a dimension equal to the CoMP-set size, and precoding is done based on the CoMP-users' channel gains). Therefore, CB-CoMP is not applicable in for a CoMP-NOMA system.

4.3 Deployment Scenarios for CoMP in Downlink NOMA Systems

In this section, we discuss different CoMP-NOMA deployment models based on the users' distribution (i.e., number of CoMP-users and non-CoMP-users) in a two-cell

CoMP set.

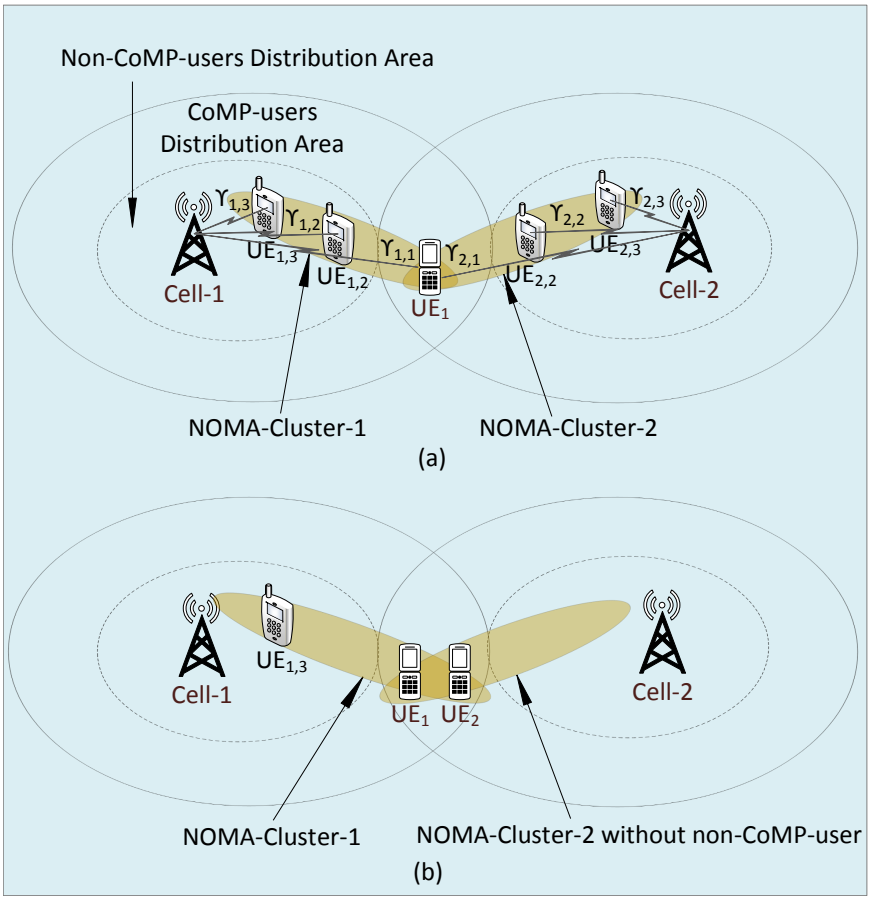

Figure 4.3: Illustrations of the various CoMP-NOMA deployment scenarios: (a) deployment scenario−1, (b) deployment scenario−3.

CoMP-NOMA Deployment Scenario−1

In this scenario, only one CoMP-user is considered for a CoMP-set, while one or multiple non-CoMP-users are considered in each CoMP-cell of that CoMP-set. Since there is only one CoMP-user, the JT-CoMP-NOMA and DPS-CoMP-NOMA schemes are applicable in this scenario. Fig. 4.3(a) illustrates the deployment scenario−1 for a two-cell CoMP set in a JT-CoMP-NOMA set up, where the CoMP-user is included

in both of the NOMA clusters formed in cell−1 and cell−2, and utilizes the same spectrum resources. By exploiting the NOMA principle, each cell superposes their NOMA users' message signals in the same spectrum resources, and thus the CoMP-user's message signal is superposed at both cells. To decode the desired signal, the decoding order for the CoMP-user needs to be same in both the NOMA clusters.

Let $\gamma_{1,1}$, $\gamma_{1,2}$, and $\gamma_{1,3}$ denote the normalized channel power gains (with respect to noise power) for UE_1, $\mathrm{UE}_{1,2}$ and $\mathrm{UE}_{1,3}$ in cell−1, respectively, and $\gamma_{2,1}$, $\gamma_{2,2}$, and $\gamma_{2,3}$ are the normalized channel power gains for UE_1, $\mathrm{UE}_{2,2}$ and $\mathrm{UE}_{2,3}$ in cell−2, respectively. If the decoding order is based on the user's subscript, i.e., the message signal for UE_1 is decoded prior to decoding the other users' signals in NOMA cluster−1 and NOMA cluster−2, then the achievable throughput for the CoMP-user is:

$$R_1 = B\log_2\left(1+\frac{\sum\limits_{i=1}^{2} p_{i,1}\gamma_{i,1}}{\sum\limits_{i=1}^{2}\sum\limits_{j=2}^{3} p_{i,j}\gamma_{i,1}+1}\right). \tag{4.4}$$

The achievable throughput for the j-th non-CoMP-user in cell−i is:

$$R_{i,j} = B\log_2\left(1+\frac{p_{i,j}\gamma_{i,j}}{\sum\limits_{k=j+1}^{3} p_{i,k}\gamma_{i,j}+\sum\limits_{m=1,m\neq i}^{2}\sum\limits_{l=2}^{3} p_{m,l}\gamma'_{i,j}+1}\right) \tag{4.5}$$

where $i = 1, 2$ and $j = 2, 3$. The term $\gamma'_{m,j}$ is the normalized channel power gain for the j-th non-CoMP-user in i-th cell but measured from m-th cell ($m \neq i$) of the CoMP set, and represents the inter-cell interference for non-CoMP-users. If the inter-cell interference for a non-CoMP-user from any cell of a CoMP set is negligible, then

the achievable NOMA throughput for the non-CoMP users can be approximated as:

$$R_{i,j} = B\log_2\left(1+\frac{p_{i,j}\gamma_{i,j}}{\sum_{k=j+1}^{3} p_{i,k}\gamma_{i,j}+1}\right), \quad \forall i=1,2, \text{ and } \forall j=2,3. \tag{4.6}$$

4.3.1 CoMP-NOMA Deployment Scenario−2

In this scenario, we assume multiple CoMP-users in a CoMP set, while one or multiple non-CoMP-users in each of the CoMP-cells of that CoMP set. This scenario is similar to those models illustrated in Fig. 1, in which all of the CS-CoMP, JT-CoMP, and DPS-CoMP schemes are applicable. In case of JT-CoMP-NOMA for Fig. 4.1(b), the achievable throughput formulas for CoMP-user and non-CoMP users for each NOMA cluster pair, which includes a common CoMP-user, are similar to those for scenario−1. For Fig. 4.1(b), it is noted that each NOMA cluster can only include one CoMP-user, thus the spectrum resource for different CoMP-users are orthogonal. However, for the JT-CoMP-NOMA deployment scenario−2 in Fig. 4.1(c), multiple CoMP-users are grouped into each NOMA cluster formed at different CoMP-cells but their decoding order will be similar in all cases. Similar to the scenario−1, if the decoding order is based on the user's subscript, then the achievable throughput formula for CoMP-users can be expressed as:

$$R_j = B\log_2\left(1+\frac{\sum_{i=1}^{2} p_{i,j}\gamma_{i,j}}{\sum_{i=1}^{2}\sum_{k=j+1}^{3} p_{i,k}\gamma_{i,j}+1}\right), \quad \forall j=1,2. \tag{4.7}$$

On the other hand, the formulas for achievable throughput for non-CoMP users are similar to those for scenario−1.

4.3.2 CoMP-NOMA Deployment Scenario−3

In a user-centric CoMP system, different CoMP-users of a particular cell can receive CoMP transmissions from CoMP-cells belonging to different CoMP sets. In such a case, for a JT-CoMP-NOMA system, the CoMP-users of different CoMP sets will interfere with each other and thus will not form NOMA cluster. Although they can form NOMA cluster by maintaining their decoding order requirement, the inter-cell interference that we have neglected in scenario−1 would be excessively high. Therefore, it can be recommended that NOMA clusters are formed by including CoMP-users from one CoMP set at a time.

Based on the aforementioned idea for CoMP-NOMA clustering, for a particular CoMP-set, some cells may not have non-CoMP-user to form NOMA cluster with the CoMP-users, while other cells of that CoMP set may have sufficient non-CoMP-users. Fig. 4.3(b) illustrates the CoMP-NOMA deployment scenario−3 for a two-cell CoMP set, where cell−2 does not have any non-CoMP-user to form a NOMA-cluster with the CoMP-users, while cell−1 forms a NOMA cluster by grouping both of the CoMP-users and the non-CoMP-user. In this situation, in addition to the requirement of same decoding order for CoMP-users, the decoding order among the CoMP-users itself significantly affects the spectrum efficiency. In the section on numerical results, we will demonstrate the spectral efficiency performance for two different decoding orders of CoMP-users. The achievable throughput formulas for CoMP and non-CoMP users can, however, be expressed similarly as in scenario−2.

4.4 Spectral Efficiency Performance of Downlink CoMP-NOMA Systems

4.4.1 Simulation Assumptions

In this section, I analyze the gain in spectral efficiency for downlink CoMP-NOMA systems for different CoMP-NOMA schemes and deployment scenarios discussed earlier when compared to the CoMP-OMA systems. The average spectral efficiency (in bits/sec/Hz) is evaluated for all the cells in a CoMP set by using the Shannon's capacity formula. We assume that the BSs do not use sectorization and a BS is located at the center of a circular coverage area. In this proposed CoMP-NOMA systems, to allocate optimal downlink power among the users in a cell, I use the dynamic power allocation model derived in Chapter 2. It is to be noted that the optimal power allocation in Chapter 2 is derived assuming that decoding is performed in an ascending order of channel power gains, that is, a particular user can decode and then cancel all users' signals who have lower channel power gain while all the higher channel gain users act as interferer. In the proposed CoMP-NOMA models, the same CoMP-users would be grouped into multiple NOMA clusters at different CoMP-cells but their decoding order will be same for all clusters. Therefore, the decoding order for a CoMP-user will not follow the the ascending channel gain at all NOMA clusters. For each NOMA cluster, however, I utilized the optimal power allocation solution for the resultant decoding order for CoMP-users by following the same procedure as in Chapter 2.

In case of orthogonal multiple access (OMA), the transmit power is allocated in proportional to the amount of spectrum resources. The major simulation parameters are as follows: inter-BS distance is 1 Km, BS transmit power is 43 dBm, noise spectral

density is -139 dBm/Hz, system overall bandwidth is 8.64 MHz, path-loss coefficient is 4, the minimum difference between received power (normalized with respect to noise power) of the decoded signal and the non-decoded signal(s) (i.e., p_{tol}) is 20 dBm, and single antenna at BS and UE ends. I also assume that the non-CoMP-users are distributed within the cell-center areas for 400 m radius in each cell, and the non-CoMP-users of two different cells do not interfere with each other. In addition, in each NOMA cluster, the user who can decode and then cancel all the other users' signals (and hence does not experience any inter-user interference), is referred to as the *cluster-head.*.

A flat-fading Rayleigh channel having channel power gain with zero mean and unit variance as well as path-loss is considered. For all simulations, the non-CoMP-users are considered at a fixed distance within their distribution areas, while a random distance is considered for CoMP-users outside the non-CoMP-user's coverage areas (measured in terms of the *cell-edge coverage distance*). Perfect channel state information (CSI) is assumed to be available at the BS ends. All the simulations are done for a single transmission time interval. However, these instantaneous channel gains are averaged over fifty thousands channel realizations. It is also noted that a NOMA cluster achieves maximum throughput gain if the decoding order follows the ascending channel power gain. However, to observe the impact for different decoding orders, we consider that the NOMA cluster in one CoMP-cell follows the ascending channel power gain decoding, while another CoMP-cell follows a different decoding order while maintaining the same decoding order for CoMP-users. Since the working principles of CB-CoMP-NOMA, and DPS-CoMP-NOMA are the same as that of the conventional single-cell NOMA, I mainly evaluate the performance for JT-CoMP-NOMA in this thesis.

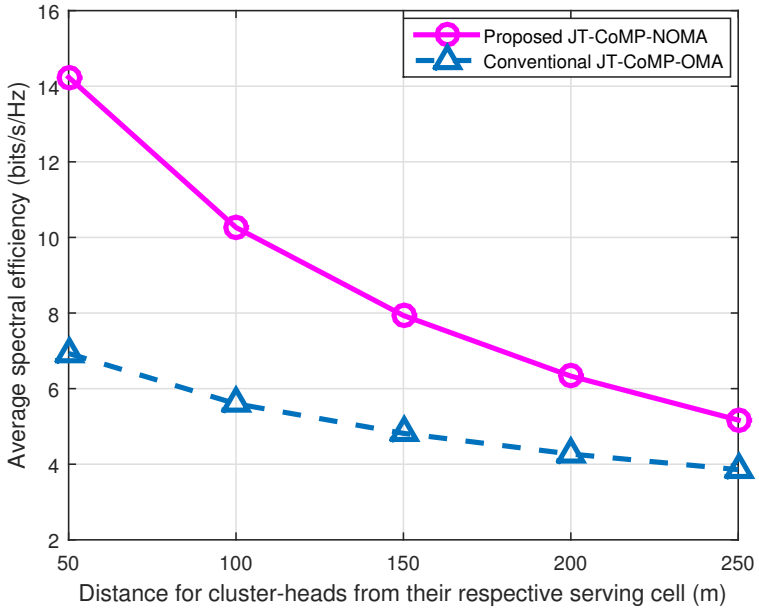

Figure 4.4: Average spectral efficiency for JT-CoMP-NOMA and JT-CoMP-OMA systems for deployment scenario−1 with one CoMP-user and two non-CoMP-users in each CoMP-cell.

4.4.2 Simulation Results and Discussions

I simulate three different models for three aforementioned *deployment scenarios*. Fig. 4.4 shows the average spectral efficiency for the proposed JT-CoMP-NOMA and the conventional JT-CoMP-OMA for *deployment scenario*−1 illustrated in Fig. 4.3(a), where we consider one CoMP-user in a two-cell CoMP set and two non-CoMP-users in each cell. The guaranteed throughput requirement for each user in JT-CoMP-NOMA system is equal to its achievable JT-CoMP-OMA throughput considering equal spectrum allocation. For example, if B be the system bandwidth, for OMA operations, each CoMP-user and non-CoMP-user will be allocated $B/3$ bandwidth from each cell. For the CoMP-user, both the cells allocate the same spectrum resource and transmit the same data stream, thus the receiver performance is improved. The

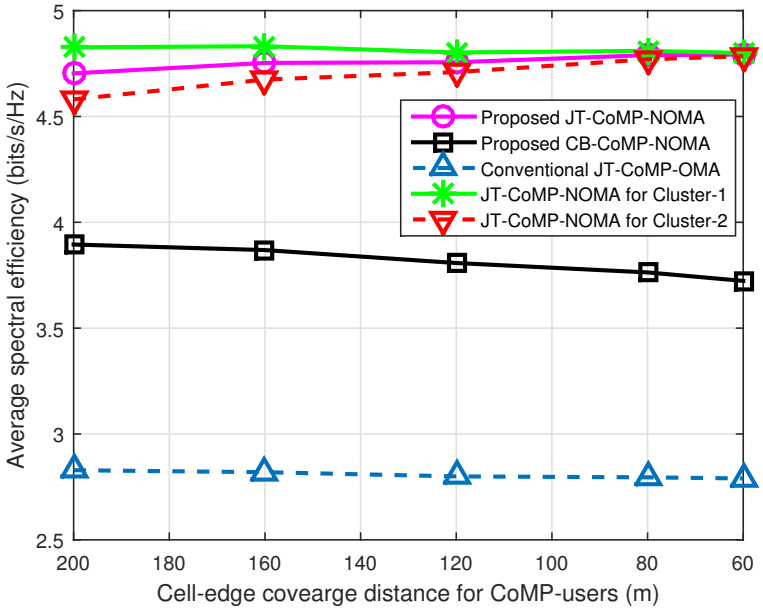

Figure 4.5: Average spectral efficiency for JT-CoMP-NOMA, CS-CoMP-NOMA and JT-CoMP-OMA systems for deployment scenario−2 with two CoMP-users and one non-CoMP-user in each CoMP-cell.

random distance for CoMP-user is considered at 200 m cell edge radius. The average spectral efficiency is measured for different distance for cluster-heads, while the second non-CoMP-user in each cell is assumed at 300 m distance from the BS.

The key observation from Fig. 4.4 is that the average spectral efficiency gain of JT-CoMP-NOMA system for *deployment scenario*−1 is much higher in comparison to that of a JT-CoMP-OMA system, and the performance gain largely depends on the channel gain for cluster-head. Since the cluster-head is the highest channel gain user in each cluster, thus the performance gain is very obvious. In this case, the more distinct channel for cluster-head than the other NOMA users provides more spectral efficiency compare to their OMA counterparts.

The average spectral efficiency for JT-CoMP-NOMA, CS-CoMP-NOMA, and JT-CoMP-OMA for *deployment scenario*−2 *(illustrated in Fig. 4.1(c) for JT-COMP-*

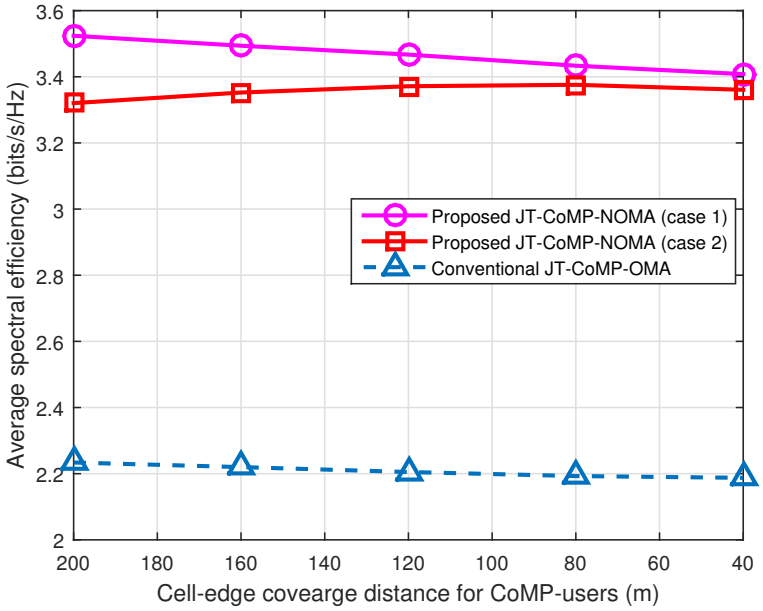

Figure 4.6: Average spectral efficiency for JT-CoMP-NOMA and JT-CoMP-OMA systems for deployment scenario−3 with two CoMP-users and one non-CoMP-user in cell−1 but none non-CoMP-user in cell−2.

NOMA), are shown in Fig. 4.5. Here, we consider one non-CoMP-user in each CoMP-cell at a distance 250 m from its serving BS, while two CoMP-users are randomly distributed at various cell-edge coverage distance. The guaranteed throughput requirement for each user in JT-CoMP-NOMA and CS-CoMP-NOMA systems is equal to their achievable JT-CoMP-OMA throughput by considering equal spectrum resource allocation. As we mentioned earlier, for JT-CoMP-NOMA, both CoMP-users can use full spectrum resource by forming 3-user NOMA cluster (two CoMP-users and one non-CoMP-user) at both CoMP-cells, while each CoMP-user can use at most 50% spectrum resources (orthogonal resources) in CB-CoMP-NOMA system by forming 2-user NOMA cluster (one CoMP-users and one non-CoMP-user). The additional 50% spectrum is allocated only to non-CoMP-user at both cell in CB-CoMP-NOMA system.

Fig. 4.5 shows the average spectral efficiency gain for CoMP-NOMA systems over CoMP-OMA systems. It is observed that JT-CoMP NOMA provides a much higher spectral efficiency than CS-CoMP-NOMA. Since there are two CoMP-users in each JT-CoMP-NOMA cluster, the NOMA cluster that uses optimal decoding order (ascending channel gain order) will have a higher spectral efficiency than the other which uses a non-optimal decoding order. In Fig. 4.5, we consider that cluster-1 formed in cell-1 uses the optimal decoding order, while cluster-2 formed in cell-2 uses a non-optimal decoding order. However, as the cluster-head in both the both JT-CoMP-NOMA clusters is the highest channel gain non-CoMP-user, the variation for spectral efficiency is not significant.

Fig. 4.6 shows the spectral efficiency gain for JT-CoMP-NOMA and JT-CoMP-OMA in *deployment scenario*-3 illustrated in Fig. 4.3(b), where two CoMP-users are assumed in a two-cell CoMP set, while one non-CoMP-user in cell-1 but there is no non-CoMP-user in cell-2. Two CoMP-users are randomly distributed at various cell-edge coverage distance, while the non-CoMP-user in cell-1 is located at a distance of 250 m from the BS. The guaranteed throughput requirement for each user in JT-CoMP-NOMA system is equal to the achievable JT-CoMP-OMA throughput by considering equal spectrum allocation to all users. In the corresponding OMA system, cell-2 allocates more spectrum resources (50%) to each CoMP-user than what cell-1 allocates (33.33%) but both allocations are in the same band, and thus each CoMP-user gets the same message signal over the same 33.33% spectrum resource from both the CoMP-cells. In the additional OMA spectrum resource (16.67%), cell-2 sends additional data to the CoMP-users.

Similar to the two other simulation results, Fig. 4.6 also shows significant spectral efficiency gain of JT-CoMP-NOMA system over the OMA system. Since the cluster-

head in cell−2 is a cell-edge user, the performance gain in Fig. 4.6 is not as good as the other two results. As the cluster-head in NOMA cluster−2 formed in cell−2 is a CoMP-user, the performance gain is better for optimal decoding order for cluster−2 (*case 1* in Fig. 4.6). However, this performance gain is not significantly high in comparison to that in the case of optimal decoding order for cluster−1 (*case 2* in Fig. 4.6). The reason is that the cluster-head in cluster−2 is a cell-edge user (i.e., has a low channel power gain) and the channel gains among the cluster-head and another user in cluster−2 is less distinctive, while the cluster-head in NOMA cluster−1 is a non-CoMP user with more distinctive channel gain than the other users in that cluster.

4.5 Summary

In this chapter, a general framework is proposed to use CoMP transmission technology in downlink multi-cell NOMA systems considering distributed power allocation at each cell. In this framework, CoMP transmission is used for users experiencing strong receive-signals from multiple cells while each cell adopts NOMA for resource allocation to its active users. After a brief review of the working principles of different CoMP schemes, I have identified their applicability and necessary conditions for their use in downlink multi-cell NOMA system. After that, I have discussed different network scenarios with different spatial distributions of users and study the applicability of CoMP schemes in these network scenarios. To the end, a numerical performance evaluation has been carried out for the proposed CoMP-NOMA systems and the results are compared with those for conventional orthogonal multiple access (OMA)-based CoMP systems. The numerical results quantify the spectral efficiency gain of the proposed CoMP-NOMA models over CoMP-OMA.

Chapter 5

Conclusion and Future Work

5.1 Conclusion

In this thesis, I have mainly investigated for the optimal power allocation solutions for the downlink and uplink NOMA systems, in the target of cell overall sum throughput maximization. However, due to the excessive complexity of SIC processing and strong inter-user interference in NOMA operations, cluster based NOMA has been proposed as a potential approach for wide applications of NOMA in wireless cellular systems. Toward that directions, I have sub-grouped the users into different NOMA clusters, and then optimal power allocation is employed within each cluster. In both of the downlink and uplink NOMA systems, I have formulated a MINLP joint optimization problem of dynamic user clustering and optimal power allocation in each cluster, in order to maximize the overall system throughput. I also have proposed a low-complexity sub-optimal user clustering algorithm by exploiting the channel gain differences among the NOMA users. The benefits of the proposed user clustering algorithm is that it does not require any matching operation, whilst optimal user clustering requires exhaustive matching operations which makes it extremely ineffi-

cient.

After clustering users, I have formulated convex optimization problem of power allocation at each downlink and uplink NOMA clusters in the target of sum throughput maximization. I also have developed closed-form solutions of the optimal power allocation for both of the downlink and uplink NOMA clusters with any number of users. All of the above researches and their throughput performances are presented in Chapter 2.

In Chapter 3, I have investigated the application of NOMA in downlink multiuser MIMO system where the total number of users' receive antennas is much higher than the number of BS transmit antennas. The receive antennas are grouped into a number of clusters and each cluster of MIMO-NOMA is served by a single MIMO beam which is orthogonal to the other clusters' beams, while all users in a cluster are scheduled on a NOMA basis. In Chapter 3, I have introduced a new inter-cluster zero-forcing beamforming technique for downlink MIMO-NOMA. The proposed technique can significantly eliminate inter-cluster interference when the more distinctive channel gain users are formed MIMO-NOMA clusters. I have also provided the dynamic power allocation solution for inter-cluster and intra-cluster power allocation in downlink MIMO-NOMA system. Moreover, a low-complexity suboptimal user-clustering algorithm has been proposed which potentially mitigates inter-cluster interference and also helps for achieving optimal intra-cluster power allocation in order to maximize the overall throughput in a cell. Simulation results have demonstrated the spectral efficiency gain of the proposed MIMO-NOMA model over the MIMO-OMA and other existing MIMO-NOMA solutions.

In Chapter 4, I have investigated the application of CoMP transmission technique in downlink multi-cell NOMA systems under co-channel homogeneous network sce-

narios . Here, I have demonstrated the gain in spectral efficiency performance for CoMP transmission in downlink homogeneous multi-cell NOMA systems by considering distributed power allocation. I also have identified the necessary conditions required to perform CoMP-NOMA in downlink transmission under distributed power allocation. Different CoMP-NOMA schemes have been numerically analyzed under various network deployment scenarios. All of the simulation results reveal the superior spectral efficiency performance of CoMP-NOMA systems over their counterpart CoMP-OMA systems. However, among all the CoMP schemes, JT-CoMP-NOMA provides the highest spectral efficiency gain. This is due to the fact that, all the CoMP-users can use the same spectrum resources by forming NOMA clusters at all coordinating cells. On the other hand, orthogonal spectrum resource allocation is required among the CoMP-users in other CoMP-NOMA schemes.

5.2 Future Work

Based on the research presented in this thesis, the following potential research could be conducted:

- In this thesis, I have considered ideal SIC operation, but the performances of NOMA systems mainly depend on the practical SIC processing. In a rigorous downlink NOMA system, each of the NOMA candidate signals need to be identically encoded, modulated and precoded at transmitter end; while SIC receiver successively demodulates, decodes, and then re-encodes and re-modulates each of the lower channel gain signals in order to suppress that from the received signal. Therefore, for a higher order NOMA system, error propagation in SIC process may drastically reduce the NOMA performance. Also, the SIC processing involve sufficient latency that may not be supported by many applications.

Therefore, by considering the practical SIC application the performance evaluation of NOMA systems may would be great beneficial for implementation in real network.

- The proposed MIMO-NOMA model in Chapter 4 has been evaluated in a single cell scenario, while a multi-cell system may introduce additional inter-cell interference which could affect the performance of the proposed beamforming solution. Therefore, the performance evaluation of the proposed MIMO-NOMA model in multi-cell scenarios may would be a potential research opportunity.

- In CoMP-NOMA, I have used optimal power allocation for a given decoding order for each NOMA cluster. However, determining the optimal decoding order among all the coordinating cells is a challenging task. An exhaustive search algorithm could be a solution for optimal decoding order but the complexity of such a solution would be very high for a CoMP set with more than two cells and or two CoMP-users. Finding low-complexity near-optimal user clustering schemes for CoMP-NOMA systems is an open challenge.

- Also in CoMP-NOMA, when the cluster-head is the highest channel gain user of a NOMA cluster, our optimal power allocation solution for sum-throughput maximization provides minimum power to meet the guaranteed throughput requirement for all NOMA users except the cluster-head who gets all the residual power, by maintaining the SIC decoding requirements. Thus, the sum-throughput would be the maximum for the given minimum throughput requirement of each NOMA user. However, in JT-CoMP-NOMA, each CoMP-user receives the same data stream transmitted over the same spectrum resources from multiple cells, while their channel gains at each coordinating cell are differ-

ent. Thus how much power to allocate to a JT-CoMP user at each coordinating cell to satisfy the user's rate requirement while achieving the optimal spectral efficiency in all the coordinating cells is another open research challenge. Determining the optimal decoding order and optimal rate requirement for a CoMP-NOMA system is a joint optimization problem.

- In downlink co-channel HetNets, all the small-cell users experience strong inter-cell interference signal from the high power macro-cell. While in NOMA system, it is required for a NOMA user to decode and and ten cancel, i.e. SIC application, the other NOMA users signal whose decoding order is prior to the considered user. Since the SIC application explicitly depends on the power domain, the co-channel macro-cell interference may make the small-cell users unable to perform SIC application. Therefore, the general NOMA application in co-channel downlink HetNets is a open challenge. However, the use of CoMP technology may would be a potential solution for such NOMA-based downlink co-channel HetNets.

- In HetNets, since multiple small cells underlay a macro-cell, a CoMP set may be formed among multiple small cells and one macro cell. In a two-tier HetNet, all users in a small cell could be treated as CoMP-users by the macro cell and the corresponding small cell, while all users in a small cell cannot be treated as CoMP-users by another small cell. Therefore, application of CoMP in such a NOMA-based downlink HetNet is a challenging task. The concept of location-aware CoMP [28], in which, the small cell users close to the small cell BSs are treated as non-CoMP-user, would provide a potential solution to this problem. However, the inter-cell interference for small cell non-CoMP-users would be very high. Therefore, the selection of CoMP-users and non-CoMP-users should be

done carefully.

Bibliography

[1] Y. Saito, Y. Kishiyama, A. Benjebbour, T. Nakamura, A. Li, and K. Higuchi, "Non-orthogonal multiple access (noma) for cellular future radio access," in *Vehicular Technology Conference (VTC Spring), 2013 IEEE 77th.* IEEE, 2013, pp. 1–5.

[2] A. Benjebbour, Y. Saito, Y. Kishiyama, A. Li, A. Harada, and T. Nakamura, "Concept and practical considerations of non-orthogonal multiple access (noma) for future radio access," in *Intelligent Signal Processing and Communications Systems (ISPACS), 2013 International Symposium on.* IEEE, 2013, pp. 770–774.

[3] A. Benjebbour, A. Li, Y. Saito, Y. Kishiyama, A. Harada, and T. Nakamura, "System-level performance of downlink noma for future lte enhancements," in *Globecom Workshops (GC Wkshps), 2013 IEEE.* IEEE, 2013, pp. 66–70.

[4] A. Benjebbour, K. Saito, A. Li, Y. Kishiyama, and T. Nakamura, "Non-orthogonal multiple access (noma): Concept, performance evaluation and experimental trials," in *Wireless Networks and Mobile Communications (WINCOM), 2015 International Conference on.* IEEE, 2015, pp. 1–6.

[5] K. Higuchi and A. Benjebbour, "Non-orthogonal multiple access (noma) with successive interference cancellation for future radio access," *IEICE Transactions on Communications*, vol. 98, no. 3, pp. 403–414, 2015.

[6] Q. H. Spencer, A. L. Swindlehurst, and M. Haardt, "Zero-forcing methods for downlink spatial multiplexing in multiuser mimo channels," *IEEE Transactions on Signal Processing*, vol. 52, no. 2, pp. 461–471, 2004.

[7] S. Sun, Q. Gao, Y. Peng, Y. Wang, and L. Song, "Interference management through comp in 3gpp lte-advanced networks," *IEEE Wireless Communications*, vol. 20, no. 1, pp. 59–66, 2013.

[8] M. S. Ali, "On the evolution of coordinated multi-point (comp) transmission in lte-advanced," *International Journal of Future Generation Communication and Networking*, vol. 7, no. 4, pp. 91–102, 2014.

[9] Z. Ding, Z. Yang, P. Fan, and H. V. Poor, "On the performance of non-orthogonal multiple access in 5g systems with randomly deployed users," *IEEE Signal Processing Letters*, vol. 21, no. 12, pp. 1501–1505, 2014.

[10] Z. Ding, P. Fan, and H. V. Poor, "Impact of user pairing on 5g non-orthogonal multiple access," *arXiv preprint arXiv:1412.2799*, 2014.

[11] S. Timotheou and I. Krikidis, "Fairness for non-orthogonal multiple access in 5g systems," *IEEE Signal Processing Letters*, vol. 22, no. 10, pp. 1647–1651, 2015.

[12] Z. Ding, M. Peng, and H. V. Poor, "Cooperative non-orthogonal multiple access in 5g systems," *IEEE Communications Letters*, vol. 19, no. 8, pp. 1462–1465, 2015.

[13] Y. Endo, Y. Kishiyama, and K. Higuchi, "Uplink non-orthogonal access with mmse-sic in the presence of inter-cell interference," in *Wireless Communication Systems (ISWCS), 2012 International Symposium on.* IEEE, 2012, pp. 261–265.

[14] M. Al-Imari, P. Xiao, M. A. Imran, and R. Tafazolli, "Uplink non-orthogonal multiple access for 5g wireless networks," in *Wireless Communications Systems (ISWCS), 2014 11th International Symposium on.* IEEE, 2014, pp. 781–785.

[15] N. Zhang, J. Wang, G. Kang, and Y. Liu, "Uplink nonorthogonal multiple access in 5g systems," *IEEE Communications Letters*, vol. 20, no. 3, pp. 458–461, 2016.

[16] L. Anxin, A. Benjebbour, C. Xiaohang, H. Jiang, and H. Kayama, "Uplink non-orthogonal multiple access (noma) with single-carrier frequency division multiple access (sc-fdma) for 5g systems," *IEICE Transactions on Communications*, vol. 98, no. 8, pp. 1426–1435, 2015.

[17] B. Kim, S. Lim, H. Kim, S. Suh, J. Kwun, S. Choi, C. Lee, S. Lee, and D. Hong, "Non-orthogonal multiple access in a downlink multiuser beamforming system," in *Military Communications Conference, MILCOM 2013-2013 IEEE*. IEEE, 2013, pp. 1278–1283.

[18] Y. Hayashi, Y. Kishiyama, and K. Higuchi, "Investigations on power allocation among beams in non-orthogonal access with random beamforming and intra-beam sic for cellular mimo downlink," in *Vehicular Technology Conference (VTC Fall), 2013 IEEE 78th*. IEEE, 2013, pp. 1–5.

[19] Y. Lan, A. Benjebboiu, X. Chen, A. Li, and H. Jiang, "Considerations on downlink non-orthogonal multiple access (noma) combined with closed-loop su-mimo," in *Signal Processing and Communication Systems (ICSPCS), 2014 8th International Conference on*. IEEE, 2014, pp. 1–5.

[20] Z. Ding, F. Adachi, and H. V. Poor, "The application of mimo to non-orthogonal multiple access," *IEEE Transactions on Wireless Communications*, vol. 15, no. 1, pp. 537–552, 2016.

[21] Q. Sun, S. Han, I. Chin-Lin, and Z. Pan, "On the ergodic capacity of mimo noma systems," *IEEE Wireless Communications Letters*, vol. 4, no. 4, pp. 405–408, 2015.

[22] J. Choi, "Non-orthogonal multiple access in downlink coordinated two-point systems," *IEEE Communications Letters*, vol. 18, no. 2, pp. 313–316, 2014.

[23] Y. Tian, A. R. Nix, and M. Beach, "On the performance of opportunistic noma in downlink comp networks," *IEEE Communications Letters*, vol. 20, no. 5, pp. 998–1001, 2016.

[24] A. Beylerian and T. Ohtsuki, "Coordinated non-orthogonal multiple access (co-noma)," in *Global Communications Conference (GLOBECOM), 2016 IEEE*. IEEE, 2016, pp. 1–5.

[25] W. Shin, M. Vaezi, B. Lee, D. J. Love, J. Lee, and H. V. Poor, "Non-orthogonal multiple access in multi-cell networks: Theory, performance, and practical challenges," *arXiv preprint arXiv:1611.01607*, 2016.

[26] E. K. Chong and S. H. Zak, *An introduction to optimization*. John Wiley & Sons, 2013, vol. 76.

[27] M. M. Do and H. J. Son. "comp type". [Online]. Available: www.netmanias.com/en/post/blog/6558/comp-lte-lte-a/comp-1-comp-types-cs-cb-jt-and-dps

[28] A. H. Sakr and E. Hossain, "Location-aware cross-tier coordinated multipoint transmission in two-tier cellular networks," *IEEE Transactions on Wireless Communications*, vol. 13, no. 11, pp. 6311–6325, 2014.

[29] T. Wang. "inequality constrained optimization". [Online]. Available: http://privatewww.essex.ac.uk/~wangt/Presession\%20Math/Lecture\%205.pdf

Appendix A

A.1 Proof of Lemma 2.3.1 by Induction.

In this Appendix, I will consider one satisfied KKT condition (i.e. a particular set of values of Lagrange multipliers) of a particular downlink NOMA cluster. Using the considered Lagrange multipliers, I will determine the optimal solution of power allocation by manipulating the KKT conditions of Lagrange multipliers. After that, the Lagrange multipliers will be determined by using the optimal power allocation solution in KKT conditions of power allocation. The optimality will be proofed by obtaining non-zero Lagrange multipliers as similar to those are initially considered [29]. The detail procedures are as follows:

Let us consider $m = 4$ which is a 4-user downlink NOMA cluster. Then, the set of Lagrange multipliers can be expressed as $A = \{\lambda\}$ $B = \{\mu_1, \mu_2, \mu_3, \mu_4\}$ and $C = \{\psi_2, \psi_3, \psi_4\}$. The solution sets that satisfy KKT conditions are, $S = \{\lambda, \mu_2 \text{ or } \psi_2, \mu_3 \text{ or } \psi_3, \mu_4 \text{ or } \psi_4\}$. Now, consider one set of Lagrange multipliers, say $S_1 = \{\lambda, \mu_2, \mu_3, \mu_4\}$, that satisfy KKT condition, and thus the value of the Lagrange multipliers are $\lambda^* > 0$, $\mu_2^* > 0$, $\mu_3^* > 0$, $\mu_4^* > 0$, and $\mu_1^* = \psi_2^* = \psi_3^* = \psi_4^* = 0$.

With the aforementioned Lagrange multipliers, equations (2.5) to (2.7) could be

expressed as

$$p_t - \sum_{i=1}^{4} p_i = 0 \tag{A.1}$$

$$p_i\gamma_i - \Big(\sum_{j=1}^{i-1} p_j\gamma_i + \omega\Big)\Big(\varphi_i - 1\Big) = 0, \quad \forall i = 2, 3, 4 \tag{A.2}$$

$$p_i\gamma_i - \Big(\sum_{j=1}^{i-1} p_j\gamma_i + \omega\Big)\Big(\varphi_i - 1\Big) > 0, \quad \forall i = 1 \tag{A.3}$$

$$p_i\gamma_{i-1} - \sum_{j=1}^{i-1} p_j\gamma_{i-1} - p_{tol} > 0, \quad \forall i = 2, 3, 4. \tag{A.4}$$

Equations (A.1) to (A.2) provides the optimal solution of p_1, p_2, p_3 and p_4, while equations (A.3) to (A.4) provides the necessary conditions of these optimal solutions. Now, solving equations (A.1) to (A.2), the optimal power allocation solution can be obtained as

$$p_1 = \frac{p_t}{\varphi_2\varphi_3\varphi_4} - \frac{\omega(\varphi_2 - 1)}{\varphi_2\gamma_2} - \frac{\omega(\varphi_3 - 1)}{\varphi_2\varphi_3\gamma_3} - \frac{\omega(\varphi_4 - 1)}{\varphi_2\varphi_3\varphi_4\gamma_4}$$

$$p_2 = \frac{p_t(\varphi_2 - 1)}{\varphi_2\varphi_3\varphi_4} + \frac{\omega(\varphi_2 - 1)}{\varphi_2\gamma_2} - \frac{\omega(\varphi_2 - 1)(\varphi_3 - 1)}{\varphi_2\varphi_3\gamma_3} - \frac{\omega(\varphi_2 - 1)(\varphi_4 - 1)}{\varphi_2\varphi_3\varphi_4\gamma_4}$$

$$p_3 = \frac{p_t(\varphi_3 - 1)}{\varphi_3\varphi_4} + \frac{\omega(\varphi_3 - 1)}{\varphi_3\gamma_3} - \frac{\omega(\varphi_3 - 1)(\varphi_4 - 1)}{\varphi_3\varphi_4\gamma_4}$$

$$p_4 = \frac{p_t(\varphi_4 - 1)}{\varphi_4} + \frac{\omega(\varphi_4 - 1)}{\varphi_4 \gamma_4}$$

Since $\varphi_i = 2^{\frac{R_1}{\omega B}} > 1, \quad \forall i$; thus the solution of p_1, p_2, p_3 and p_4 all are positive. Now, with the considered Lagrange multipliers and the positive $p_i, \quad \forall i$, and after some algebraic manipulations, equations (2.3) to (2.4) can be expressed as

$$\sum_{j=1}^{3} \frac{\omega^2 B(\gamma_j - \gamma_{j+1})}{\left(\sum_{k=1}^{j} p_k \gamma_j + \omega\right)\left(\sum_{k=1}^{j} p_k \gamma_{j+1} + \omega\right)} + \frac{\omega B \gamma_4}{\sum_{l=1}^{4} p_l \gamma_4 + \omega} = \lambda + \sum_{j=2}^{4} (\varphi_j - 1)\mu_j \gamma_j \quad \text{(A.5)}$$

$$\sum_{j=i}^{3} \frac{\omega^2 B(\gamma_j - \gamma_{j+1})}{\left(\sum_{k=1}^{j} p_k \gamma_j + \omega\right)\left(\sum_{k=1}^{j} p_k \gamma_{j+1} + \omega\right)} + \frac{\omega B \gamma_4}{\sum_{l=1}^{4} p_l \gamma_4 + \omega} = \lambda - \mu_i \gamma_i + \sum_{j=i+1}^{4} (\varphi_j - 1)\mu_j \gamma_j, \quad \forall i = 2, 3, 4. \quad \text{(A.6)}$$

Now, after performing some algebraic manipulations into equations (A.5) to (A.6), we can obtain the Lagrange multipliers as follows:

$$\mu_2 = \frac{\omega^2 B(\gamma_1 - \gamma_2)}{\varphi_2 \gamma_2 (p_1 \gamma_1 + \omega)(p_1 \gamma_2 + \omega)} \quad \text{(A.7)}$$

$$\mu_i = \frac{\omega^2 B(\gamma_{i-1} - \gamma_i)}{\varphi \gamma_i \left(\sum_{j=1}^{i-1} p_j \gamma_{i-1} + \omega\right)\left(\sum_{j=1}^{i-1} p_j \gamma_i + \omega\right)} + \mu_{i-1}\gamma_{i-1}, \quad \forall i = 3, 4 \quad \text{(A.8)}$$

$$\lambda = \frac{\omega B \gamma_4}{\sum_{j=1}^{4} p_j \gamma_4 + \omega} + \mu_4 \gamma_4. \quad \text{(A.9)}$$

In this proposed dynamic power allocation solutions, I sort the UEs according to the descending order of their channel gain, i.e $\gamma_1 > \gamma_2 > \gamma_3 > \gamma_4$. Therefore, the solutions for λ and $\mu_i \quad \forall i = 2, 3, 4$, of equations (A.7) to (A.9) all are positives. Therefore, the Lagrange multipliers set $S_1 = \{\lambda, \mu_2, \mu_3, \mu_4\}$ satisfies the KKT conditions. All the other cases can easily be verified using similar approach.

By verifying all the necessary KKT conditions, the optimal transmission powers and the corresponding necessary conditions for 2- and 3-user downlink NOMA clusters are provided in **Table A.1**; while 4-user downlink NOMA cluster is provided in **Table A.2**. By observing the optimal solutions in **Table A.1** and **Table A.2**, the closed-form solution of **Lemama** 2.3.1 can be proofed by induction.

Table A.1: Optimal power allocation solution for 2- and 3-user downlink NOMA.

NOMA	Optimal transmit power	Necessary conditions
2-user	$p_1 = \frac{p_t}{\varphi_2} - \frac{\omega(\varphi_2-1)}{\varphi_2\gamma_2}$, $p_2 = \frac{p_t(\varphi_2-1)}{\varphi_2} + \frac{\omega(\varphi_2-1)}{\varphi_2\gamma_2}$	$p_i\gamma_i - \Big(\varphi_1 - 1\Big)\Big(\sum_{j=1}^{i-1} p_j\gamma_i + \omega\Big) > 0, \forall\, i = 1,$ $\Big(p_i - \sum_{j=1}^{i-1} p_j\Big)\gamma_{i-1} - p_{tol} > 0, \forall\, i = 2$
	$p_1 = \frac{p_t}{2} - \frac{p_{tol}}{2\gamma_1}$, $p_2 = \frac{p_t}{2} + \frac{p_{tol}}{2\gamma_1}$	$p_i\gamma_i - \Big(\varphi_1 - 1\Big)\Big(\sum_{j=1}^{i-1} p_j\gamma_i + \omega\Big) > 0, \forall\, i = 1, 2$
3-user	$p_1 = \frac{p_t}{\varphi_2\varphi_3} - \frac{\omega(\varphi_2-1)}{\varphi_2\gamma_2} - \frac{\omega(\varphi_3-1)}{\varphi_2\varphi_3\gamma_3}$, $p_2 = \frac{p_t(\varphi_2-1)}{\varphi_2\varphi_3} + \frac{\omega(\varphi_2-1)}{\varphi_2\gamma_2} - \frac{\omega(\varphi_2-1)(\varphi_3-1)}{\varphi_2\varphi_3\gamma_3}$, $p_3 = \frac{p_t(\varphi_3-1)}{\varphi_3} + \frac{\omega(\varphi_3-1)}{\varphi_3\gamma_3}$	$p_i\gamma_i - \Big(\varphi_1 - 1\Big)\Big(\sum_{j=1}^{i-1} p_j\gamma_i + \omega\Big) > 0, \forall\, i = 1,$ $\Big(p_i - \sum_{j=1}^{i-1} p_j\Big)\gamma_{i-1} - p_{tol} > 0, \forall\, i = 2, 3$
	$p_1 = \frac{p_t}{2\varphi_2} - \frac{\omega(\varphi_2-1)}{\varphi_2\gamma_2} - \frac{p_{tol}}{2\varphi_2\gamma_2}$, $p_2 = \frac{p_t(\varphi_2-1)}{2\varphi_2} + \frac{\omega(\varphi_2-1)}{\varphi_2\gamma_2} - \frac{p_{tol}(\varphi_2-1)}{2\varphi_2\gamma_2}$, $p_3 = \frac{p_t}{2} + \frac{p_{tol}}{2\gamma_2}$	$p_i\gamma_i - \Big(\varphi_1 - 1\Big)\Big(\sum_{j=1}^{i-1} p_j\gamma_i + \omega\Big) > 0, \forall\, i = 1, 3,$ $\Big(p_i - \sum_{j=1}^{i-1} p_j\Big)\gamma_{i-1} - p_{tol} > 0, \forall\, i = 2$
	$p_1 = \frac{p_t}{2\varphi_3} - \frac{p_{tol}}{2\gamma_1} - \frac{\omega(\varphi_3-1)}{2\varphi_3\gamma_3}$, $p_2 = \frac{p_t}{2\varphi_3} + \frac{p_{tol}}{2\gamma_1} - \frac{\omega(\varphi_3-1)}{2\varphi_3\gamma_3}$, $p_3 = \frac{p_t(\varphi_3-1)}{\varphi_3} + \frac{\omega(\varphi_3-1)}{\varphi_3\gamma_3}$	$p_i\gamma_i - \Big(\varphi_1 - 1\Big)\Big(\sum_{j=1}^{i-1} p_j\gamma_i + \omega\Big) > 0, \forall\, i = 1, 2,$ $\Big(p_i - \sum_{j=1}^{i-1} p_j\Big)\gamma_{i-1} - p_{tol} > 0, \forall\, i = 3$
	$p_1 = \frac{p_t}{4} - \frac{p_{tol}}{2\gamma_1} - \frac{p_{tol}}{4\gamma_2}$, $p_2 = \frac{p_t}{4} + \frac{p_{tol}}{2\gamma_1} - \frac{p_{tol}}{4\gamma_2}$, $p_3 = \frac{p_t}{2} + \frac{p_{tol}}{2\gamma_2}$	$p_i\gamma_i - \Big(\varphi_1 - 1\Big)\Big(\sum_{j=1}^{i-1} p_j\gamma_i + \omega\Big) > 0, \forall\, i = 1, 2, 3$

Table A.2: Optimal power allocation solution for 4-user downlink NOMA.

NOMA	Optimal transmit power	Necessary conditions
4-user	$p_1 = \frac{p_t}{\varphi_2\varphi_3\varphi_4} - \frac{\omega(\varphi_2-1)}{\varphi_2\gamma_2} - \frac{\omega(\varphi_3-1)}{\varphi_2\varphi_3\gamma_3} - \frac{\omega(\varphi_4-1)}{\varphi_2\varphi_3\varphi_4\gamma_4}$, $p_2 = \frac{p_t(\varphi_2-1)}{\varphi_2\varphi_3\varphi_4} + \frac{\omega(\varphi_2-1)}{\varphi_2\gamma_2} - \frac{\omega(\varphi_2-1)(\varphi_3-1)}{\varphi_2\varphi_3\gamma_3} - \frac{\omega(\varphi_2-1)(\varphi_4-1)}{\varphi_2\varphi_3\varphi_4\gamma_4}$, $p_3 = \frac{p_t(\varphi_3-1)}{\varphi_3\varphi_4} + \frac{\omega(\varphi_3-1)}{\varphi_3\gamma_3} - \frac{\omega(\varphi_3-1)(\varphi_4-1)}{\varphi_3\varphi_4\gamma_4}$, $p_4 = \frac{p_t(\varphi_4-1)}{\varphi_4} + \frac{\omega(\varphi_4-1)}{\varphi_4\gamma_4}$	$p_i\gamma_i - \Big(\varphi_1 - 1\Big)\Big(\sum_{j=1}^{i-1} p_j\gamma_i + \omega\Big) > 0, \forall\, i = 1,$ $\Big(p_i - \sum_{j=1}^{i-1} p_j\Big)\gamma_{i-1} - p_{tol} > 0, \forall\, i = 2,3,4$
	$p_1 = \frac{p_t}{2\varphi_2\varphi_3} - \frac{\omega(\varphi_2-1)}{\varphi_2\gamma_2} - \frac{\omega(\varphi_3-1)}{\varphi_2\varphi_3\gamma_3} - \frac{p_{tol}}{2\varphi_2\varphi_3\gamma_3}$, $p_2 = \frac{p_t(\varphi_2-1)}{2\varphi_2\varphi_3} + \frac{\omega(\varphi_2-1)}{\varphi_2\gamma_2} - \frac{\omega(\varphi_2-1)(\varphi_3-1)}{\varphi_2\varphi_3\gamma_3} - \frac{p_{tol}(\varphi_2-1)}{2\varphi_2\varphi_3\gamma_3}$, $p_3 = \frac{p_t(\varphi_3-1)}{2\varphi_3} + \frac{\omega(\varphi_3-1)}{\varphi_3\gamma_3} - \frac{p_{tol}(\varphi_3-1)}{2\varphi_3\gamma_3}$, $p_4 = \frac{p_t}{2} + \frac{p_{tol}}{2\gamma_3}$	$p_i\gamma_i - \Big(\varphi_1 - 1\Big)\Big(\sum_{j=1}^{i-1} p_j\gamma_i + \omega\Big) > 0, \forall\, i = 1,4,$ $\Big(p_i - \sum_{j=1}^{i-1} p_j\Big)\gamma_{i-1} - p_{tol} > 0, \forall\, i = 2,3$
	$p_1 = \frac{p_t}{2\varphi_2\varphi_4} - \frac{\omega(\varphi_2-1)}{\varphi_2\gamma_2} - \frac{\omega(\varphi_4-1)}{2\varphi_2\varphi_4\gamma_4} - \frac{p_{tol}}{2\varphi_2\gamma_2}$, $p_2 = \frac{p_t(\varphi_2-1)}{2\varphi_2\varphi_4} + \frac{\omega(\varphi_2-1)}{\varphi_2\gamma_2} - \frac{\omega(\varphi_2-1)(\varphi_4-1)}{2\varphi_2\varphi_4\gamma_4} - \frac{p_{tol}(\varphi_2-1)}{2\varphi_2\gamma_2}$, $p_3 = \frac{p_t}{2\varphi_4} + \frac{p_{tol}}{2\gamma_2} - \frac{\omega(\varphi_4-1)}{2\varphi_4\gamma_4}$, $p_4 = \frac{p_t(\varphi_4-1)}{\varphi_4} + \frac{\omega(\varphi_4-1)}{\varphi_4\gamma_4}$	$p_i\gamma_i - \Big(\varphi_1 - 1\Big)\Big(\sum_{j=1}^{i-1} p_j\gamma_i + \omega\Big) > 0, \forall\, i = 1,3,$ $\Big(p_i - \sum_{j=1}^{i-1} p_j\Big)\gamma_{i-1} - p_{tol} > 0, \forall\, i = 2,4$
	$p_1 = \frac{p_t}{2\varphi_3\varphi_4} - \frac{p_{tol}}{2\gamma_1} - \frac{\omega(\varphi_3-1)}{2\varphi_3\gamma_3} - \frac{\omega(\varphi_4-1)}{2\varphi_3\varphi_4\gamma_4}$, $p_2 = \frac{p_t}{2\varphi_3\varphi_4} + \frac{p_{tol}}{2\gamma_1} - \frac{\omega(\varphi_3-1)}{2\varphi_3\gamma_3} - \frac{\omega(\varphi_4-1)}{2\varphi_3\varphi_4\gamma_4}$, $p_3 = \frac{p_t(\varphi_3-1)}{\varphi_3\varphi_4} + \frac{\omega(\varphi_3-1)}{\varphi_3\gamma_3} - \frac{\omega(\varphi_3-1)(\varphi_4-1)}{\varphi_3\varphi_4\gamma_4}$, $p_4 = \frac{p_t(\varphi_4-1)}{\varphi_4} + \frac{\omega(\varphi_4-1)}{\varphi_4\gamma_4}$	$p_i\gamma_i - \Big(\varphi_1 - 1\Big)\Big(\sum_{j=1}^{i-1} p_j\gamma_i + \omega\Big) > 0, \forall\, i = 1,2,$ $\Big(p_i - \sum_{j=1}^{i-1} p_j\Big)\gamma_{i-1} - p_{tol} > 0, \forall\, i = 3,4$
	$p_1 = \frac{p_t}{4\varphi_2} - \frac{\omega(\varphi_2-1)}{\varphi_2\gamma_2} - \frac{p_{tol}}{2\varphi_2\gamma_2} - \frac{p_{tol}}{4\varphi_2\gamma_3}$, $p_2 = \frac{p_t(\varphi_2-1)}{4\varphi_2} + \frac{\omega(\varphi_2-1)}{\varphi_2\gamma_2} - \frac{p_{tol}(\varphi_2-1)}{2\varphi_2\gamma_2} - \frac{p_{tol}(\varphi_2-1)}{4\varphi_2\gamma_3}$, $p_3 = \frac{p_t}{4} + \frac{p_{tol}}{2\gamma_2} - \frac{p_{tol}}{4\gamma_3}$, $p_4 = \frac{p_t}{2} + \frac{p_{tol}}{2\gamma_3}$	$p_i\gamma_i - \Big(\varphi_1 - 1\Big)\Big(\sum_{j=1}^{i-1} p_j\gamma_i + \omega\Big) > 0, \forall\, i = 1,3,4,$ $\Big(p_i - \sum_{j=1}^{i-1} p_j\Big)\gamma_{i-1} - p_{tol} > 0, \forall\, i = 2$
	$p_1 = \frac{p_t}{4\varphi_3} - \frac{p_{tol}}{2\gamma_1} - \frac{\omega(\varphi_3-1)}{2\varphi_3\gamma_3} - \frac{p_{tol}}{4\varphi_3\gamma_3}$, $p_2 = \frac{p_t}{4\varphi_3} + \frac{p_{tol}}{2\gamma_1} - \frac{\omega(\varphi_3-1)}{2\varphi_3\gamma_3} - \frac{p_{tol}}{4\varphi_3\gamma_3}$, $p_3 = \frac{p_t(\varphi_3-1)}{2\varphi_3} + \frac{\omega(\varphi_3-1)}{\varphi_3\gamma_3} - \frac{p_{tol}(\varphi_3-1)}{2\varphi_3\gamma_3}$, $p_4 = \frac{p_t}{2} + \frac{p_{tol}}{2\gamma_3}$	$p_i\gamma_i - \Big(\varphi_1 - 1\Big)\Big(\sum_{j=1}^{i-1} p_j\gamma_i + \omega\Big) > 0, \forall\, i = 1,2,4,$ $\Big(p_i - \sum_{j=1}^{i-1} p_j\Big)\gamma_{i-1} - p_{tol} > 0, \forall\, i = 3$
	$p_1 = \frac{p_t}{4\varphi_4} - \frac{p_{tol}}{2\gamma_1} - \frac{p_{tol}}{4\gamma_2} - \frac{\omega(\varphi_4-1)}{4\varphi_4\gamma_4}$, $p_2 = \frac{p_t}{4\varphi_4} + \frac{p_{tol}}{2\gamma_1} - \frac{p_{tol}}{4\gamma_2} - \frac{\omega(\varphi_4-1)}{4\varphi_4\gamma_4}$, $p_3 = \frac{p_t}{2\varphi_4} + \frac{p_{tol}}{2\gamma_2} - \frac{\omega(\varphi_4-1)}{2\varphi_4\gamma_4}$, $p_4 = \frac{p_t(\varphi_4-1)}{\varphi_4} + \frac{\omega(\varphi_4-1)}{\varphi_4\gamma_4}$	$p_i\gamma_i - \Big(\varphi_1 - 1\Big)\Big(\sum_{j=1}^{i-1} p_j\gamma_i + \omega\Big) > 0, \forall\, i = 1,2,3,$ $\Big(p_i - \sum_{j=1}^{i-1} p_j\Big)\gamma_{i-1} - p_{tol} > 0, \forall\, i = 4$
	$p_1 = \frac{p_t}{8} - \frac{p_{tol}}{2\gamma_1} - \frac{p_{tol}}{4\gamma_2} - \frac{p_{tol}}{8\gamma_3}$, $p_2 = \frac{p_t}{8} + \frac{p_{tol}}{2\gamma_1} - \frac{p_{tol}}{4\gamma_2} - \frac{p_{tol}}{8\gamma_3}$, $p_3 = \frac{p_t}{4} + \frac{p_{tol}}{2\gamma_2} - \frac{p_{tol}}{4\gamma_3}$, $p_4 = \frac{p_t}{2} + \frac{p_{tol}}{2\gamma_3}$	$p_i\gamma_i - \Big(\varphi_1 - 1\Big)\Big(\sum_{j=1}^{i-1} p_j\gamma_i + \omega\Big) > 0, \forall\, i = 1,2,3,4$

Appendix B

B.1 Proof of Lemma 2.3.2 by Induction.

Similar to downlink NOMA cluster, I will the KKT verification of a general m-user uplink NOMA cluster by considering a particular combination of Lagrange multipliers in a particular cluster size.

Let again consider $m = 4$, that is a 4-user uplink NOMA cluster, then the set of Lagrange multipliers can be expressed as $A = \{\lambda_1, \lambda_2, \lambda_3, \lambda_4\}$, $B = \{\mu_1, \mu_2, \mu_3, \mu_4\}$ and $C = \{\psi_1, \psi_2, \psi_3\}$. Therefore, the solution sets that satisfy KKT conditions are, $S = \{\lambda_1, \lambda_2, \lambda_3, \lambda_4 \text{ or } \mu_3 \text{ or } \psi_3\}$. Now, consider one set of Lagrange multipliers, say $S_1 = \{\lambda_1, \lambda_2, \lambda_3, \mu_3\}$, that satisfy KKT condition, and thus the value of the Lagrange multipliers are $\lambda_i^* > 0$, $\mu_3^* > 0$, and $\lambda_4^* = \mu_j^* = \psi_k^* = 0$; $\forall\, i = 1, 2, 3$, $\forall\, j = 1, 2, 4$, $\forall\, k = 1, 2, 3$. Now, with the aforementioned Lagrange multipliers, equations (2.13) to (2.15) can be expressed as

$$p_t' - p_i = 0, \quad \forall i = 1, 2, 3 \tag{B.1}$$

$$p_3\gamma_3 - \phi_3 p_4 \gamma_4 - \phi_3 \omega = 0 \tag{B.2}$$

$$p_t' - p_4 > 0 \tag{B.3}$$

$$p_i\gamma_i - \phi_i \sum_{j=i+1}^{4} p_j\gamma_j - \phi_i\omega > 0, \quad \forall i = 1, 2, 4 \tag{B.4}$$

$$p_i\gamma_i - \sum_{j=i+1}^{4} p_j\gamma_j - p_{tol} > 0, \quad \forall i = 1, 2, 3 \tag{B.5}$$

Equations (B.1) to (B.2) provides the optimal solution of p_1, p_2, p_3 and p_4; while equations (B.3) to (B.5) provides the necessary conditions of these optimal solutions. Now, solving equations (B.1) to (B.2), we can obtain the optimal power allocation as

$$p_i = p_t', \quad \forall i = 1, 2, 3$$

$$p_4 = \frac{p_t'\gamma_3}{\phi_3\gamma_4} - \frac{\omega}{\gamma_4}.$$

Since $\varphi_i = 2^{\frac{R_1'}{\omega B}} - 1 > 0, \quad \forall i = 1, 2, 3, 4$, the solution of p_1, p_2, p_3 and p_4 all are positives. Now, with the considered Lagrange multipliers and the resultant positive $p_i \quad \forall i = 1, 2, 3, 4$, equations (2.11) to (2.12) can be expressed as follows:

$$\lambda_i = \frac{\omega B\gamma_i}{\sum_{j=1}^{4} p_j\gamma_j + \omega}, \quad \forall i = 1, 2 \tag{B.6}$$

$$\mu_3 = \frac{\omega B}{\phi_3 \sum_{j=1}^{4} p_j \gamma_j + \phi_3 \omega} \tag{B.7}$$

$$\lambda_3 = \frac{\omega B \gamma_3}{\sum_{j=1}^{4} p_j \gamma_j + \omega} + \gamma_3 \mu_3. \tag{B.8}$$

Since the solutions of $p_i \ \forall i = 1, 2, 3, 4$ are positives, thus the equations (B.6) to (B.8) show that λ_1, λ_2, λ_3, and μ_3 all are positives. Therefore, the Lagrange multipliers set, $S_1 = \{\lambda_1, \lambda_2, \lambda_3, \mu_3\}$, satisfies KKT condition. All the other cases can easily be verified using similar approach.

By verifying all the necessary KKT conditions, the optimal transmission powers and the corresponding necessary conditions for 2-, 3-, and 4-user uplink NOMA clusters are provided in **Table B.1**. By observing the optimal solutions in **Table B.1**, the closed-form solution of **Lemama** 2.3.2 can be proofed by induction.

Table B.1: Optimal Power allocation solutions for 2-r, 3-, and 4-user uplink NOMA

NOMA	Optimal transmission power	Necessary conditions
2-user	$p_i = p'_t, \forall\, i = 1, 2$	$(C_1^2) \quad p_i\gamma_i - \sum_{j=i+1}^{2} \phi_i p_j \gamma_j - \phi_i \omega > 0, \forall\, i = 1, 2$ $(C_2^2) \quad p_1\gamma_1 - p_2\gamma_2 - p_{tol} > 0$
	$p_1 = p'_t,\ p_2 = \frac{p'_t\gamma_1}{\phi_1\gamma_2} - \frac{\omega}{\gamma_2}$	$(C_1^2)\, \forall\, i = 2$, (C_2^2), and $p_2 < p'_t$
	$p_1 = p'_t,\ p_2 = \frac{p'_t\gamma_1}{\gamma_2} - \frac{p_{tol}}{\gamma_2}$	(C_1^2), and $p_2 < p'_t$
3-user	$p_i = p'_t, \forall\, i = 1, 2, 3$	$(C_1^3) \quad p_i\gamma_i - \sum_{j=i+1}^{3} \phi_i p_j \gamma_j - \phi_i \omega > 0, \forall\, i = 1, 2, 3$ $(C_2^3) \quad p_i\gamma_i - \sum_{j=i+1}^{3} p_j \gamma_j - p_{tol} > 0, \,, \forall\, i = 1, 2$
	$p_i = p'_t, \forall\, i = 1, 2$ $p_3 = \frac{p'_t\gamma_2}{\phi_2\gamma_3} - \frac{\omega}{\gamma_3}$	$(C_1^3)\, \forall\, i = 1, 3$, (C_2^3), and $p_3 < p'_t$
	$p_i = p'_t, \forall\, i = 1, 2$ $p_3 = \frac{p'_t\gamma_2}{\gamma_3} - \frac{p_{tol}}{\gamma_3}$	(C_1^3), $(C_2^3)\, \forall\, i = 1$, and $p_3 < p'_t$
4-user	$p_i = p'_t, \forall\, i = 1, 2, 3, 4$	$(C_1^4) \quad p_i\gamma_i - \sum_{j=i+1}^{4} \phi_i p_j \gamma_j - \phi_i \omega > 0, \forall\, i = 1, 2, 3, 4$ $(C_2^4) \quad p_i\gamma_i - \sum_{j=i+1}^{4} p_j \gamma_j - p_{tol} > 0, \,, \forall\, i = 1, 2, 3$
	$p_i = p'_t, \forall\, i = 1, 2, 3$ $p_4 = \frac{p'_t\gamma_3}{\phi_3\gamma_4} - \frac{\omega}{\gamma_4}$	$(C_1^4)\, \forall\, i = 1, 2, 4$, (C_2^4), and $p_4 < p'_t$
	$p_i = p'_t, \forall\, i = 1, 2, 3$ $p_4 = \frac{p'_t\gamma_3}{\gamma_4} - \frac{p_{tol}}{\gamma_4}$	(C_1^4), $(C_2^4)\, \forall\, i = 1, 2$, and $p_4 < p'_t$